

2015

Development of light- and chemo-sensitive probes for biochemical methods

Pratik Pran Goswami
Iowa State University

Follow this and additional works at: <https://lib.dr.iastate.edu/etd>

 Part of the [Organic Chemistry Commons](#)

Recommended Citation

Goswami, Pratik Pran, "Development of light- and chemo-sensitive probes for biochemical methods" (2015). *Graduate Theses and Dissertations*. 14369.
<https://lib.dr.iastate.edu/etd/14369>

This Dissertation is brought to you for free and open access by the Iowa State University Capstones, Theses and Dissertations at Iowa State University Digital Repository. It has been accepted for inclusion in Graduate Theses and Dissertations by an authorized administrator of Iowa State University Digital Repository. For more information, please contact digirep@iastate.edu.

Development of light- and chemo-sensitive probes for biochemical methods

by

Pratik Pran Goswami

A dissertation submitted to the graduate faculty
in partial fulfillment of the requirements for the degree of

DOCTOR OF PHILOSOPHY

Major: Organic Chemistry

Program of Study Committee:
Arthur H. Winter, Major Professor
William S. Jenks
Nicola L. B. Pohl
Emily A. Smith
Brett VanVeller

Iowa State University

Ames, Iowa

2015

Copyright © Pratik Pran Goswami, 2015. All rights reserved.

Dedication

I would like to dedicate this dissertation to *Ma* and *Deuta*, whose love and support made this journey possible.

TABLE OF CONTENTS

ACKNOWLEDGEMENTS	iv
ABSTRACT.....	vii
CHAPTER 1 INTRODUCTION TO PHOTOCAGES	1
CHAPTER 2 BODIPY-DERIVED PHOTOREMOVABLE PROTECTING GROUPS UNMASKED WITH GREEN LIGHT	25
CHAPTER 3 SHIFTING BODIPY PHOTOREMOVABLE GROUPS INTO THE RED	41
GENERAL CONCLUSIONS FOR PART I	52
CHAPTER 4 INTRODUCTION TO SELF-IMMOLATIVE LINKERS.....	53
CHAPTER 5 SELF-IMMOLATIVE ARYL PHTHALATE ESTERS	73
CHAPTER 6 SELF-IMMOLATIVE PHTHALATE ESTERS SENSITIVE TO HYDROGEN PEROXIDE AND LIGHT	88
GENERAL CONCLUSIONS FOR PART II.....	99
APPENDIX A SUPPORTING INFORMATION FOR CHAPTER 2.....	100
APPENDIX B SUPPORTING INFORMATION FOR CHAPTER 5.....	133
APPENDIX C SUPPORTING INFORMATION FOR CHAPTER 6.....	142

ACKNOWLEDGEMENTS

First, I would like to thank my major professor, Arthur Winter, for being an excellent mentor. His research ideas have always excited and inspired me. Even during particularly stubborn and difficult projects, Art's zeal and excellent ideas have consistently kept me going. With his *hands free* approach, he has always encouraged me to develop and shape my research. As such, the success I have, has been more fruitful and gratifying. At the same time, he has an *open door policy* for all his graduate students. I have walked into his office innumerable times, unannounced, and he always had an answer for me, be it about chemistry or anything else. I would like to thank him for all those answers, discussions, encouragements and laughters. Being one of his first students, I feel extremely fortunate to have witnessed Art grow as a teacher and a scientist. Be it setting up his fresh new lab to staining the floors with BODIPY; from the first overflowing hood with leaking reflux condenser to the first JACS paper of the lab; from his first few projects (read amplifier) to the new and exciting direction of the lab; from dejection with repeated failed experiments to relief and 'hell yeah' when something finally clicks; from disappointment with various grant rejections to finally getting one; from nervous anticipation of his tenure talk to proudly cheering with cheap champagne; I feel honored to be a part of Art's journey.

I would also like to thank my committee members' throughout my Ph.D. I greatly appreciate their help and suggestions during this period. I would like to thank Prof. Nicola Pohl for encouraging me and always being available whenever I needed her. I cherish her suggestions and am always inspired by her. I would also like to thank the staff in chemistry teaching labs and chemistry office. Sarah and Shu have been excellent help throughout my Ph.D. They always seem to have time for everyone and have assisted me with their

valuable inputs. I would also like to thank Lynette for being so helpful and an all-round wonderful person. I thank Allen for helping me throughout while I was an organic T.A.

I would like to thank Prof. Emily Smith for agreeing to collaborate for my projects. I am extremely lucky to have worked with Aleem Syed, a great professional and a good friend.

I would like to sincerely thank each member of Winter lab. I have been very fortunate to spend these years with you and lucky to have each one of you as a close friend. Christickle, Patrickle and Toscars will always be special as we started our journey in the Winter lab together. It was a new and unknown adventure for us and I am glad we had each other. I would like to point out the immense help of Christie and Katie towards my Ph.D. research. Christie had graciously allowed me to continue on her projects when mine were failing. Katie has been kind as well as bold to trust me with her own projects. She has been an outstanding co-worker and I owe a significant part of my success in graduate career to her. I have some unique and great memories with all my lab mates including group trips, group lunches, NMR parties, robot unicorn attacks, apple events, inappropriate office discussions, civilization games, real Russian story times, contemplating next koala attack, TFW etc., to name just a few. I enjoyed some great moments in the classy and ever-clean *west side winter lab*. Mark, Alex and Katie; your swagger, awful and awkward humor and general goofiness made working inside the lab so much fun.

I would like to thank my parents who always had faith in my ability and constantly encouraged me. This journey would not have been possible without their blessings. I am indebted to Sanghamitra Goswami and Nayan Goswami for helping me embark on the graduate school journey.

I would like to thank Abhi and Kanika for helping out with my dissertation. I can always trust you both.

I would like to thank all the friends I made during the course of my graduate studies. I would like to especially thank Nitin and Gargey. Their company made the after-work hours so much fun.

Finally, I would like to thank my wonderful wife, Manibarsha Goswami. An excellent chemist, she has been more than a life partner for me. She has always found time to discuss and give invaluable suggestions on my research even when she was busy with her own. She has always inspired me to be a better scientist and a better person. I am extremely lucky to have spent most of my graduate life with her and it has been an outstanding journey together.

ABSTRACT

Part I. Photocages, which are light cleavable protecting groups, are an important class of chemical tools that allow light to unmask bioactive substrates with precise spatiotemporal resolution in biological microenvironments. Due to their effectiveness in biological systems, it has become increasingly important to find logically designed photocages that can cleave under visible light and Near IR conditions, wavelengths with minimal phototoxicity and increased tissue penetration compared to ultraviolet light. The scope of this research is to both rationally design and synthesize a new class of photocage based on the BODIPY moiety, as well as to modify these photocages to absorb in region of the biological window (600-1000 nm), where tissues have maximal transparency.

In chapter 1, photocages derived from *meso*-substituted BODIPY dyes were synthesized that release acetic acid when irradiated with green wavelengths (>500 nm). The structures of the photocages were derived by computationally searching for carbocations with low-energy diradical states as a possible indicator of nearby productive conical intersections. These photocages were found to have superior optical properties than the popular *o*-nitrobenzyl systems, which make them promising alternatives. The utility of these photocages in living cells was successfully demonstrated by our collaborators (Prof. Emily Smith and Aleem Syed) in cultured *S2* cells.

In Chapter 2, Knoevenagel type reactions were used to extend the π electron conjugation of the aromatic rings of the BODIPY photocages. This extended conjugation of these BODIPY photocages resulted in a bathochromic shift in absorbance towards red light (>600 nm) and allows cleavage using wavelengths in the biological window.

Part II. Self-immolative linkers can be used to trigger the release of an important cargo molecule like a drug or a biomolecule. A variety of trigger stimulants including light, chemo and enzyme are known in literature. However, there is a need for new linker units which would have fast and controllable kinetics of cargo release. During my research, I identified improved self-immolative linker units based on aryl phthalate esters with a modular design, which can tolerate a range of different trigger and cargo units.

In Chapter 3, new types of self-immolative linkers based on the phenyl hydrogen phthalate system were synthesized. The fast kinetic rate for the hydrolysis of phenyl hydrogen phthalate system and the resulting benign byproducts promise a robust self-immolative linker system that can be used in biological systems. The linker system was shown to release phenol based cargo molecules including phenol and coumarin dyes upon cleavage by a fluoride sensitive trigger. This type of linker can also be potentially used as an efficient fluoride sensor.

In Chapter 4, the scope of self-immolative linkers based on phenyl hydrogen phthalate system was extended. Light and peroxide sensitive triggers were incorporated into the linker system. Coumarin based cargo molecules were used as reporter molecules and the increase in their fluorescence after release was monitored. The light-sensitive aryl phthalate ester was further demonstrated as a pro-fluorophore in cultured *S2* cells.

CHAPTER 1

INTRODUCTION TO PHOTOCAGES

Light brings us the news of the Universe.

— Sir William Bragg

Photoremovable protecting groups, also known as photocages, have found increasing use in biology and chemistry. These groups can be bound to a bioactive molecule through a chemical bond, thus rendering them biologically inert. However, upon irradiation with light, the chemical bond between the photocage and the bioactive molecule is broken, restoring the activity of the biomolecule. Since light is the trigger, there is high temporal and spatial control over these photocages for the release of the chemical cargo using focused pulsed laser light, thus making these chemical tools indispensable for biological studies. Temporal resolution refers to the precision of a measurement with respect to time while spatial resolution describes the ability to unmask the substrate within a focused area of 3-dimensional space. For a photocage, high temporal resolution can be achieved by initiating photorelease with light pulses of short duration while spatial resolution can be achieved by irradiation with focused light. Applications of photocages in the field of biology involve activated gene expression,¹⁻⁴ photoactivation of fluorophores (“pro-fluorophores”) and signal transduction,⁵⁻⁷ photorelease of small molecules (e.g. ATP, cAMP) for studying cell behavior,^{8,9} photocontrolled processing of RNA,^{10,11} light-activated prodrugs,¹²⁻¹⁴ photocaged unnatural amino acids that can be genetically encoded into proteins^{15,16} etc., amongst many others.

Apart from biology, photocages have important applications in multiple areas such as organic synthesis,¹⁷⁻¹⁹ photolithography^{20,21} and light-responsive organic materials.²²⁻²⁴ Application of photocages towards organic synthesis is of singular interest due to these groups permitting a traceless reagent process.²⁵ Since no reagents apart from light are used for the photorelease process, no further separation of spent reagents is required.

To evaluate the efficiency of a photocage, several guidelines are proposed by various researchers including Umezawa *et al.*²⁶ and Nerbonne *et al.*²⁷ The important criteria for a useful photocage include (a) strong absorption at wavelengths well above 300 nm, (b) good aqueous solubility for biological studies, (c) efficient photochemical release, (d) biocompatible photochemical byproducts, (e) reasonable absorptivity (ϵ) to capture the incident light efficiently, (f) excitation by a short light pulse and (g) the appearance rate constant (k_{app}) of the desired free substrate exceeding the rate constant of the response under investigation. A strong absorption at wavelengths above 300 nm is highly significant, as absorption in the UV region considerably hinders the biological utility of the photocage. Also, absorption of UV light is toxic for biological systems while at the same time the penetration of light in this wavelength is very poor in a biological entity.

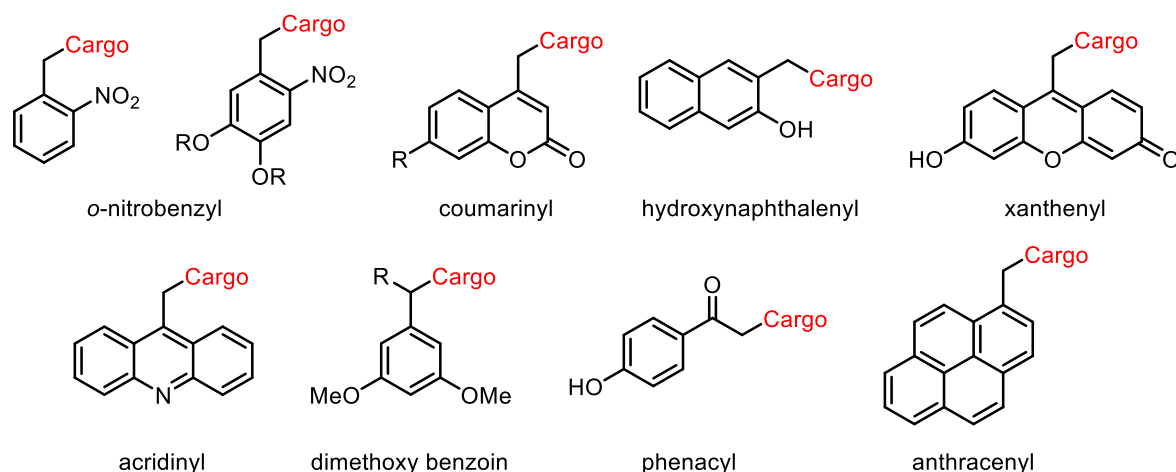


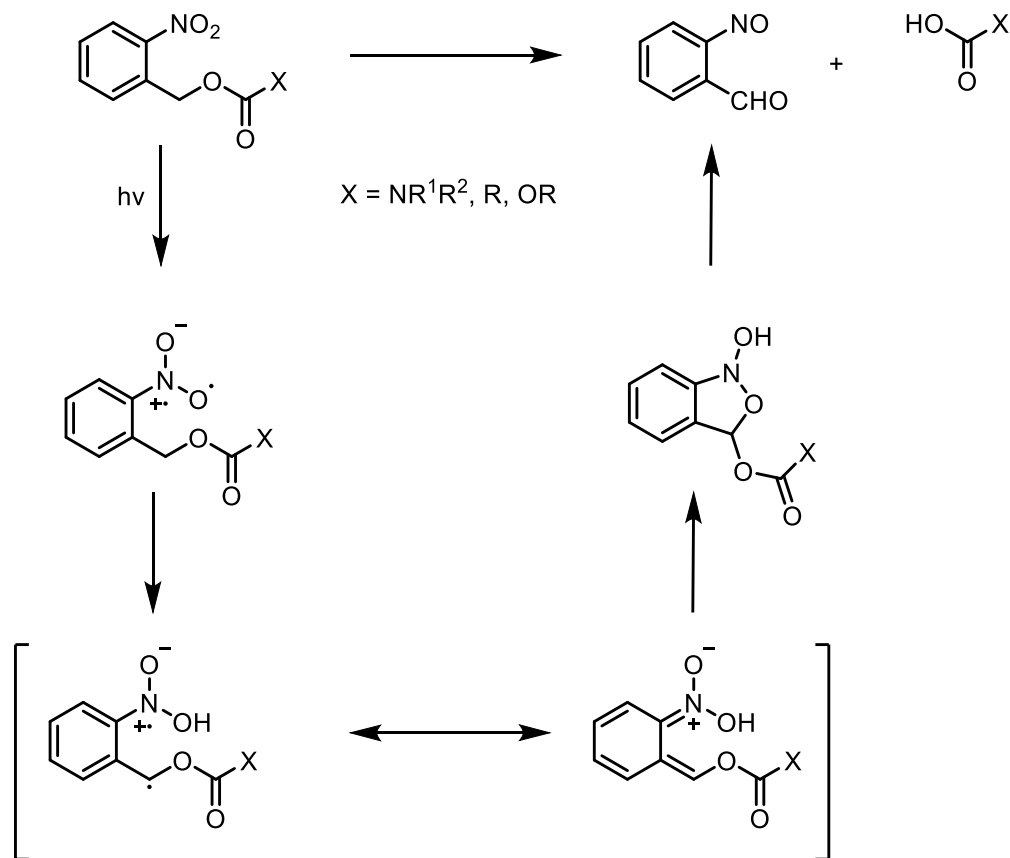
Figure 1.1 Common photocages.

Structures of the most commonly known photocages are given in **Figure 1.1**. Although the phenacyl,²⁸ acridinyl,²⁹ benzoinyl,^{30,31} coumarinyl,³² xanthenyl,³³ and *o*-hydroxynaphthyl³⁴ based photocages have found increasing use in recent times, *o*-nitrobenzyl systems and their derivatives^{8,9,35} remain the most commonly used photocage systems.

***o*-nitrobenzyl systems:**

o-nitrobenzyl based protecting groups were originally developed for organic synthesis³⁵, but the pioneering work of Kaplan *et al.*⁸ in 1978 opened the doors for its use in biochemistry. This work highlighted the protection of ATP with an *o*-nitrobenzyl photocage, which was released upon irradiation with light (342 nm). Furthermore, his work explored the possibility of using the photocaged compounds towards subsequent release of a bioactive molecule under physiological conditions. This greatly piqued the interest of biochemists and led to the use of the *o*-nitrobenzyl system in various other biochemical systems.

As shown in **Scheme 1.1**, *o*-nitrobenzyl photocage is based on the photochemically induced photoisomerisation of *o*-nitrobenzyl alcohol derivatives into *o*-nitrosobenzaldehyde.³⁶ Acetal derivatives of carbamates, carbonates and esters are formed, which then spontaneously forms an aldehyde and the uncaged cargo. Photoisomerisation of meta and para nitrobenzyl alcohol has also been shown in literature.³⁷



Scheme 1.1 Proposed mechanism of *o*-nitrobenzyl photocage system³⁶

The *o*-nitrobenzyl photocage systems have been extensively researched and their properties are well established. This coupled with their relative ease of synthesis, thermal stability and low cost is responsible for more than 80% of the studied photocages being based on the *o*-nitrobenzyl backbone. Various alterations have been done to the core

structure of *o*-nitrobenzyl photocages to revise and enhance several important properties of the photocage. This includes substitution in the benzylic position³⁸⁻⁴⁰ to increase efficiency and enhance electronic effect, substitution on the aromatic ring⁴¹⁻⁴³ for easier synthesis without inducing chirality and promote bathochromic shift of the absorbance spectrum, as well as incorporating two-photon irradiation technique⁴⁴⁻⁴⁷ to enhance temporal resolution of the cargo delivery into a biological system.

Despite the various existing studies done on making the *o*-nitrobenzyl moiety a better photocage, they still suffer from critical limitations such as:

- a) *o*-Nitrosobenzaldehyde is the by-product of *o*-nitrobenzyl based protecting groups (**Scheme 1.1**). This highly reactive nitroso functional group is very toxic in biological systems.⁴⁸ Moreover, as shown by Patchornik *et al.*,⁴⁹ nitrosoaldehyde derived side-products can act as an internal filter, thus preventing efficient light absorption and thereby causing a significant darkening of the solution. Also, the nitroso group may react with the released cargo thereby causing inhibition and inefficient cargo release.^{50,51}
- b) The cleavage of the cargo follows a mechanism which operates *via* a neighboring group participation, rather than *via* a direct heterolytic scission from the excited state (**Scheme 1.1**). This generally results in a slow pH dependent photorelease ($k_{\text{release}} = 10^2 - 10^{-2} \text{ s}^{-1}$ depending on the pH microenvironment).^{8,52}
- c) Quantum efficiency of a photocage is an important property, which gives a quantitative knowledge of how efficient a photocage is towards photocleavage. Mathematically, it is the product of quantum yield of

photolysis and the molar absorptivity of a photocage. Since *o*-nitrobenzyl compounds are very weak chromophores and have low molar absorptivity ($\epsilon < 10^4 \text{ M}^{-1} \text{ cm}^{-1}$ at selected λ_{max}), the quantum efficiency of these photocages is generally very poor.

- d) The most significant limitation of *o*-nitrobenzyl based photocages is that the maximum absorption (λ_{max}) lies in the UV region. The *o*-nitrobenzyl group has its λ_{max} at 280 nm while substitution in the aromatic ring e.g. dimethoxy analog, can improve $\lambda_{\text{max}} \sim 350$ nm. Due to this, the photocage can be uncaged only by using cytotoxic UV irradiations. Also, light with wavelengths around 300 nm is readily absorbed by biological systems (causing damage to the system), thereby severely limiting the penetration of the light into the system upon irradiation.

Structure Relationship of Photocages:

Most of the known photocages have been discovered serendipitously or through empirical investigations. The lack of a structure-reactivity relationship for heterolysis in the excited state is a significant hurdle towards understanding why a compound can act as a photocage, which in turn is a major stumbling block in the rationale design of photocages. On the one hand, ground state heterolysis is well documented with developed quantitative and qualitative structure-reactivity principles. The stabilized transition state along the heterolysis coordinate can be used to induce thermal heterolysis. However, since photoheterolysis is carried out in the excited state potential energy surface, there is no correlation known between stabilizing the ground state transition state and a subsequent photochemical reaction. Several studies have been done to comprehend photoheterolysis

and the mechanism involved. Interestingly, several reports by Zimmerman's,^{53,54} Turro's,⁵⁵ and Michl's⁵⁶ suggested that photoheterolysis may involve a conical intersection pathway.

Are Photoheterolysis Reactions Under Conical Intersection Control?

A conical intersection between two potential energy surfaces is the set of molecular geometry points where they intersect (degenerate energy and geometries). The Born–Oppenheimer approximation breaks down near the vicinity of a conical intersection, thereby allowing non-adiabatic processes to take place. A non-adiabatic photochemical reaction involves two potential energy surfaces. As shown in **Figure 1.2**, a molecule is first excited from a stable ground state S_0 to an excited state S_1 . This molecule can relax on the excited surface to move to the excited state minima. In case of a nearby conical intersection, this excited state minima is energetically degenerate with the maximum on the ground state S_0 . This allows for *funneling* or crossing of the molecule from one energy surface to another, i.e. from excited state S_1 back to S_0 . In **Figure 1.2**, the conical intersection is represented by CI.

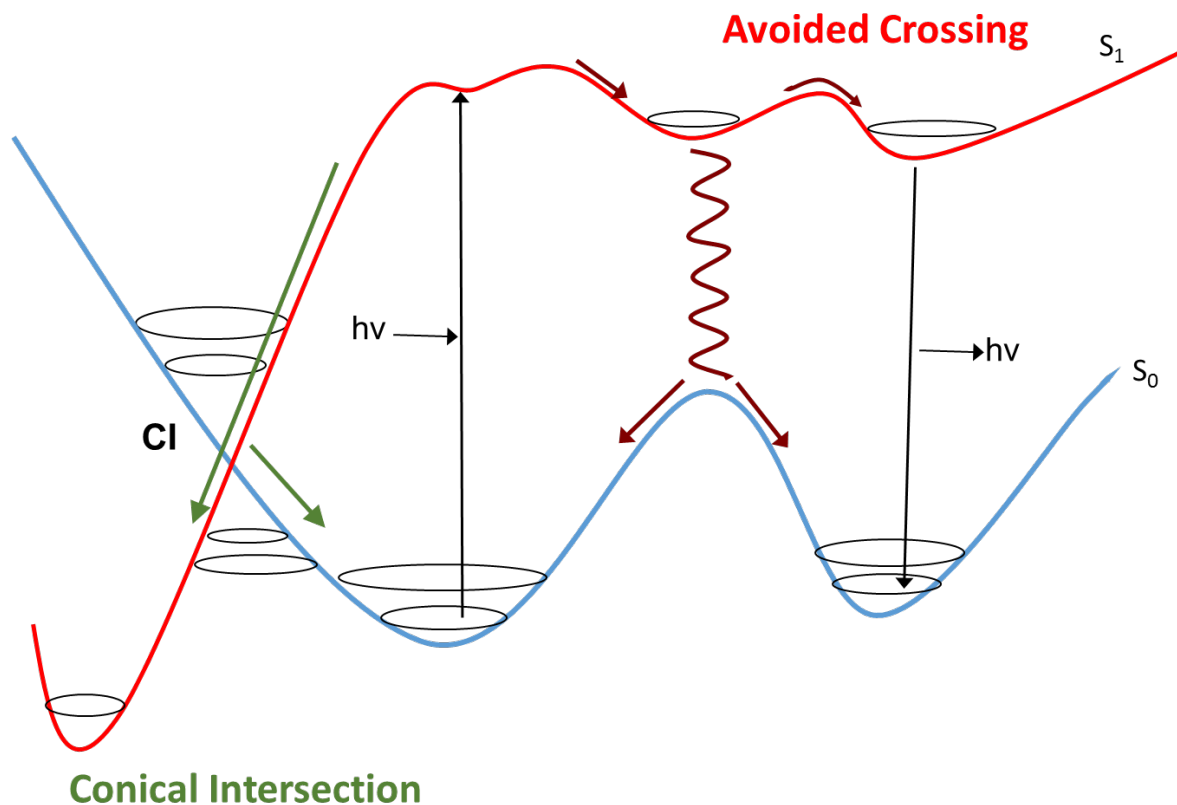


Figure 1.2 Energy diagram showing ground state S_0 and excited state S_1 . CI represents the conical intersection between the two states.

The relation of a photochemical reaction and the conical intersection control was studied in previous work by the Winter lab.⁵⁷ This work is based on the underlying argument that if the ground state maxima of a compound was elevated, i.e. made more unstable while the excited state minima was stabilized and hence lowered in energy, both the potential energy surfaces should be close enough to have a productive conical intersection. This is in contrast to thermal heterolysis, which requires the ground state minima to stabilize the carbocation, and hence has very less likelihood of a nearby conical intersection (as shown in **Figure 1.3**). This argument came from the general observation of known compounds that undergo photoheterolysis reactions, which usually generate

destabilized carbocations (antiaromatic ions, donor-unconjugated ions, dicoordinated aryl/vinyl cations), the opposite of thermal heterolysis preferences.

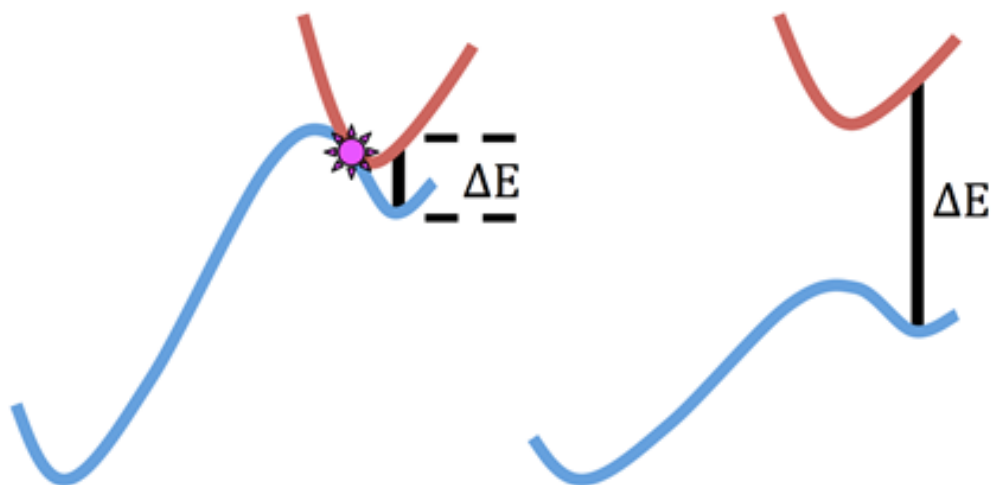


Figure 1.3 Schematic of hypothesis that a destabilized ground state and a stabilized excited state can lead to a favorable, nearby conical intersection.

To probe this theory, Buck *et al.* employed high level computational conical intersection searches. As shown in **Figure 1.4**, the studies confirmed their hypothesis that the unstabilized cations from a photoheterolysis reaction, which have a stabilized excited state also have a nearby conical intersection. Moreover, stabilized cations have high energy, distant conical intersections relative to the excited-state minima. As shown in **Figure 1.4 (I)**, one of the compounds studied was a simplified model of a popular 9-aminocoumarinyl photocage. This model was examined instead of the actual photocage as it preserved the unconjugated nature and connectivity of the amine donor while at the same time was small enough to be computationally viable. As postulated, the authors were able to find low-energy conical intersections relative to the excited-state minimum for the cation [**Figure 1.4 (I)**].

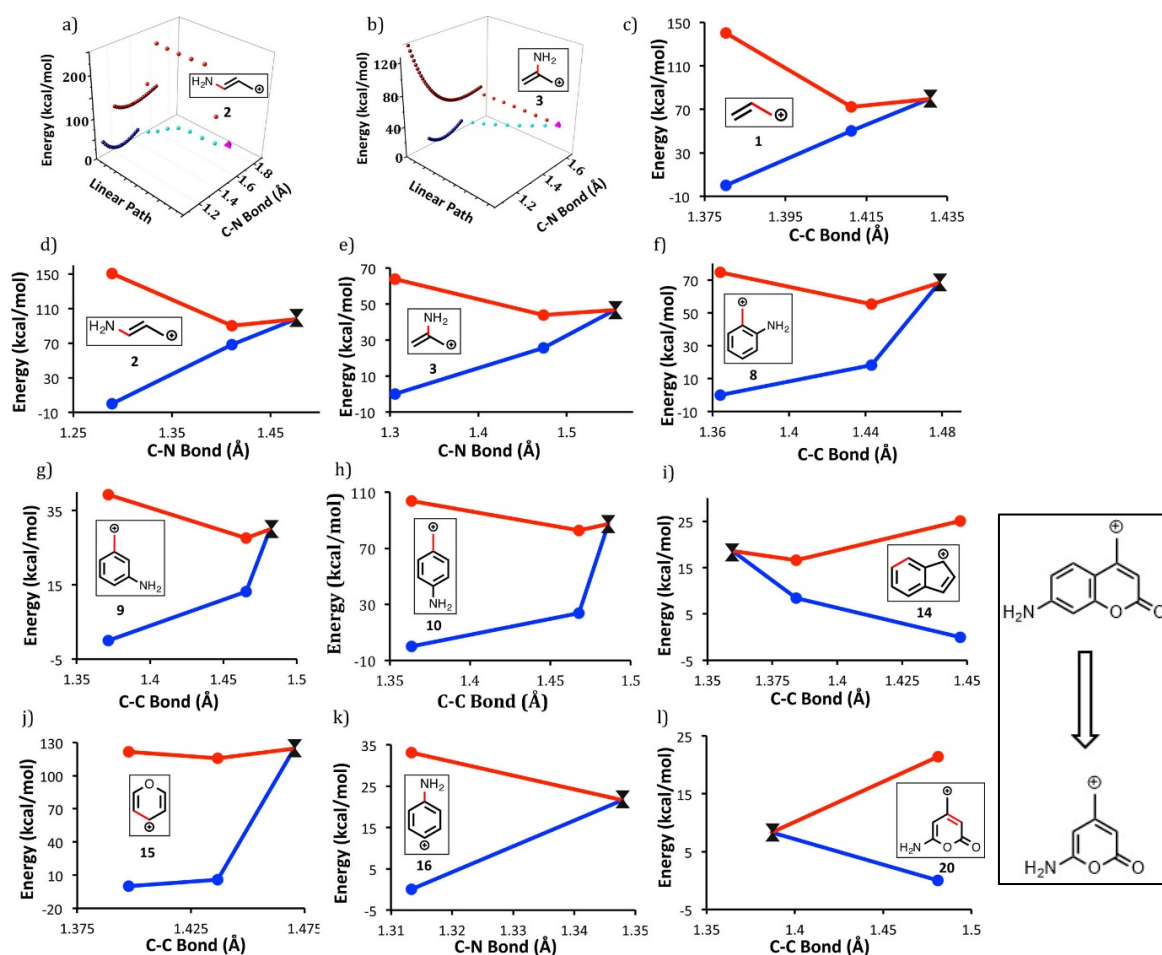


Figure 1.4 Calculated points on the potential energy surfaces of the cations studied by CASSCF with full pi active space. a,b) 3D graphs of calculated points on S_0 and S_1 surface with linear path to the nearest conical intersection (pink tetrahedron). The linear paths are only linear least motion paths and are not minimum energy points (MEP). c - l) graphs of the energies of the potential energy surfaces relative to respective ground states. c) allyl **1**, d) 1-aminoallyl **2**, e) 2-aminoallyl **3**, f) o-aminobenzyl **8**, g) m-aminobenzyl **9**, h) p-aminobenzyl **10**, i) indenium **14**, j) pyrylium **15**, k) p-aminophenyl **16**, and l) aminocoumarin analog **20** (The insert shows the full structure for the aminocoumarin). Red bond in the inset shows the bond chosen for the geometrical coordinate, which was chosen based on the bond with the largest deformation between S_0 , S_1 and the CI. For a), all points at 250 kcal/mol are off scale.

The authors do note that for this particular cation, they were unable to locate an excited-state minima, and suggested a direct channel from the Franck–Condon excited state to the conical intersection bypassing the excited state minimum.

Calculating conical intersection however has practical difficulty, as it is computationally very expensive. As such, an easier way to probe nearby conical intersection is by calculating the excited state energy gaps. This vertical energy gap can be easily estimated using Time Dependent Density Functional Theory (TD-DFT) calculations (**Figure 1.5**). It was found that vertical energy gap for cations which are photoactive is below ~ 60 kcal/mol (**Figure 1.5**, green portion). Cations lying in the red sections would not be expected to have low energy conical intersections. Thus, it is relatively easy to compute the structure reactivity of a carbocation under photochemical conditions, and this novel method can be used as an invaluable tool to predict whether a compound under investigation can be used as a photocage.

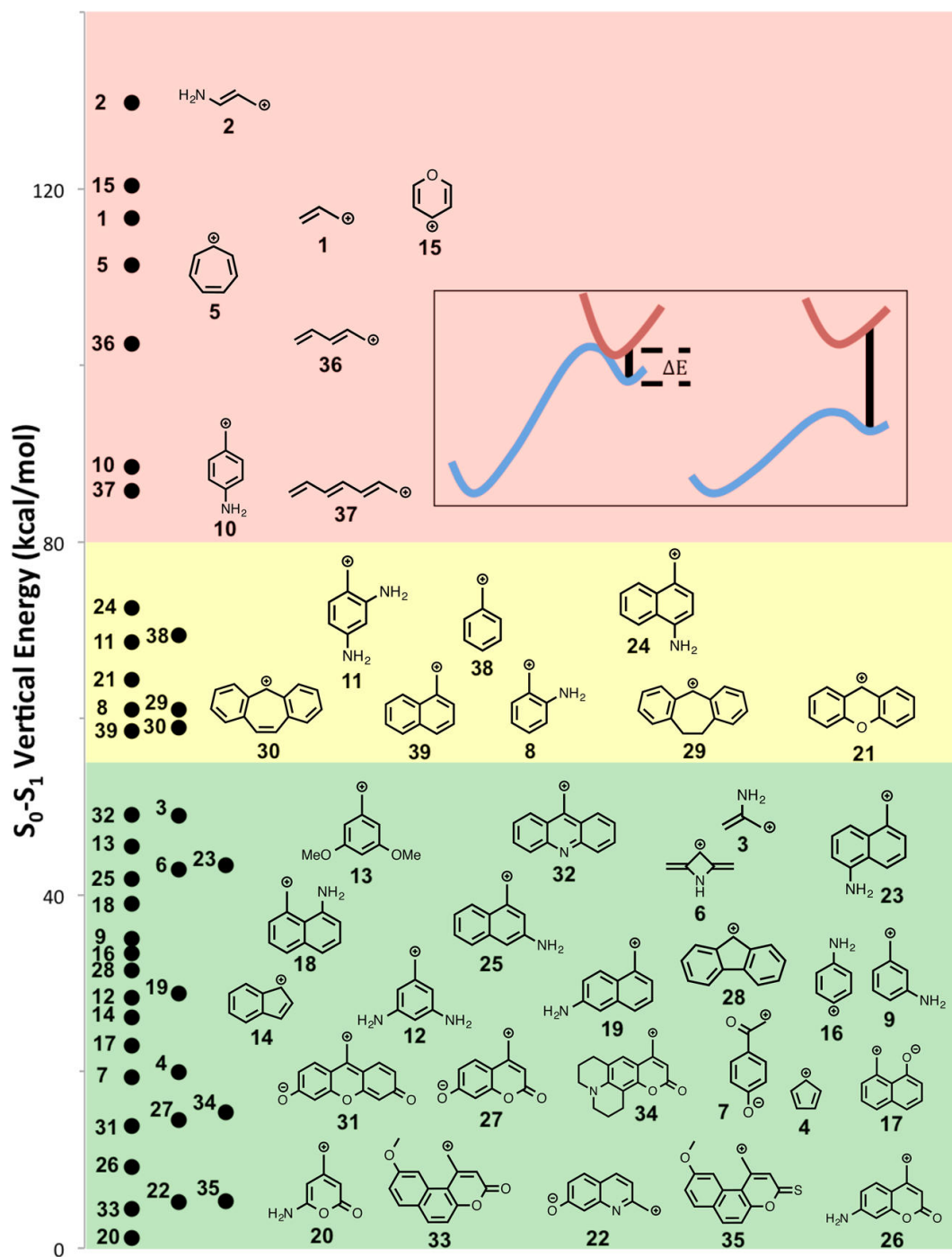


Figure 1.5 An energy level diagram comparing the Franck-Condon vertical energy gap (TD-B3LYP/6-311+G(2d,p)) of all of the cations studied. Compounds in the green section encompass most of the cations from the photoactive species. The maximum of the green section is where the TD-DFT gap for the experimentally known cations for photoheterolysis end. Cations in the red sections would not be expected to have low-energy conical intersections. Inset: Hypothesis that a small vertical energy gap suggests a nearby

conical intersection.

Visible Light Absorbing Photocages Derived from BODIPY Dyes:

BODIPY dyes are a class of fluorescent dyes discovered by Treibs and Kreuzer in 1968.⁵⁸ These dyes consist of the core structure of 4,4-difluoro-4-bora-3a,4a-diaza-s-indacene (henceforth abbreviated to BODIPY) (**Figure 1.6**), and generally display a strong absorbance in the visible region along with high quantum yield of fluorescence.⁵⁹ BODIPY dyes are usually uncharged and hence are independent of solvent polarity, being reasonably stable in physiological pH-range. Toxicological studies on these dyes have shown them to be relatively benign,⁶⁰ making them an ideal choice as probes in biological systems.⁶¹⁻⁶⁴ For example, these dyes have already found widespread use as labeling agents,⁶⁵ fluorescent switches,⁶⁶ chemosensors^{67,68} and as laser dyes.⁶⁹

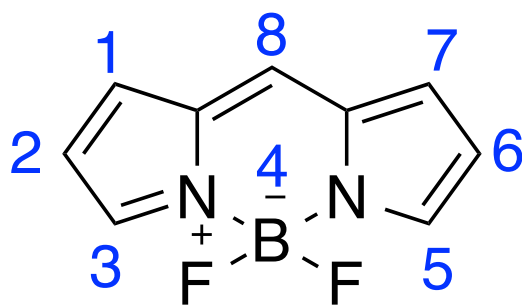


Figure 1.6 The BODIPY core

The spectroscopic properties of BODIPY dyes is characterized by narrow bands of absorption and emission with small Stokes shift. Although, BODIPY dyes normally have absorption and emission in the green region of visible light, various substitutions on the pyrrole ring have been able to modify the absorbance of the dyes across the visible region up to the infrared region. The extinction coefficient of BODIPY dyes are generally very

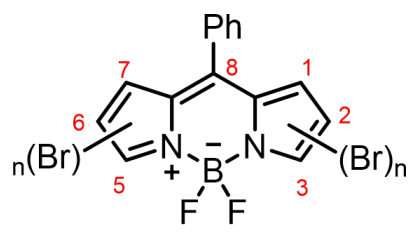
high ($>40,000 \text{ cm}^{-1}\text{M}^{-1}$) along with high fluorescence quantum yield. BODIPY dyes have been found to have fluorescence quantum yields generally approaching 1 along with great compatibility with various organic and aqueous mediums. These dyes in general also have a relatively long excited state lifetime, making them useful for fluorescence polarization-based assays. These characteristics make them extremely versatile and superior to similar dyes/fluorophores like fluorescein, tetramethylrhodamine, Texas Red and other known longer wavelength dyes.

Halogen incorporated BODIPY dyes: The importance of the Heavy Atom Effect

BODIPY dyes incorporated with halogens like fluorine, bromine and iodine have been synthesized and studied. The halogen atom are either included in the pyrrole ring used for the construction of the BODIPY core^{70,71} or as a post BODIPY core synthesis modification.⁷²⁻⁷⁴ These dyes are generally used as pre-cursors, as a number of reactions may then be done on the halogenated aromatic heterocyclic structure of these BODIPY compounds.

Another important utility of incorporating halogen atoms into BODIPY moieties have been to exploit the heavy atom effect.⁷⁵ The heavy atom effect has been defined by IUPAC as “*the enhancement of the rate of a spin-forbidden process by the presence of an atom of high atomic number, which is either part of, or external to, the excited molecular entity. Mechanistically, it responds to a spin-orbit coupling enhancement produced by a heavy atom.*”⁷⁶ The presence of the halogen atom tends to enhance the intersystem crossing. This would lead to possible quenching of fluorescence but in turn opens up opportunity for other electronic changes including red shift of UV-absorption and

fluorescence emission maxima. The heavy atom effect of halogens in BODIPY moiety has been exploited to generate singlet oxygen, which in turn has been used to target malignant cells in photodynamic therapy.^{75,77} A more recent study on the heavy atom effect on the BODIPY core was done by Zhang and Yang.⁷⁷ They studied four dyes (**Figure 1.7**) which had one, two, four and six bromine atoms on the BODIPY core structure. The BODIPY compound with no bromine atom has a negligible triplet quantum yield (ϕ_T). However, addition of 1 bromine atom to the parent compound significantly enhances the ϕ_T from 0.0 to 0.39. Further addition of bromine atom increases the ϕ_T to 0.46, 0.50 and 0.66 for 2, 4 and 6 additional bromine atoms respectively.



	n	Position of Br atom	Triplet Quantum Yield
0 Bromine	0		0.00
1 Bromine	1	2	0.39
2 Bromine	2	2,6	0.46
4 Bromine	4	2,3,5,6	0.50
6 Bromine	6	1,2,3,4,5,6	0.66

Figure 1.7 The BODIPY structure illustrating the positions where bromine was substituted. The table gives information on the substitution positions and the corresponding triplet quantum yields.

BODIPY dyes with Extended Conjugation:

As previously noted, the core of BODIPY can be modified to redshift the absorption and emission of these dyes. The idea behind these modifications in the BODIPY system is to extend the delocalization of the electronic π -systems of BODIPY chromophoric core by conjugating with suitable substituents. Delocalization reduces the energy gap between π and π^* orbitals, thereby reducing the energy required for the promotion of the electron, which in turn means longer wavelength. An example of this

concept would be that while naphthalene and anthracene are colorless, tetracene is orange.

(Figure 1.8)

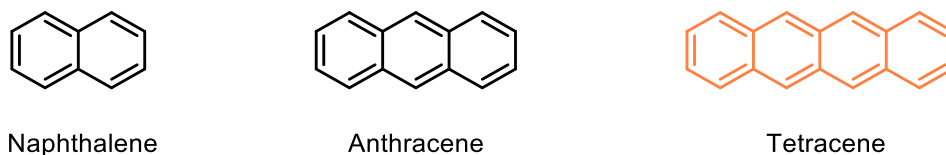


Figure 1.8 The structure of naphthalene, anthracene and tetracene. The orange color of tetracene structure represents the actual color of this compound. Both naphthalene and anthracene are colorless.

The conjugation of BODIPY was shown in terms of contour maps of the HOMO and LUMO electronic states by A. Costela *et al.*⁷⁸ In their study, they compared the absorbances of the commercially available BODIPY dye PM567 with the synthesized PMS BODIPY. The PMS BODIPY dye has a styryl group at the 3-position of the PM567 core. The extension of the delocalized electronic π -system through the styryl group induces a bathochromic shift (around 50 nm) in the absorption band (**Figure 1.9**). This extended conjugated electronic cloud is shown by the contour maps of the HOMO and LUMO electronic states obtained by quantum mechanical calculations (**Figure 1.9**).

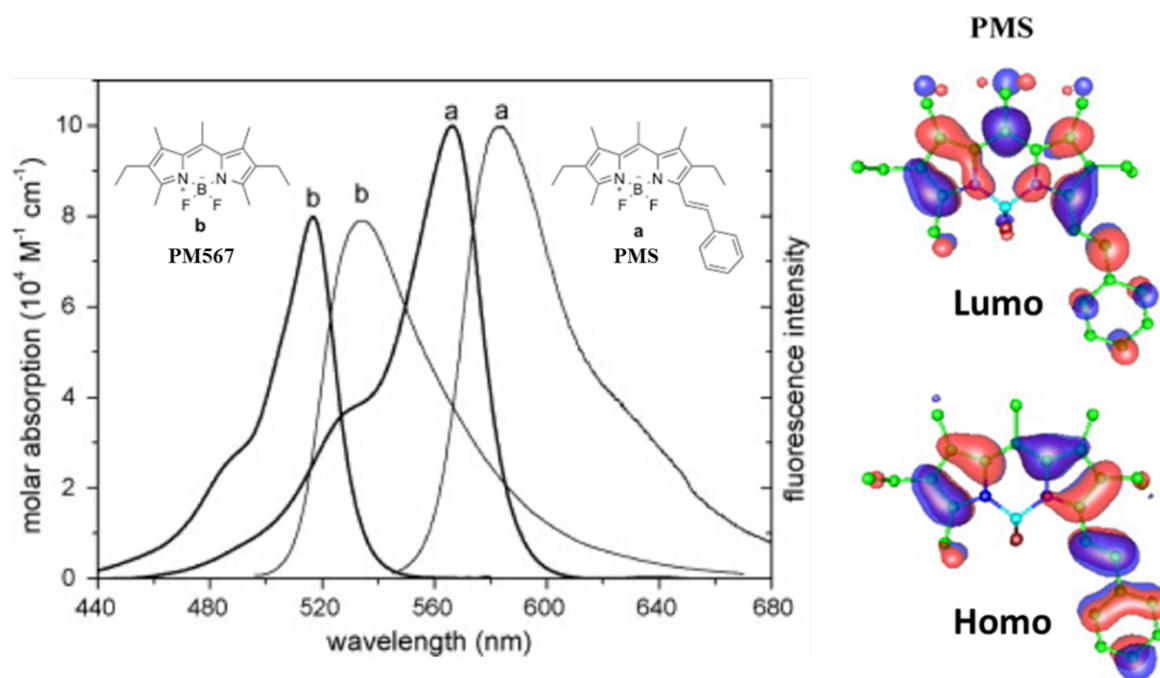


Figure 1.9 Normalized absorption and fluorescence spectra of PMS (a) and PM567 (b) in diluted solutions of methanol. The contour maps of the HOMO and LUMO of PMS are also included.

BODIPY dyes conjugated by Knoevenagel reaction

Methyl groups in the 3 and 5 position of BODIPY cores (**Figure 1.6**) are known to be acidic in nature, being similar to pyridinyl systems.⁷⁹ The acidity of these methyl groups has been exploited for Knoevenagel type reactions where condensation of a base is done with an aromatic aldehyde.^{80,81} Knoevenagel reactions are aldol type reactions which consists of a nucleophilic addition of an active hydrogen compound to a carbonyl center followed by dehydration.⁸² These reactions are generally done under basic conditions with the azeotropic removal of water during the course of the reaction, such as the Dean-Stark method. However, the yields of the Knoevenagel reaction with BODIPY dyes are generally quite low. These reactions for BODIPY dyes have been shown to work in microwave assisted way with similar results to those done with conventional method.⁸³ Although both the methyl groups have shown to undergo Knoevenagel type reactions (position 3 and 5) to

give bis substituted products, they are generally even lower yielding. The addition of aromatic rings to the BODIPY core using Knoevenagel reaction extends the conjugation of the π -system of the fluorophore and further red shifts the absorbance and the fluorescence. As shown in **Figure 1.10**, there is a significant change in absorbance moving from the BODIPY dye towards the mono-Knoevenagel product and finally to the bis-Knoevenagel product.⁸⁴⁻⁸⁶ This variation in absorbance and the relative ease of synthesis has prompted a number of BODIPY modifications using Knoevenagel reactions. The conjugated dyes have increasingly found use as laser dyes and cell imaging probes.⁸³

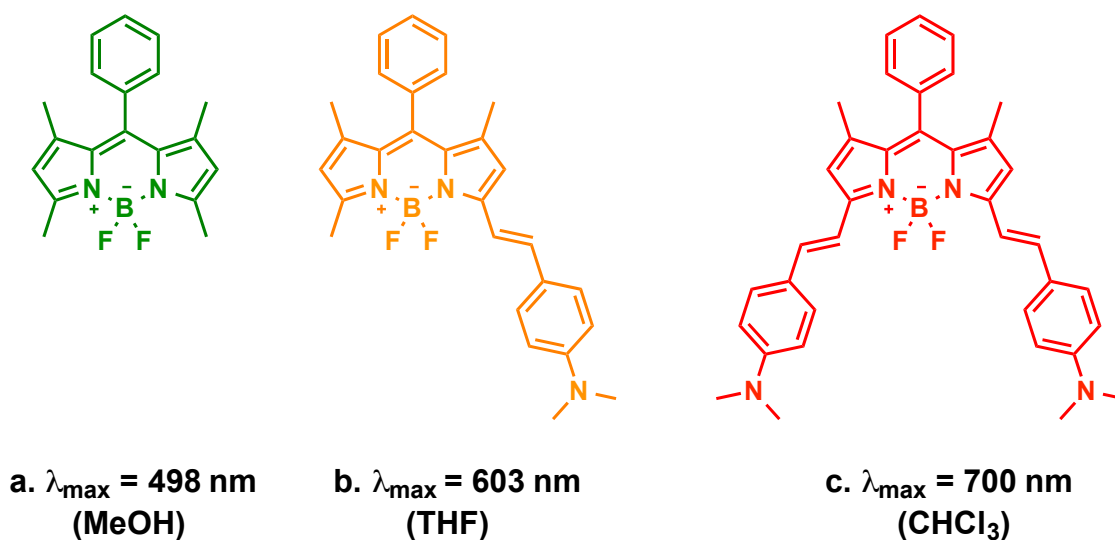


Figure 1.10 The change in maximum absorbance (λ_{\max}) is shown with increasing conjugation in the BODIPY core

More recently, reactions involving methyl groups in positions 1- and 7- have further extended the scope of Knoevenagel reactions on BODIPY moieties.⁸⁷ Bromine substitutions have been purposefully used in positions 2- and 6- of the BODIPY moiety to induce higher acidity of the methyl groups in 1-, 7- positions, which results in higher reactivity of these dyes. It has also been shown that formylation at positions 1,7 leads to a

more controlled approach towards making 1-, 3-, 5-, 7- substituted Knoevenagel BODIPY products.⁸⁸

Conclusion:

Photocages have become indispensable chemical tools which can be used in chemical and biological systems. As highlighted above, in spite of the work done in this field, there is an urgent need to come up with a way to rationally design better photocages. The structure relationship of photocages have been recently explored and this can be used to make better photocages. BODIPY dyes due to its various benefits can act as an excellent core to base a photocage. In the subsequent chapters I have tried to use these information to rationally design a photocage and study its properties and viability in various systems.

References:

- (1) Liu, Q.; Deiters, A. *Acc. Chem. Res.* **2013**, *47*, 45.
- (2) Tang, X.; Dmochowski, I. *J. Mol. BioSyst.* **2007**, *3*, 100.
- (3) Wang, Y.; Wu, L.; Wang, P.; Lv, C.; Yang, Z.; Tang, X. *Nucleic Acids Res.* **2012**.
- (4) Deiters, A.; Garner, R. A.; Lusic, H.; Govan, J. M.; Dush, M.; Nascone-Yoder, N. M.; Yoder, J. A. *J. Am. Chem. Soc.* **2010**, *132*, 15644.
- (5) Fukaminato, T. *J. Photochem. Photobiol., C* **2011**, *12*, 177.
- (6) Li, W.-h.; Zheng, G. *Photochem. Photobiol. Sci.* **2012**, *11*, 460.
- (7) Puliti, D.; Warther, D.; Orange, C.; Specht, A.; Goeldner, M. *Bioorg. Med. Chem.* **2011**, *19*, 1023.
- (8) Kaplan, J. H.; Forbush, B.; Hoffman, J. F. *Biochemistry* **1978**, *17*, 1929.
- (9) Engels, J.; Schlaeger, E. J. *J. Med. Chem.* **1977**, *20*, 907.
- (10) Chaulk, S. G.; MacMillan, A. M. *Nat. Protocols* **2007**, *2*, 1052.
- (11) Pinheiro, A. V.; Baptista, P.; Lima, J. o. C. *Nucleic Acids Res.* **2008**, *36*, e90.
- (12) Blake, J. A.; Bareiss, B.; Jimenez, L.; Griffith, M.; Scaiano, J. C. *Photochem. Photobiol. Sci.* **2012**, *11*, 539.
- (13) Skwarczynski, M.; Noguchi, M.; Hirota, S.; Sohma, Y.; Kimura, T.; Hayashi, Y.; Kiso, Y. *Bioorg. Med. Chem. Lett.* **2006**, *16*, 4492.
- (14) Crespy, D.; Landfester, K.; Schubert, U. S.; Schiller, A. *Chem. Commun.* **2010**, *46*, 6651.
- (15) Lemke, E. A.; Summerer, D.; Geierstanger, B. H.; Brittain, S. M.; Schultz, P. G. *Nat. Chem. Biol.* **2007**, *3*, 769.
- (16) Nguyen, D. P.; Mahesh, M.; Elsässer, S. J.; Hancock, S. M.; Uttamapinant, C.; Chin, J. W. *J. Am. Chem. Soc.* **2014**, *136*, 2240.
- (17) Wuts, P. G. M.; Greene, T. W. *Greene's Protective Groups in Organic Synthesis*; Wiley, 2006.
- (18) Barltrop, J. A.; Schofield, P. *Tetrahedron Lett.* **1962**, *3*, 697.
- (19) Patchornik, A.; Amit, B.; Woodward, R. B. *J. Am. Chem. Soc.* **1970**, *92*, 6333.
- (20) Wöll, D.; Laimgruber, S.; Galetskaya, M.; Smirnova, J.; Pfeleiderer, W.; Heinz, B.; Gilch, P.; Steiner, U. E. *J. Am. Chem. Soc.* **2007**, *129*, 12148.
- (21) Woll, D.; Lukzen, N.; Steiner, U. E. *Photochem. Photobiol. Sci.* **2012**, *11*, 533.

- (22) Pawle, R. H.; Eastman, V.; Thomas, S. W. *J. Mater. Chem.* **2011**, *21*, 14041.
- (23) Park, B. S.; Lee, H. M. *Bull. Korean Chem. Soc.* **2008**, *29*, 2054.
- (24) Hensarling, R. M.; Hoff, E. A.; LeBlanc, A. P.; Guo, W.; Rahane, S. B.; Patton, D. *L. J. Polym. Sci., Part A: Polym. Chem.* **2013**, *51*, 1079.
- (25) Givens, R. S. C., P.G; Yousef, A.L; Lee, J *CRC Handbook of Organic Photochemistry and Photobiology, Volumes 1 & 2, Second Edition*; Second ed.; CRC Press: Boca Raton, 2003.
- (26) Sheehan, J. C.; Umezawa, K. *J. Org. Chem.* **1973**, *38*, 3771.
- (27) Lester, H. A.; Nerbonne, J. M. *Annual Review of Biophysics and Bioengineering* **1982**, *11*, 151.
- (28) Anderson, J. C.; Reese, C. B. *Tetrahedron Lett.* **1962**, *3*, 1.
- (29) Ackmann, A. J.; Frechet, J. M. J. *Chem. Commun.* **1996**, 605.
- (30) Sheehan, J. C.; Wilson, R. M. *J. Am. Chem. Soc.* **1964**, *86*, 5277.
- (31) Sheehan, J. C.; Wilson, R. M.; Oxford, A. W. *J. Am. Chem. Soc.* **1971**, *93*, 7222.
- (32) Givens, R. S.; Matuszewski, B. *J. Am. Chem. Soc.* **1984**, *106*, 6860.
- (33) Šebej, P.; Wintner, J.; Müller, P.; Slanina, T.; Al Anshori, J.; Antony, L. A. P.; Klán, P.; Wirz, J. *J. Org. Chem.* **2013**, *78*, 1833.
- (34) Arumugam, S.; Popik, V. V. *J. Am. Chem. Soc.* **2009**, *131*, 11892.
- (35) Ciamician, G.; Silbert, P. *Chem. Ber.* **1901**, *34*, 2040.
- (36) Bochet, C. G. *Perkin Trans. 1* **2002**, 125.
- (37) Wan, P.; Yates, K. *Can. J. Chem.* **1986**, *64*, 2076.
- (38) Barltrop, J. A.; Plant, P. J.; Schofield, P. *Chem. Commun.* **1966**, 822.
- (39) Baldwin, J. E.; McConnaughie, A. W.; Moloney, M. G.; Pratt, A. J.; Bo Shin, S. *Tetrahedron* **1990**, *46*, 6879.
- (40) Kevitch, R. M.; McGrath, D. V. *New J. Chem.* **2007**, *31*, 1332.
- (41) Allan, A. C.; Ward, J. L.; Beale, M. H.; Trewavas, A. J. In *Methods Enzymol.*; Gerard, M., Ed.; Academic Press: 1998; Vol. Volume 291, p 474.
- (42) Lusic, H.; Young, D. D.; Lively, M. O.; Deiters, A. *Org. Lett.* **2007**, *9*, 1903.
- (43) Klán, P.; Šolomek, T.; Bochet, C. G.; Blanc, A.; Givens, R.; Rubina, M.; Popik, V.; Kostikov, A.; Wirz, J. *Chem. Rev.* **2013**, *113*, 119.

- (44) Zhao, J.; Gover, T. D.; Muralidharan, S.; Auston, D. A.; Weinreich, D.; Kao, J. P. *Y. Biochemistry* **2006**, *45*, 4915.
- (45) Neveu, P.; Aujard, I.; Benbrahim, C.; Le Saux, T.; Allemand, J.-F.; Vrizz, S.; Bensimon, D.; Jullien, L. *Angew. Chem., Int. Ed.* **2008**, *47*, 3744.
- (46) Yan, B.; Boyer, J.-C.; Branda, N. R.; Zhao, Y. *J. Am. Chem. Soc.* **2011**, *133*, 19714.
- (47) Carling, C.-J.; Nourmohammadian, F.; Boyer, J.-C.; Branda, N. R. *Angew. Chem., Int. Ed.* **2010**, *49*, 3782.
- (48) Swann, P. F. *J. Sci. Food Agric.* **1975**, *26*, 1761.
- (49) Rubinstein, M.; Amit, B.; Patchornik, A. *Tetrahedron Lett.* **1975**, *16*, 1445.
- (50) Zou, K.; Cheley, S.; Givens, R. S.; Bayley, H. *J. Am. Chem. Soc.* **2002**, *124*, 8220.
- (51) Zou, K.; Miller, W. T.; Givens, R. S.; Bayley, H. *Angew. Chem., Int. Ed.* **2001**, *40*, 3049.
- (52) Il'ichev, Y. V.; Schwöbber, M. A.; Wirz, J. *J. Am. Chem. Soc.* **2004**, *126*, 4581.
- (53) Zimmerman, H. E. *J. Am. Chem. Soc.* **1966**, *88*, 1564.
- (54) Zimmerman, H. E. *J. Am. Chem. Soc.* **1966**, *88*, 1566.
- (55) Turro, N. *Modern Molecular Photochemistry* 1978.
- (56) Michl, J. *Mol. Photochem.* **1972**, *4*, 243.
- (57) Buck, A. T.; Beck, C. L.; Winter, A. H. *J. Am. Chem. Soc.* **2014**, *136*, 8933.
- (58) Treibs, A.; Kreuzer, F.-H. *Justus Liebigs Annalen der Chemie* **1968**, *718*, 208.
- (59) Loudet, A.; Burgess, K. *Chem. Rev.* **2007**, *107*, 4891.
- (60) Choyke, P. L.; Alford, R.; Simpson, H. M.; Duberman, J.; Hill, G. C.; Regino, O.; Celeste, M.; Hisataka, K. *Mol. Imaging* **2009**, *8*, 1536.
- (61) Johnson, I. D.; Kang, H. C.; Haugland, R. P. *Anal. Biochem.* **1991**, *198*, 228.
- (62) Metzker, M. L.; Lu, J.; Gibbs, R. A. *Science* **1996**, *271*, 1420.
- (63) Farber, S. A.; Pack, M.; Ho, S.-Y.; Johnson, I. D.; Wagner, D. S.; Dosch, R.; Mullins, M. C.; Hendrickson, H. S.; Hendrickson, E. K.; Halpern, M. E. *Science* **2001**, *292*, 1385.
- (64) Reents, R.; Wagner, M.; Kuhlmann, J.; Waldmann, H. *Angew. Chem., Int. Ed.* **2004**, *43*, 2711.
- (65) Gocze, P. M.; Freeman, D. A. *Cytometry* **1994**, *17*, 151.

- (66) Xu, J.; Li, Q.; Yue, Y.; Guo, Y.; Shao, S. *Biosensors and Bioelectronics* **2014**, *56*, 58.
- (67) Barba-Bon, A.; Calabuig, L.; Costero, A. M.; Gil, S.; Martinez-Manez, R.; Sancenon, F. *RSC Advances* **2014**, *4*, 8962.
- (68) Culzoni, M. J.; Munoz de la Pena, A.; Machuca, A.; Goicoechea, H. C.; Babiano, R. *Analytical Methods* **2013**, *5*, 30.
- (69) Amat-Guerri, F.; Liras, M.; Carrascoso, M. L.; Sastre, R. *Photochem. Photobiol.* **2003**, *77*, 577.
- (70) Kim, T. G.; Castro, J. C.; Loudet, A.; Jiao, J. G. S.; Hochstrasser, R. M.; Burgess, K.; Topp, M. R. *J. Phys. Chem. A* **2006**, *110*, 20.
- (71) Wan, C.-W.; Burghart, A.; Chen, J.; Bergström, F.; Johansson, L. B. Å.; Wolford, M. F.; Kim, T. G.; Topp, M. R.; Hochstrasser, R. M.; Burgess, K. *Chem. Eur. J.* **2003**, *9*, 4430.
- (72) Baruah, M.; Qin, W.; Vallée, R. A. L.; Beljonne, D.; Rohand, T.; Dehaen, W.; Boens, N. *Org. Lett.* **2005**, *7*, 4377.
- (73) Rihn, S.; Retailleau, P.; Bugsaliewicz, N.; Nicola, A. D.; Ziesel, R. *Tetrahedron Lett.* **2009**, *50*, 7008.
- (74) Krumova, K.; Cosa, G. *J. Am. Chem. Soc.* **2010**, *132*, 17560.
- (75) Yogo, T.; Urano, Y.; Ishitsuka, Y.; Maniwa, F.; Nagano, T. *J. Am. Chem. Soc.* **2005**, *127*, 12162.
- (76) McNaught, A. D.; Wilkinson, A. In *XML on-line corrected version*; 2nd ed.; Nic, M., Jirat, J., Kosata, B., Eds.; Blackwell Scientific Publications: Oxford, 1997; Vol. 2014.
- (77) Zhang, X.-F.; Yang, X. *J. Phys. Chem. B* **2013**, *117*, 5533.
- (78) Costela, A.; García-Moreno, I.; Pintado-Sierra, M.; Amat-Guerri, F.; Liras, M.; Sastre, R.; Arbeloa, F. L.; Prieto, J. B.; Arbeloa, I. L. *J. Photochem. Photobiol., A* **2008**, *198*, 192.
- (79) Shimizu, S.; Watanabe, N.; Kataoka, T.; Shoji, T.; Abe, N.; Morishita, S.; Ichimura, H. In *Ullmann's Encyclopedia of Industrial Chemistry*; Wiley-VCH Verlag GmbH & Co. KGaA: 2000.
- (80) Rurack, K.; Kollmannsberger, M.; Daub, J. *New J. Chem.* **2001**, *25*, 289.
- (81) Coskun, A.; Akkaya, E. U. *Tetrahedron Lett.* **2004**, *45*, 4947.

- (82) Knoevenagel, E. *Berichte der deutschen chemischen Gesellschaft* **1898**, *31*, 2596.
- (83) Lee, J.-S.; Kang, N.-y.; Kim, Y. K.; Samanta, A.; Feng, S.; Kim, H. K.; Vendrell, M.; Park, J. H.; Chang, Y.-T. *J. Am. Chem. Soc.* **2009**, *131*, 10077.
- (84) Yu, Y.-H.; Descalzo, A. B.; Shen, Z.; Röhr, H.; Liu, Q.; Wang, Y.-W.; Spieles, M.; Li, Y.-Z.; Rurack, K.; You, X.-Z. *Chem. Asian. J.* **2006**, *1*, 176.
- (85) Baruah, M.; Qin, W.; Flors, C.; Hofkens, J.; Vallée, R. A. L.; Beljonne, D.; Van der Auweraer, M.; De Borggraeve, W. M.; Boens, N. *J. Phys. Chem. A* **2006**, *110*, 5998.
- (86) Rurack, K.; Kollmannsberger, M.; Daub, J. *Angew. Chem., Int. Ed.* **2001**, *40*, 385.
- (87) Buyukcakil, O.; Bozdemir, O. A.; Kolemen, S.; Erbas, S.; Akkaya, E. U. *Org. Lett.* **2009**, *11*, 4644.
- (88) Zhu, S.; Zhang, J.; Vegesna, G.; Tiwari, A.; Luo, F.-T.; Zeller, M.; Luck, R.; Li, H.; Green, S.; Liu, H. *RSC Advances* **2012**, *2*, 404.

CHAPTER 2

BODIPY-DERIVED PHOTOREMOVABLE PROTECTING GROUPS UNMASKED WITH GREEN LIGHT

Taken in part from: **Goswami, P. P.**; Syed, A; Beck, C.L.; Albright T.R.; Mahoney, K. M.; Unash, R.; Smith, S.A.; Winter, A. H., *J. Am. Chem. Soc.* **2015**, 137(11), 3783-3786

Introduction

Photoremovable protecting groups, sometimes called photocages or phototriggers, are popular light-sensitive chemical moieties that mask substrates through covalent linkages that render the substrates inert. Upon irradiation, the masked substrates are released, restoring their reactivity or function. While photocages have important applications in areas such as organic synthesis,¹⁻³ photolithography,^{4,5} and light-responsive organic materials,⁶⁻⁸ these structures are particularly prized for their ability to trigger biological activity with high spatial and temporal resolution⁹⁻¹³. Examples of such chemical tools include photocaged proteins,¹⁴⁻¹⁶ nucleotides,^{17,18} ions,¹⁹⁻²³ neurotransmitters,^{24,25} pharmaceuticals,^{26,27} fluorescent dyes,²⁸⁻³⁰ and small molecules^{31,32} (e.g., caged ATP). These biologically relevant caged molecules and ions can be released from the caging structure within particular biological microenvironments using pulses of focused light. The most popular photocages used in biological studies are the *o*-nitrobenzyl systems³¹⁻³³ and their derivatives, but other photocages that see significant use include those based on the phenacyl,³⁴ acridinyl,³⁵ benzoinyl,^{36,37} coumarinyl,³⁸ xanthenyl,³⁹ and *o*-hydroxynaphthyl structures.⁴⁰ Unfortunately, with few exceptions described below,^{41,42} a serious limitation of most popular photocages is that they absorb mostly in the ultraviolet where the limited

penetration of UV light into tissues largely restricts these studies to fixed cells and thin tissue slices. Furthermore, prolonged exposure of cells or tissues to UV light can lead to cellular damage or death.

Consequently, new photocaging structures that absorb visible light are urgently needed. Advantages of visible light irradiation include diminished phototoxicity compared to UV light and deeper optical penetration into tissue. Additionally, visible light photolysis can be performed with cheap lamps and Pyrex glassware, while UV photolysis requires expensive UV sources. Unfortunately, the major problem that has hindered the development of new photocages that absorb visible light is the lack of a structure-reactivity relationship for excited state heterolysis. That is, it is difficult to predict a priori which structures, when irradiated with light, will undergo an efficient photoheterolysis reaction. Thus, attempts to prepare visible light absorbing photocages have mostly bypassed this problem by using metal-ligand photoreleasing systems⁴²⁻⁴⁴ or by using creative indirect schemes. Examples of such creative schemes include upconverting nanoparticles with surface-attached UV-absorbing photocages,⁴⁵⁻⁴⁷ using two photon uncaging⁴⁸⁻⁵⁰ or release mediated by photoinduced electron transfer with a sacrificial electron donor.⁵¹

However, visible light absorbing organic structures that offer simple photorelease schemes and structures would potentially make a more compelling case for widespread use in biologically-oriented labs.⁵² A recent computational study performed in our lab suggested the hypothesis that photoheterolysis reactions may be under conical intersection control.⁵³ That is, photoheterolysis of C-LG (carbon—leaving group) bonds to generate ion pairs⁵⁴ may be favored if the ion pair has access to a nearby productive conical intersection that provides an efficient channel for the excited state of the photoprecursor to decay to the

ground-state ion pair. Because conical intersections are challenging to compute, we further suggested using the vertical energy gap of the carbocation to its first excited state as a simple predictor of a nearby conical intersection (CI). A low S_0 - S_1 energy gap of the cation would suggest the possibility of a nearby CI between the S_0 and S_1 surfaces, and the potential for a productive mechanistic channel for the photochemistry to proceed from the excited state of the photocaged precursor to the ion pair.

Thus, to find visible light absorbing photocages, we searched for potential photocaging structures that would generate carbocations with low-lying diradical states. A time-dependent density functional theory (TD-DFT) computational investigation of carbocations attached to the BODIPY scaffold at the meso position indicated that these ions have low-lying excited states. For example, the TD-DFT computed S_0 - S_1 vertical energy gap of the carbocation derived from C-O scission of **2** is 8 kcal/mol (TD-B3LYP/6-311+G (2d,p)), suggesting a near-degenerate diradical configuration. Indeed, all of the cations derived from C-O scission of **1-6** have vertical gaps < 13 kcal/mol (see Appendix A for computational details), and have singlet states with considerable diradical character. Large singlet stabilizations upon switching from restricted \rightarrow spin-purified unrestricted singlet computations indicate that the singlet states can be described as diradicals or possessing considerable diradical character (see Appendix A for details). Thus, the exact vertical energies from the TD-DFT computations are to be viewed with suspicion, but it is clear that there are low-energy diradical forms for these ions, suggesting a CI between the closed-shell singlet and singlet diradical forms of the carbocations in the vicinity of the ion pair geometry. Further, the singlet-triplet gaps of all the carbocations derived from **1-6** are \sim 5 kcal/mol in favor of the triplet state, suggesting that the “carbocations” produced by

heterolysis of **1-6** may in fact be better described as ion diradicals in their thermodynamic ground state than by traditional closed-shell carbocation structures.⁵⁵

Encouraged by these computational studies, we synthesized structures **1-6** as photocages for acetic acid. Advantages of the BODIPY scaffold include simple syntheses, a compact structure, known biological compatibility,⁵⁶ and high extinction coefficients in the visible.⁵⁷ Other studies have shown BODIPYs can be used as laser dyes⁵⁸ and have photochemical reactivity at boron.⁵⁹ Photorelease studies, described below, indicate that these structures release carboxylic acids upon photolysis with wavelengths >500 nm.

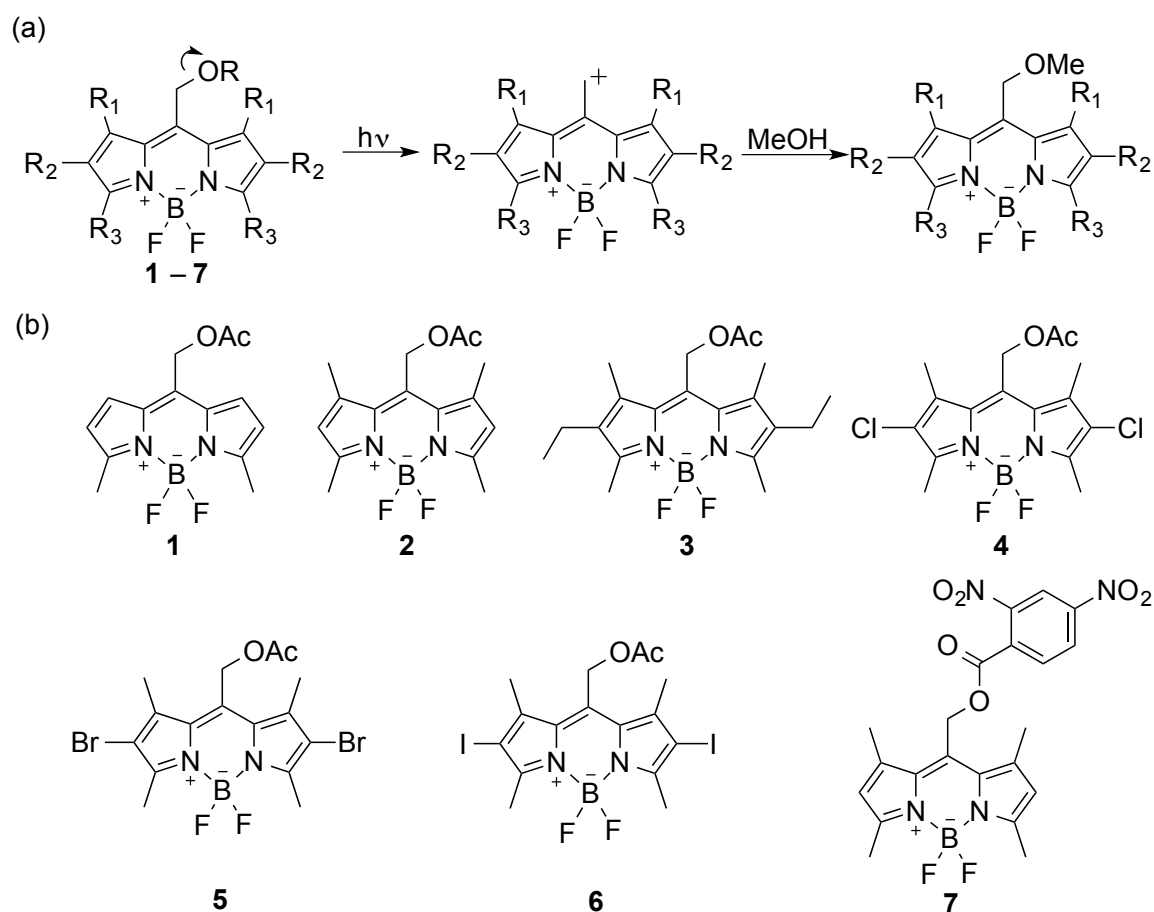


Figure 2.1 (a) Possible pathway for the photolysis of photocaged acetic acid; (b) Substrates described in this study.

Photorelease studies and quantum efficiencies. The observed substrate release rate as a function of photolysis time is quantified by the quantum efficiency parameter ($\epsilon \Phi$), which is the product of the extinction coefficient at the irradiation wavelength (ϵ) and the quantum yield of release (Φ). Extinction coefficients for **1-6** were determined by UV-Vis spectroscopy (see Table 1). To compute the quantum yields of photorelease (Φ), the flux of a 532 nm laser excitation beam (ND:YAG, 1st harmonic) was determined using potassium ferrioxalate actinometry. Release of acetic acid as a function of laser irradiation time in MeOH was followed by quantitative LC/UV (see SI for details). Each quantum yield reported is the average of 3 separate runs. Identical actinometry measurements performed after photolysis demonstrated high flux stability of the laser. Additionally, repeating the quantum yield measurement for **2** on a different day with a different laser power setting (in triplicate) gave essentially the same value for the quantum yield, indicating reproducibility. A preparative photolysis of **2** in MeOH gave a meso-substituted methyl ether adduct as a stable photoproduct of the photocaging moiety, suggestive of solvent trapping of an intermediate carbocation. Additionally, lamp photolysis of **2** showed no major difference in release of acetic acid under argon or air atmosphere. Curiously, unlike **1-4** and **6**, the brominated compound **5** was found to be unstable. It decomposes after 1 day stored on the shelf in the dark, and photolysis of freshly prepared and purified **5** led to secondary products in addition to acetic acid release, and photolysis was accompanied by rapid solution bleaching. Consequently, we were not confident in our quantum yield measurements for **5** and excluded it from **Table 2.1**. Probably, **5** also has access to alternative photochemical pathways (e.g., C-Br homolysis) and thermal degradation channels similar to benzyl based photocages which include bromine.⁶⁰

Photocaged compounds **1-4** and **6** are thermally stable in the dark. Boiling these compounds in MeOH for 1 h in a foil-wrapped vessel led to no change in the ¹H NMR spectrum.

In general, the quantum efficiencies for **1-4** and **6** are lower or comparable with the popular caged *o*-nitrobenzyl or coumarinyl systems.⁹ Quantum yields for **1-4** are lower than those for typical *o*-nitrobenzyl photocaged structures or coumarinyl systems, but this lower quantum yield is compensated by the much higher extinction coefficients of the BODIPY chromophores compared to the *o*-nitrobenzyl chromophore, leading to reasonable quantum efficiencies. The iodinated derivative **6** has the largest quantum efficiency, comparable to that of some caged *o*-nitrobenzyl systems, but with a λ_{max} at ~550 nm rather than in the UV (the parent *o*-nitrobenzyl system has a λ_{max} of ~280 nm while a popular dimethoxy analog has a λ_{max} of ~350 nm), although still much lower than the best known photocaging systems. A plausible explanation for the higher quantum yield of **6** is that the iodine atoms promote intersystem crossing (ISC) to a triplet state, which are usually longer lived than singlet excited states, giving more time for release. For example, the phenacyl photocage derivatives described by Givens undergo photorelease in the triplet state.³⁴ The plausibility of a rapid ISC event is supported by the very weak fluorescence of solutions of **5** and **6**, compared to solutions of **1-4**.

Table 2.1. Optical properties and quantum efficiencies of 1-6. Quantum yields of acetic acid release (Φ) determined by ferrioxalate actinometry in MeOH with a 532 nm ND:YAG laser source and release followed using quantitative LC-UV (Φ values are the average of 3 runs).

	λ_{\max} (nm)	λ_{em} (nm)	ϵ ($\times 10^4 \text{ M}^{-1} \text{ cm}^{-1}$)	Φ ($\times 10^{-4}$)	$\epsilon \Phi$ ($\text{M}^{-1} \text{ cm}^{-1}$)
1	519	527	5.7	6.4	37
2	515	526	7.1	9.9	70
3	544	560	6.2	9.5	59
4	544	570	4.8	4.0	19
5	545	575	--	--	--
6	553	576	4.9	23.8	117

Optical properties of 1-6.

The UV-Vis spectra and fluorescence spectra of **1-6** are shown in **Figure 2.2**. These structures absorb between 515 nm and 553 nm (and emit between 520 nm and 580 nm), typical of simple BODIPY dyes, and feature large extinction coefficients ($\sim 50,000$ - $70,000 \text{ M}^{-1} \text{ cm}^{-1}$).

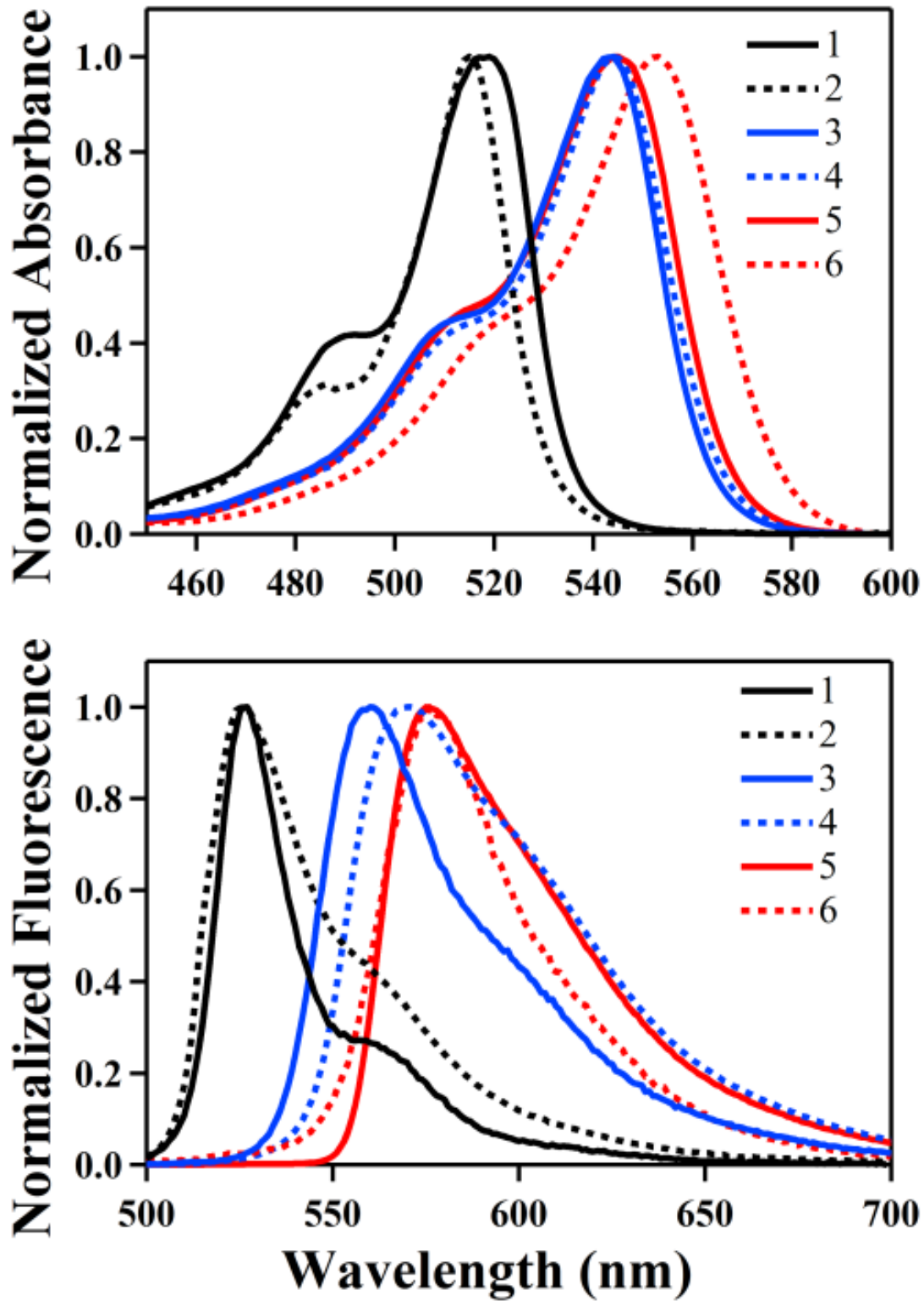


Figure 2.2 Normalized absorbance and fluorescence spectra of 1-6.

Cell Studies:

To test the viability and usefulness of the BODIPY derived photocages in biological systems, compound **7** was synthesized. 2,4-dinitrobenzoic acid is a known⁶¹ fluorescence quencher for BODIPY dyes. This quencher was coupled with our BODIPY moiety using a standard DCC/DMAP ester coupling reaction. We anticipated that **7** would be weakly fluorescent, but upon photorelease of the quencher the fluorescence would increase. Indeed, when **7** was irradiated with a mercury lamp (excitation = 500 nm) in a cuvette and its fluorescence was plotted over time (**Figure 2.3 N**), there was a growth in fluorescence attributed to release of the quencher. Photorelease of the quencher was confirmed by ¹H NMR photolysis studies. As a control, similar steady state fluorescence measurements were performed over time for compound **7** in the dark without light exposure, leading to essentially no change in fluorescence.

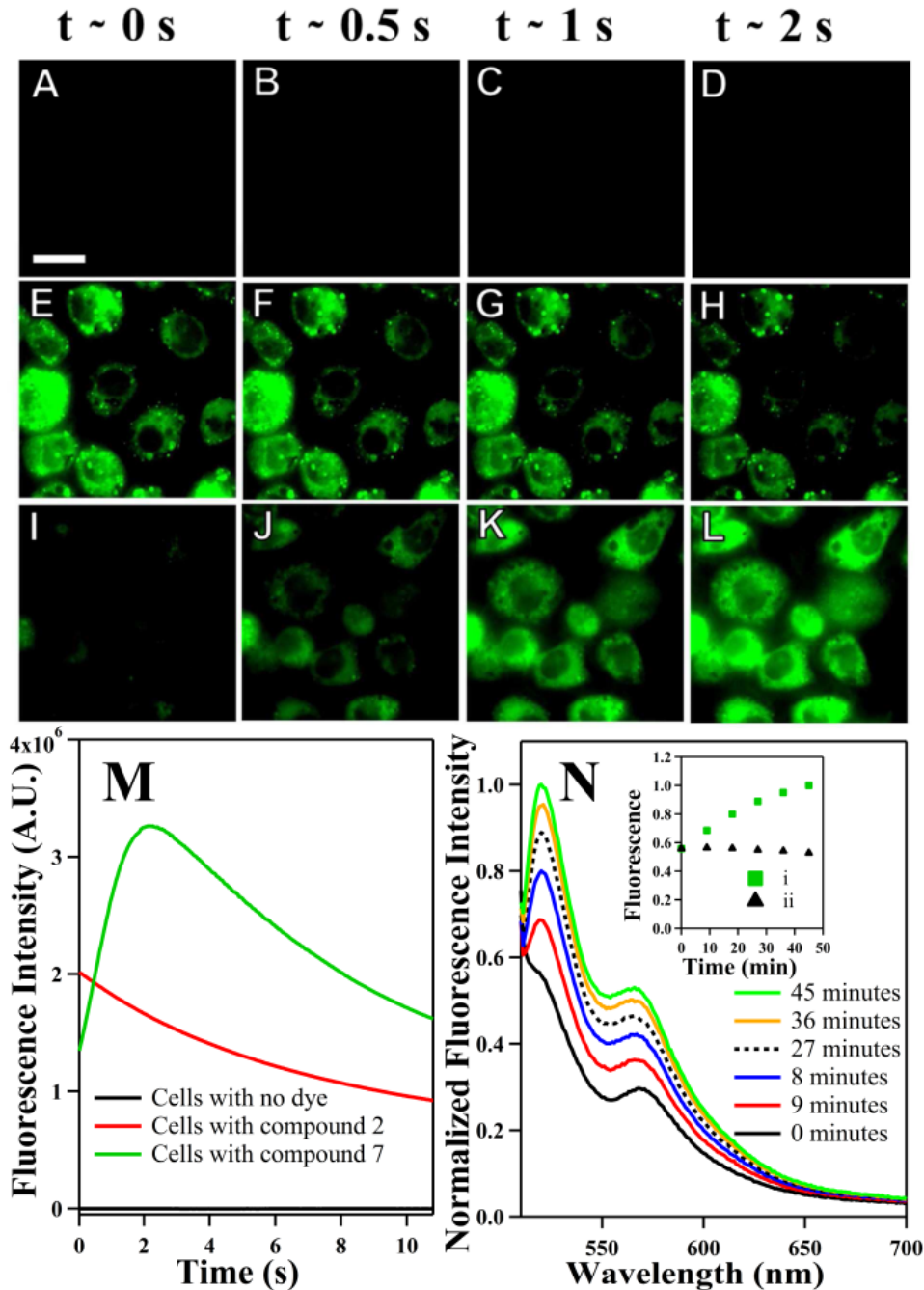


Figure 2.3 Fluorescence images of S2 cells with no BODIPY compound (A-D), cells incubated with compound 2 (E-H) and cells incubated with compound 7 (I-L) as a function of irradiation time (top). Scale bar is $20 \mu\text{m}$ (shown in panel A) and is the same for all the images. Images were adjusted to same contrast in each row. Average of at least 32 cells fluorescence intensity profile versus irradiation time using 100% lamp power for excitation in cells (M). Increase in free BODIPY fluorescence signal over time with quencher release from compound 7 in BES buffer (N). Plot insert (N) depicts the difference in growth of fluorescence vs time for compound 7 with (i) and without (ii) light irradiation in a cuvette.

Compound **2** and **7** were then incubated with *Drosophila* S2 cells and monitored using fluorescence microscopy (**Figure 2.3 A-L**). The *Drosophila* S2 cells loaded with **2** and **7** were irradiated continuously with 500 nm light. Fluorescence images were collected every 36 ms for a total of 10.8 seconds. The fluorescence intensity for compound **7** inside cell as shown in **Figure 2.3I-L** increases rapidly. This increase in fluorescence can be attributed to the release of the quencher. The same fluorescence study with **2** as a control in **Figure 2.3E-H** shows no such increase in fluorescence. For **2**, the leaving group is acetate, which is not a quencher. Thus, little change in the fluorescence would be anticipated upon photorelease of acetic acid from this moiety. The background decay in fluorescence for both **2** and **7** can be attributed to photobleaching under the intense focused light. Parts **A-D** of **Figure 2.3** show that there is a minimal change in fluorescence of cells when they are irradiated without being loaded with compound **2** or **7**. **Figure 2.3M** shows the fluorescence intensity change over time for cells incubated with compound **2**, **7**, and the control experiments without any compound.

Cytotoxicity of compounds were measured with trypan blue exclusion assay. All values are normalized with the control cells which were not incubated with any compound. At a compound concentration of 25 μM , 97% for compound **2** and 92% for compound **7** remained viable after 1h.

Conclusion

BODIPY-derived photocages unmask carboxylic acids with green light excitation >500 nm and photocleavage can be carried out in living cells. These photocages are promising alternatives for the popular *o*-nitrobenzyl photocaging systems, being easy to synthesize,

utilizing a biocompatible chromophore, and having superior optical properties to the most popular photocages in current use. More generally, our strategy of identifying new photocages by searching for carbocations with low-energy diradical states seems to be a promising one. BODIPY derivatives that release functional groups other than carboxylic acids and that have red-shifted absorptions into the biological window (~600-1000 nm) are currently under investigation.

REFERENCES

- (1) Wuts, P. G. M.; Greene, T. W. *Greene's Protective Groups in Organic Synthesis*; Wiley, 2006.
- (2) Barltrop, J. A.; Schofield, P. *Tetrahedron Lett.* **1962**, *3*, 697.
- (3) Patchornik, A.; Amit, B.; Woodward, R. B. *J. Am. Chem. Soc.* **1970**, *92*, 6333.
- (4) Wöll, D.; Laimgruber, S.; Galetskaya, M.; Smirnova, J.; Pfeleiderer, W.; Heinz, B.; Gilch, P.; Steiner, U. E. *J. Am. Chem. Soc.* **2007**, *129*, 12148.
- (5) Woll, D.; Lukzen, N.; Steiner, U. E. *Photochem. Photobiol. Sci.* **2012**, *11*, 533.
- (6) Pawle, R. H.; Eastman, V.; Thomas, S. W. *J. Mater. Chem.* **2011**, *21*, 14041.
- (7) Park, B. S.; Lee, H. M. *Bull. Korean Chem. Soc.* **2008**, *29*, 2054.
- (8) Hensarling, R. M.; Hoff, E. A.; LeBlanc, A. P.; Guo, W.; Rahane, S. B.; Patton, D. L. *J. Polym. Sci., Part A: Polym. Chem.* **2013**, *51*, 1079.
- (9) Klán, P.; Šolomek, T.; Bochet, C. G.; Blanc, A.; Givens, R.; Rubina, M.; Popik, V.; Kostikov, A.; Wirz, J. *Chem. Rev.* **2012**, *113*, 119.
- (10) Ellis-Davies, G. C. R. *Nat Meth* **2007**, *4*, 619.
- (11) Specht, A.; Bolze, F. d. r.; Omran, Z.; Nicoud, J. Ä. B.; Goeldner, M. *HFSP J* **2009**, *3*, 255.
- (12) Yu, H.; Li, J.; Wu, D.; Qiu, Z.; Zhang, Y. *Chem. Soc. Rev.* **2010**, *39*, 464.
- (13) Mayer, G.; Heckel, A. *Angew. Chem., Int. Ed.* **2006**, *45*, 4900.
- (14) Zhao, J.; Lin, S.; Huang, Y.; Zhao, J.; Chen, P. R. *J. Am. Chem. Soc.* **2013**, *135*, 7410.
- (15) Lawrence, D. S. *Curr. Opin. Chem. Biol.* **2005**, *9*, 570.
- (16) Riggsbee, C. W.; Deiters, A. *Trends Biotechnol.* **2010**, *28*, 468.
- (17) Pirrung, M. C. *Chem. Rev.* **1997**, *97*, 473.
- (18) Chee, M.; Yang, R.; Hubbell, E.; Berno, A.; Huang, X. C.; Stern, D.; Winkler, J.; Lockhart, D. J.; Morris, M. S.; Fodor, S. P. *Science* **1996**, *274*, 610.
- (19) Priestman, M. A.; Lawrence, D. S. *Biochim. Biophys. Acta* **2010**, *1804*, 547.
- (20) Gomez, T. M.; Spitzer, N. C. *Nature* **1999**, *397*, 350.

- (21) Zucker, R. In *Methods in Cell Biology*; Richard, N., Ed.; Academic Press: 1994; Vol. Volume 40, p 31.
- (22) Mbatia, H. W.; Dhammika Bandara, H. M.; Burdette, S. C. *Chem. Commun.* **2012**, *48*, 5331.
- (23) Bandara, H. M. D.; Walsh, T. P.; Burdette, S. C. *Chem. Eur. J.* **2011**, *17*, 3932.
- (24) Sjulson, L.; Miesenburg, G. *Chem. Rev.* **2008**, *108*, 1588.
- (25) Kramer, R. H.; Chambers, J. J.; Trauner, D. *Nat. Chem. Biol.* **2005**, *1*, 360.
- (26) Katz, J. S.; Burdick, J. A. *Macromol. Biosci.* **2010**, *10*, 339.
- (27) Lin, C.-C.; Anseth, K. *Pharm. Res.* **2009**, *26*, 631.
- (28) Puliti, D.; Warther, D.; Orange, C.; Specht, A.; Goeldner, M. *Bioorg. Med. Chem.* **2011**, *19*, 1023.
- (29) Li, W.-h.; Zheng, G. *Photochem. Photobiol. Sci.* **2012**, *11*, 460.
- (30) Fukaminato, T. *J. Photochem. Photobiol.* **2011**, *12*, 177.
- (31) Kaplan, J. H.; Forbush, B.; Hoffman, J. F. *Biochemistry* **1978**, *17*, 1929.
- (32) Engels, J.; Schlaeger, E. J. *J. Med. Chem.* **1977**, *20*, 907.
- (33) Ciamician, G.; Silbert, P. *Chem. Ber.* **1901**, *34*, 2040.
- (34) Anderson, J. C.; Reese, C. B. *Tetrahedron Lett.* **1962**, *3*, 1.
- (35) Ackmann, A. J.; Frechet, J. M. J. *Chem. Commun.* **1996**, 605.
- (36) Sheehan, J. C.; Wilson, R. M. *J. Am. Chem. Soc.* **1964**, *86*, 5277.
- (37) Sheehan, J. C.; Wilson, R. M.; Oxford, A. W. *J. Am. Chem. Soc.* **1971**, *93*, 7222.
- (38) Givens, R. S.; Matuszewski, B. *J. Am. Chem. Soc.* **1984**, *106*, 6860.
- (39) Šebej, P.; Wintner, J.; Müller, P.; Slanina, T.; Al Anshori, J.; Antony, L. A. P.; Klán, P.; Wirz, J. *J. Org. Chem.* **2013**, *78*, 1833.
- (40) Arumugam, S.; Popik, V. V. *J. Am. Chem. Soc.* **2009**, *131*, 11892.
- (41) Pastierik, T.; Šebej, P.; Medalová, J.; Štacko, P.; Klán, P. *J. Org. Chem.* **2014**, *79*, 3374.

- (42) Pal, A. K.; Nag, S.; Ferreira, J. G.; Brochery, V.; La Ganga, G.; Santoro, A.; Serroni, S.; Campagna, S.; Hanan, G. S. *Inorg. Chem.* **2014**, *53*, 1679.
- (43) Smith, W. J.; Oien, N. P.; Hughes, R. M.; Marvin, C. M.; Rodgers, Z. L.; Lee, J.; Lawrence, D. S. *Angew Chem Int Ed Engl* **2014**, *53*, 10945.
- (44) Shell, T. A.; Shell, J. R.; Rodgers, Z. L.; Lawrence, D. S. *Angew. Chem., Int. Ed.* **2014**, *53*, 875.
- (45) Li, W.; Wang, J.; Ren, J.; Qu, X. *J. Am. Chem. Soc.* **2014**, *136*, 2248.
- (46) Auzel, F. B. *Chem. Rev.* **2003**, *104*, 139.
- (47) Yang, Y.; Shao, Q.; Deng, R.; Wang, C.; Teng, X.; Cheng, K.; Cheng, Z.; Huang, L.; Liu, Z.; Liu, X.; Xing, B. *Angew. Chem., Int. Ed.* **2012**, *51*, 3125.
- (48) Tran, C.; Gallavardin, T.; Petit, M.; Slimi, R.; Dhimane, H.; Blanchard-Desce, M.; Acher, F. C.; Ogden, D.; Dalko, P. I. *Org. Lett.* **2015**, *17*, 402.
- (49) Brown, E. B.; Shear, J. B.; Adams, S. R.; Tsien, R. Y.; Webb, W. W. *Biophys. J.* **1999**, *76*, 489.
- (50) Weissleder, R. *Nat Biotech* **2001**, *19*, 316.
- (51) Falvey, D. E.; Sundararajan, C. *Photochem. Photobiol. Sci.* **2004**, *3*, 831.
- (52) Jacques, S. L. *Phys Med Biol* **2013**, *58*, R37.
- (53) Buck, A. T.; Beck, C. L.; Winter, A. H. *J. Am. Chem. Soc.* **2014**, *136*, 8933.
- (54) DeCosta, D. P.; Pincock, J. A. *J. Am. Chem. Soc.* **1989**, *111*, 8948.
- (55) Little, R. D.; Brown, L. M.; Masjedizadeh, M. R. *J. Am. Chem. Soc.* **1992**, *114*, 3071.
- (56) Choyke, P. L.; Alford, R.; Simpson, H. M.; Duberman, J.; Hill, G. C.; Regino, O.; Celeste, M.; Hisataka, K. *Mol. Imaging* **2009**, *8*, 1536.
- (57) Umezawa, K.; Matsui, A.; Nakamura, Y.; Citterio, D.; Suzuki, K. *Chem. Eur. J.* **2009**, *15*, 1096.
- (58) Amat-Guerri, F.; Liras, M.; Carrascoso, M. L.; Sastre, R. *Photochem. Photobiol.* **2003**, *77*, 577.

- (59) Umeda, N.; Takahashi, H.; Kamiya, M.; Ueno, T.; Komatsu, T.; Terai, T.; Hanaoka, K.; Nagano, T.; Urano, Y. *ACS Chem. Biol.* **2014**, *9*, 2242.
- (60) Ma, J.; Rea, A. C.; An, H.; Ma, C.; Guan, X.; Li, M.-D.; Su, T.; Yeung, C. S.; Harris, K. T.; Zhu, Y.; Nganga, J. L.; Fedoryak, O. D.; Dore, T. M.; Phillips, D. L. *Chem. Eur. J.* **2012**, *18*, 6854.
- (61) Kobayashi, T.; Komatsu, T.; Kamiya, M.; Campos, C.; González-Gaitán, M.; Terai, T.; Hanaoka, K.; Nagano, T.; Urano, Y. *J. Am. Chem. Soc.* **2012**, *134*, 11153.

CHAPTER 3

SHIFTING BODIPY PHOTOREMOVABLE GROUPS INTO THE RED

Taken in part from: Mahoney, K. M.; **Goswami P. P.**, Albright, T. R.; Syed, A.; Smith, E. A.; Winter, A. H. **2015**, manuscript in preparation.

INTRODUCTION

Photoremovable protecting groups (also known as photocages, phototriggers, photoreleasable and photocleavable protecting groups) are light-sensitive moieties that allow for spatial and temporal control over the release of a masked substrate by light-induced cleavage of a covalent PPG-substrate bond resulting in the restoration the substrate's function. Photocages are particularly useful for the release of biologically relevant substrates, such as proteins,¹⁻³ nucleotides,^{4,5} ions,⁶⁻¹⁰ neurotransmitters,¹¹⁻¹² pharmaceuticals,¹³⁻¹⁴ and fluorescent dyes,¹⁵⁻¹⁷ and small molecules.^{18,19}

The most popular photocages used in biological studies are *o*-nitrobenzyl^{31,33} and derivatives, but others include those based on the phenacyl,²¹ acridinyl,²² benzoinyl,^{23,24} coumarinyl,²⁵ and *o*-hydroxynaphthyl²⁶ structures. A major limitation to many of these photocages and especially to the popular *o*-nitrobenzyl photocages is that they absorb in the ultraviolet region of the spectrum where tissue penetration is limited restricting studies for fixed cells and thin tissue slices. In addition, exposure of the cells or tissues to UV light can lead to cellular damage or death.

Recently, our lab developed a new class of protecting group derived from *meso*-substituted BODIPY dyes with heterolytic bond cleavage occurring at green wavelengths >500 nm.²⁷ This BODIPY structure was first computationally explored to suggest it would undergo heterolytic bond cleavage in the excited²⁹ and was then empirically investigated. This is the

first example of a rationally designed photocage releasing a cargo molecule using visible light making meso-substituted BODIPY dyes a promising alternative to the popular *o*-nitrobenzyl photocage systems. A photocage which cleaves within the biological window of light would be exceptionally valuable for cell and tissue studies. The biological window identifies the range of wavelengths from 650 nm to 1130 nm where light can more efficiently penetrate biological tissue because these tissues scatter and absorb less light at longer wavelengths.²⁸

It has been well-established that extending the conjugation of BODIPY dyes allows for a red-shift in absorption maximum.³⁰ Here, we use a Knoevenagel condensation reaction to extend the conjugation on the highly-acidic 3,5-methyl groups of our previously synthesized BODIPY photocage structure.

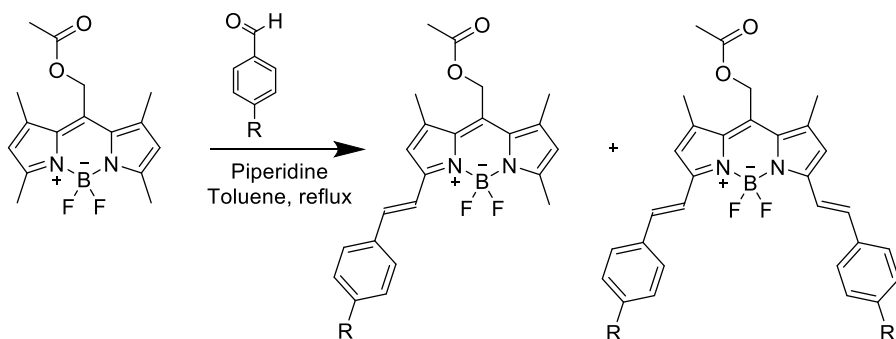


Figure 3.1 Knoevenagel condensation reaction was used to red shift the absorption maximum of BODIPY **2** from Chapter 3

The following photocages were prepared:

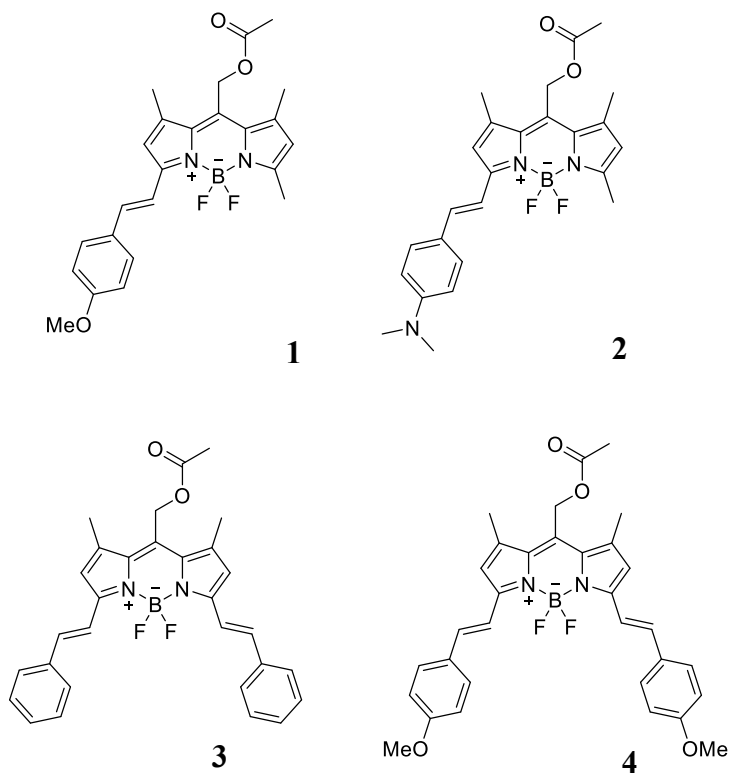


Figure 3.2 BODIPY photocages with extended conjugation

RESULTS AND DISCUSSION

To demonstrate that **1-4** could indeed release acetic acid during light irradiation, NMR was used to follow the release progress over time.

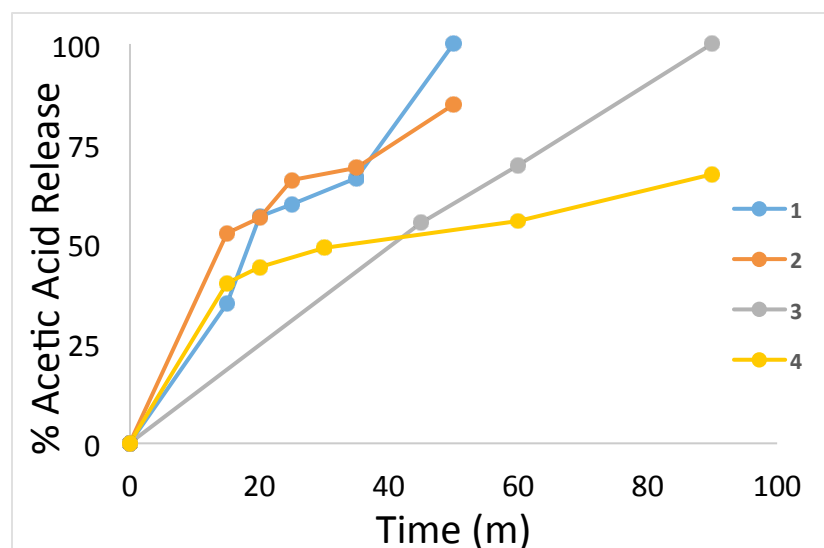


Figure 3.3 Release of acetic acid over time. 2 mM NMR samples were prepared and irradiated with a Xenon lamp.

The thermal stability of the dyes was tested by heating to 60 °C for 1 hour in the dark. No acetic acid release was observed.

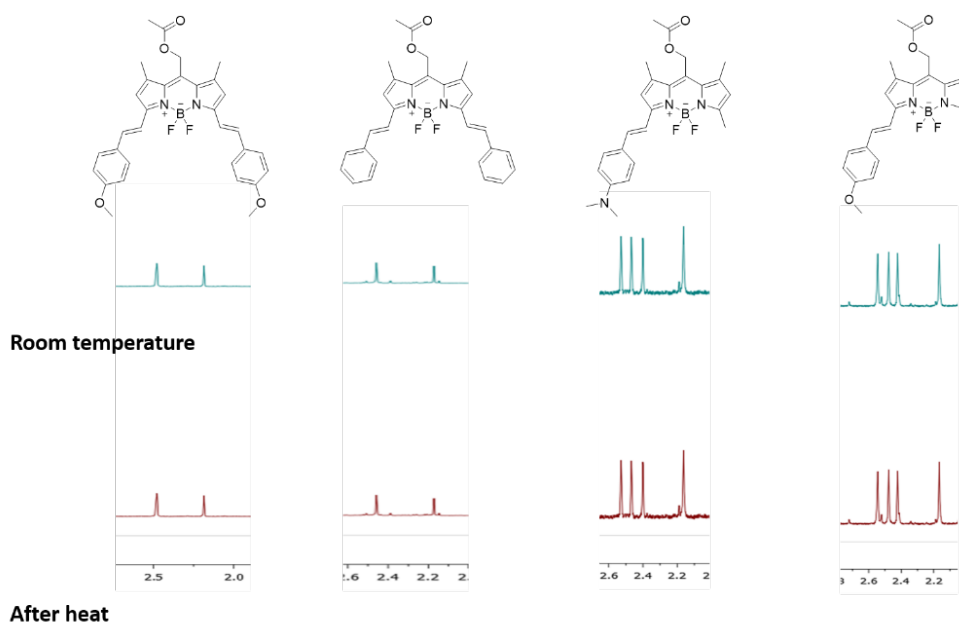


Figure 3.4 Thermal stability test of 1-4; NMR scans were taken at room temperature (blue) and the samples were heated for one hour at 60 °C and NMR was taken again (red); No

acetic acid (2.04 ppm) release was observed. The NMR spectrum has been cropped for clarity. However, there was no change in any NMR peaks after heating.

The optical properties of **1-4** are shown in **Figure 3.5**. The absorption maxima of the compounds range from 586 nm to 661 nm and the fluorescence ranges from 607-684 nm. Photocages **2-4**, absorb within the biological window of visible light making them powerful alternatives the *o*-nitrobenzyl photocage which absorbs in the UV. The extinction coefficients of the photocages are $\sim 60,000 \text{ M}^{-1} \text{ cm}^{-1}$. The quantum yields are a bit lower than the BODIPY dyes from Chapter 3. These values are relatively low, however, the high extinction coefficients of **1-4** make the quantum efficiencies similar to that of the popular *o*-nitrobenzyl photocages.

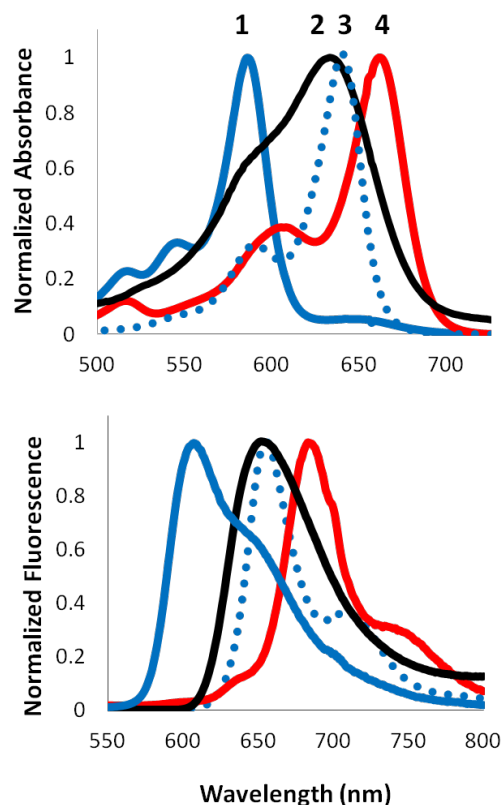


Figure 3.5 Normalized absorption and fluorescence spectra of compounds **1-4**

Table 3.1. Absorption (λ_{\max}) and fluorescence (λ_{em}) maxima, extinction coefficients (ϵ), quantum yields (Φ) and quantum efficiencies ($\epsilon \Phi$) of compounds 1-4.

	λ_{\max} (nm)	λ_{em} (nm)	ϵ ($\times 10^4 \text{ M}^{-1} \text{ cm}^{-1}$)	Φ ($\times 10^{-5}$)	$\epsilon \Phi$ ($\text{M}^{-1} \text{ cm}^{-1}$)
1	586	607	6.1	9.8	6.0
2	633	650	6.0	6.9	4.1
3	640	656	6.5	4.5	2.9
4	661	684	6.5	4.1	2.7

Work is currently underway to take **4** and replace the acetate leaving group with the 3,5 - dinitrobenzoic acid fluorescence quencher as seen in Compound **7** from Chapter 2. Similar biological studies within S2 cells are to be performed.

EXPERIMENTAL

Synthesis of Compound 1. 8-Acetoxymethyl-1,3,5,7-tetramethyl pyrromethene fluoroborate (50 mg, 0.016 mmol, 1 equiv.) and 4-methoxybenzaldehyde (4.4 mg, 0.032 mmol, 2 equiv.) were added to 8 mL of ethanol which had been previously dried over 3 Å molecular sieves for 24 h. This suspension was then placed in a dry, glass microwave reaction vessel. Both acetic acid (120 μL) and piperidine (120 μL) were then added and the vessel was sparged with argon. The microwave vessel was irradiated for 10 min at 113°C and 800 W. The solvent was evaporated under reduced pressure. The solid residue was loaded onto a silica gel flash column and eluted with 50:50 hexanes:ethyl acetate. The dark purple product was recovered and further purified using a prep TLC plate and 80:20 hexanes:ethyl acetate. The product was obtained in 58% yield (32 mg, 0.009 mmol).

^1H NMR (400 MHz, CDCl_3): δ = 7.55 (d, J = 4 Hz, 2H), 7.52 (d, J = 8 Hz, 1H), 7.24 (d, J = 8 Hz, 1H), 6.91 (d, J = 4 Hz, 2H), 6.71 (s, 1H), 6.11 (s, 1H), 5.33 (s, 2H), 3.85 (s, 3H), 2.58 (s, 3H), 2.43 (s, 3H), 2.28 (s, 3H), 2.15 (s, 3H) ppm; ^{13}C NMR (200 MHz, CDCl_3): δ = 170.77, 160.84, 155.56, 154.57, 141.15, 140.41, 137.32, 135.35, 134.46, 132.94, 131.39, 129.37, 122.18, 118.87, 116.95, 114.45, 58.16, 55.24, 20.82, 16.05, 15.74, 14.94 ppm; Hi-res MS (ESI) for formula $\text{C}_{24}\text{H}_{25}\text{BF}_2\text{N}_2\text{O}_3$, Calc. 438.2035, Found 438.2038.

Synthesis of Compound 2. 8-Acetoxymethyl-1,3,5,7-tetramethyl pyrromethene fluoroborate (50 mg, 0.016 mmol, 1 equiv..) and 4-(dimethylamino)benzaldehyde (4.8 mg, 0.032 mmol, 2 equiv.) were added to 8-mL of ethanol which had been previously dried over 3 Å molecular sieves for 24 hours. This suspension was then placed in a microwave reaction vessel. Both acetic acid (120 μL) and piperidine (120 μL) were then added and the vessel was sparged with argon. The microwave vessel was irradiated for 20 minutes at 113 °C and 800 W. The solvent was evaporated under reduced pressure. The solid residue was loaded onto a silica gel flash column and eluted with 80:20 hexanes:ethyl acetate to give 9.1 mg of **2** as a dark blue solid (24% yield). ^1H NMR (400 MHz, CDCl_3): δ = 7.50 (d, J = 8 Hz, 2H), 7.45 (d, J = 16 Hz, 1H), 7.24 (d, J = 16 Hz, 1H), 6.72 (s, 1H), 6.68 (d, J = 8 Hz, 2H), 6.07 (s, 1H), 5.32 (s, 2H), 3.04 (s, 6H), 2.57 (s, 3H), 2.41 (s, 3H), 2.36 (s, 3H), 2.15 (s, 3H) ppm; ^{13}C NMR (200 MHz, CDCl_3): δ = 170.85, 156.07, 153.42, 151.41, 141.39, 139.20, 138.64, 134.93, 132.28, 129.70, 124.56, 121.37, 119.21, 114.25, 112.12, 58.31, 40.36, 24.02, 20.85, 16.12, 15.60 ppm; Hi-res MS (ESI) for formula $\text{C}_{25}\text{H}_{28}\text{BF}_2\text{N}_3\text{O}_2$, Calc. 451.2352, Found 451.2339.

Synthesis of Compound 3. 8-Acetoxymethyl-1,3,5,7-tetramethyl pyrromethene fluoroborate (50 mg, 0.016 mmol, 1 equiv.) and benzaldehyde (3.4 mg, 0.032 mmol, 2

equiv.) were added to 8 mL of ethanol which had been previously dried over 3 Å molecular sieves for 24 h. This suspension was then placed in a microwave reaction vessel. Both acetic acid (120 µL) and piperidine (120 µL) were then added and the vessel was sparged with argon. The microwave vessel was irradiated for 20 minutes at 113 °C and 800W. The solvent was evaporated under reduced pressure. The solid residue was loaded onto a silica gel flash column and eluted with 80:20 hexanes:ethyl acetate to give 23.7 mg of **3** as a dark blue solid (38% yield). ¹HNMR (400 MHz, CDCl₃): δ = 7.71 (d, *J* = 8 Hz, 2H), 7.64, (d, *J* = 4 Hz, 4 H), 7.42 (t, *J* = 8 Hz, 4H), 7.34 (t, *J* = 8 Hz, 2H), 7.30 (d, *J* = 8 Hz, 2H), 6.77 (s, 2H), 5.37 (s, 2H), 2.44 (s, 6H), 2.17 (s, 3H) ppm; ¹³CNMR (200 MHz, CDCl₃): δ = 170.62, 153.35, 140.42, 137.06, 136.43, 134.79, 130.23, 129.18, 128.82, 127.68, 118.94, 58.02, 22.71, 15.88, 14.14 ppm; Hi-res MS (ESI) for formula C₃₀H₂₇BF₂N₂O₂Na⁺, Calc. 519.2026, Found 519.2041.

Synthesis of Compound 4. 8-Acetoxymethyl-1,3,5,7-tetramethyl pyrromethene fluoroborate (50 mg, 0.016 mmol, 1 equiv.), 4-methoxybenzaldehyde (9.6 mg, 0.064 mmol, 4 equiv.) were added to a 10 mL Erlenmeyer flask. Dry toluene (3 mL) was added to the flask, followed by piperidine (1 mL). The flask was heated until the toluene evaporated. More toluene (1 mL) was then added and solvent allowed to evaporate again. The solvent was completely evaporated under reduced pressure. The solid residue was then loaded onto a silica gel flash column and eluted with 50:50 hexanes:ethyl acetate to give **4** as a dark blue solid. The product was further purified using a prep TLC plate and 80:20 hexanes:ethyl acetate providing 17.8 mg of **4** (26% yield). ¹HNMR (400 MHz, CDCl₃): δ = 7.59 (d, *J* = 4Hz, 4H), 7.58 (d, *J* = 8 Hz, 2H), 7.24 (d, *J* = 8 Hz, 2H), 6.94 (d, *J* = 4 Hz, 4H), 6.73 (s, 2H), 5.35 (s, 2H), 3.87 (s, 6H), 2.43 (s, 6H), 2.16 (s, 3H) ppm; ¹³CNMR (200 MHz,

CDCl_3): $\delta = 170.82, 160.73, 153.52, 140.06, 136.71, 134.73, 129.58, 129.35, 118.76, 117.24, 114.46, 58.28, 55.54, 20.87, 15.99$ ppm; Hi-res MS (ESI) for formula $\text{C}_{32}\text{H}_{31}\text{BF}_2\text{N}_2\text{O}_4$, Calc. 556.2454, Found 556.2451.

CONCLUSIONS

Four new BODIPY based photocages were synthesized, **1-4**. They were found to successfully release acetic acid when irradiated with white light. They were also found to be thermally stable for 1 hour at 60°C . The optical properties of these photocages are outstanding with absorbances of 586 nm to 661 nm and extinction coefficients $\sim 60,000\text{ M}^{-1}\text{ cm}^{-1}$. The quantum efficiencies were found to be on-par with the common 2-nitrobenzyl photocages making **1-4** potentially powerful alternatives. Compounds **2**, **3**, and **4** absorb within the coveted biological window of light making them promising candidates for applications in cells and tissues. Studies are currently underway to show the biocompatibility of a BODIPY dye within *S2* cells.

REFERENCES

- (1) Zhao, J.; Lin, S.; Huang, Y.; Zhao, J.; Chen, P. R. *J. Am. Chem. Soc.* **2013**, 135, 7410.
- (2) Lawrence, D. S. *Curr. Opin. Chem. Biol.* **2005**, 9, 570.
- (3) Riggsbee, C. W.; Deiters, A. *Trends Biotechnol.* **2010**, 28, 468.
- (4) Pirrung, M. C. *Chem. Rev.* **1997**, 97, 473.
- (5) Chee, M.; Yang, R.; Hubbell, E.; Berno, A.; Huang, X. C.; Stern, D.; Winkler, J.; Lockhart, D. J.; Morris, M. S.; Fodor, S. P. *Science* **1996**, 274, 610.
- (6) Priestman, M. A.; Lawrence, D. S. *Biochim. Biophys. Acta* **2010**, 1804, 547.
- (7) Gomez, T. M.; Spitzer, N. C. *Nature* **1999**, 397, 350.
- (8) Zucker, R. In *Methods in Cell Biology*; Richard, N., Ed.; Academic Press: **1994**; Vol. Volume 40, p 31.
- (9) Mbatia, H. W.; Dhammika Bandara, H. M.; Burdette, S. C. *Chem. Commun.* **2012**, 48, 5331.
- (10) Bandara, H. M. D.; Walsh, T. P.; Burdette, S. C. *Chem. Eur J.* **2011**, 17, 3932.
- (11) Sjulson, L.; Miesenbock, G. *Chem. Rev.* **2008**, 108, 1588.
- (12) Kramer, R. H.; Chambers, J. J.; Trauner, D. *Nat. Chem. Biol.* **2005**, 1, 360.
- (13) Katz, J. S.; Burdick, J. A. *Macromol. Biosci.* **2010**, 10, 339.
- (14) Lin, C.-C.; Anseth, K. *Pharm. Res.* **2009**, 26, 631.
- (15) Puliti, D.; Warther, D.; Orange, C.; Specht, A.; Goeldner, M. *Biorg. Med. Chem.* **2011**, 19, 1023.
- (16) Li, W.-h.; Zheng, G. *Photochem. Photobio. Sci.* **2012**, 11, 460.
- (17) Fukaminato, T. *J. Photochem. Photobio. C: Photochem. Rev.* **2011**, 12, 177.
- (18) Kaplan, J. H.; Forbush, B.; Hoffman, J. F. *Biochemistry* **1978**, 17, 1929.

- (19) Engels, J.; Schlaeger, E. J. *J. Med. Chem.* **1977**, 20, 907.
- (20) Ciamician, G.; Silbert, P. *Chem. Ber.* **1901**, 34, 2040.
- (21) Anderson, J. C.; Reese, C. B. *Tetrahedron Lett.* **1962**, 3, 1.
- (22) Ackmann, A. J.; Frechet, J. M. J. *Chem. Commun.* **1996**, 605.
- (23) Sheehan, J. C.; Wilson, R. M. *J. Am. Chem. Soc.* **1964**, 86, 5277.
- (24) Sheehan, J. C.; Wilson, R. M.; Oxford, A. W. *J. Am. Chem. Soc.* **1971**, 93, 7222.
- (25) Givens, R. S.; Matuszewski, B. *J. Am. Chem. Soc.* **1984**, 106, 6860.
- (26) Arumugam, S.; Popik, V. V. *J. Am. Chem. Soc.* **2009**, 131, 11892.
- (27) Goswami, P. P.; Syed, A.; Beck, C. L.; Albright, T. R.; Mahoney, K. M.; Unash, R.; Smith, E. A.; Winter, A. H. *J. Am. Chem. Soc.*, **2015**, 137, 3787.
- (28) Smith, Andrew M.; Mancini, Michael C.; Nie, Shuming. *Nature Nanotech.* **2009**, 4, 710.
- (29) Buck, A. T.; Beck, C. L.; Winter, A. H. *J. Am. Chem. Soc.* **2014**, 136, 8933.
- (30) Buyukcakir, O.; Bozdemir, O.A.; Kolemen, S.; Erbas, S.; Akkaya, E. U. *Org. Lett.* **2009**, 11, 4644

GENERAL CONCLUSIONS FOR PART I

A time-dependent density functional theory (TD-DFT) computational investigation of carbocations attached to the BODIPY scaffold at the *meso* position indicated that these ions have a small S_0 - S_1 gap. The S_0 - S_1 gap for all the investigated carbocations were less than 13 kcal/mol suggesting a low energy diradical character that in turn indicates a nearby productive conical intersection. These structures were then synthesized as photocages for acetic acid. Irradiation of these compounds with green light (>500 nm) showed the release of acetic acid. The absorbance in the visible light along with comparable quantum efficiency of photocleavage makes these photocages promising alternative to the popular *o*-nitrobenzyl based systems. The photorelease of the BODIPY based photocage was also demonstrated in *S2* cells.

The aromatic core of the BODIPY photocage was further conjugated using Knoevenagel type reactions. This resulted in a bathochromic shift in the absorbance of the dyes (~600nm). These conjugated BODIPY dyes were also made into acetic acid photocages. Irradiation of these compounds with green light showed the release of acetic acid. The quantum efficiency of the conjugated BODIPY photocages were however lower than the non-conjugated BODIPY photocages.

Further work is underway to modify the BODIPY photocage core and study their properties. New conjugation methods may be tried to red shift the absorbance of these BODIPY photocages towards the biological window. Also, other leaving groups besides acetic acid can be tried to verify the broad use of these photocages.

CHAPTER 4

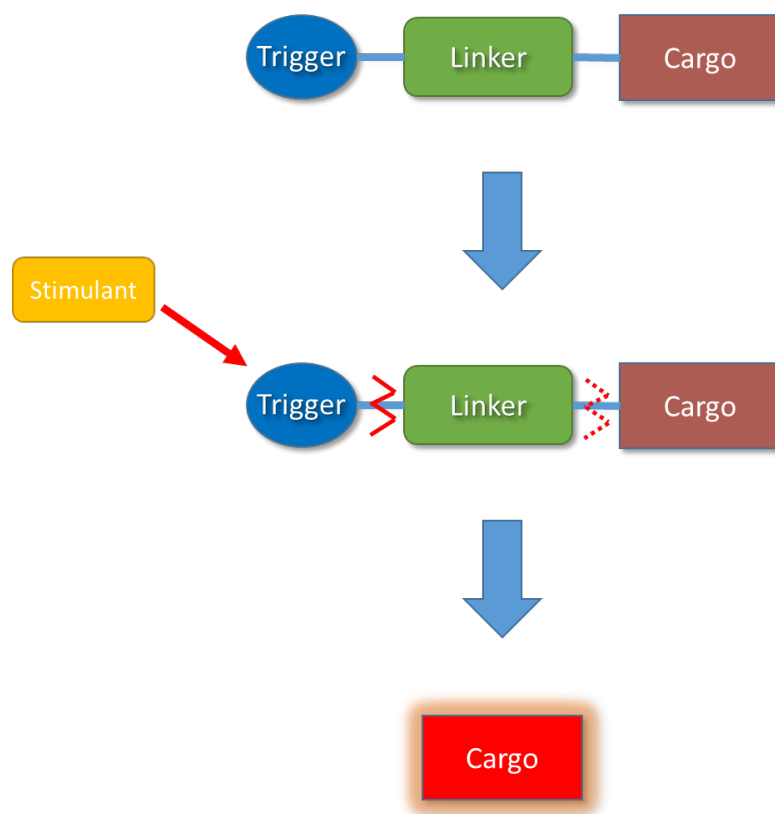
INTRODUCTION TO SELF-IMMOLATIVE LINKERS

The important thing is this: to be ready at any moment to sacrifice what you are for what you could become.

— Charles Dickens

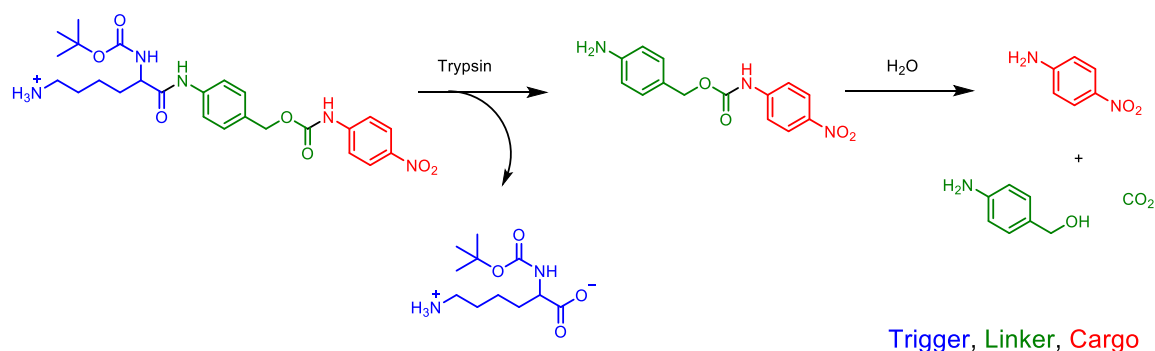
Self-immolative linkers

Self-immolative linkers are a class of linkers that can be used to connect a cleavable trigger to an output cargo molecule. Once the trigger is initiated by an input reaction, there is a cascade event leading to the release of the output cargo. As shown in **Figure 4.1**, the cargo remains inactive until it is released.



Scheme 4.1 A general scheme of self-immolative linker system

Katzenellenbogen *et al.* suggested the self-immolative moniker during their work published in 1981.¹ Their work was the first known class of self-immolative linkers and used a trypsin sensitive trigger with a quinone methide linker (**Scheme 4.1**). Since then, self-immolative linkers have found use in enzyme-activated prodrugs,²⁻¹⁰ chemical sensors,¹¹⁻¹⁵ traceless linkers,¹⁶⁻¹⁹ biological probes,²⁰⁻²³ and degradable polymers.^{2,24-31} Released chemical cargos are often biomolecules, drugs, or reporters such as fluorescent dyes. Linker structure can aid prodrugs by improving stability, solubility, biodistribution, pharmacokinetics, bioavailability and activation. These linker systems can be used as modular systems with changeable triggers and cargos.



Scheme 4.2 Quinone methide based linker used by Katzenellenbogen *et al.*

Common types of self-immolative linkers:

Quinone methide

Quinone methide is a type of organic molecule that is structurally related with quinones, with one of the carbonyls replaced by a methylene group. As shown in **Figure 4.1**, it has a conjugated cyclohexadiene with a carbonyl and an exocyclic methylene group. The carbonyl and the methylene group are generally ortho or para to one another. Being common constituents in a number of biomolecules, for e.g. celastrol, pristimerin, taxadone, Elansolid A3 etc.,³² quinone methide and its derivatives are an important class of compound. The general scheme of incorporating quinone methide linker in a self-immolative system has been shown in **Scheme 4.3**.

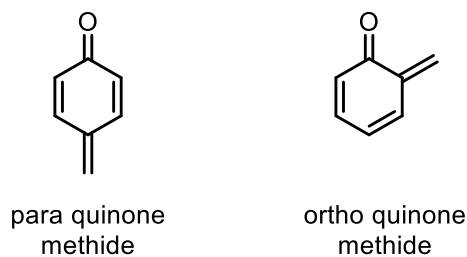
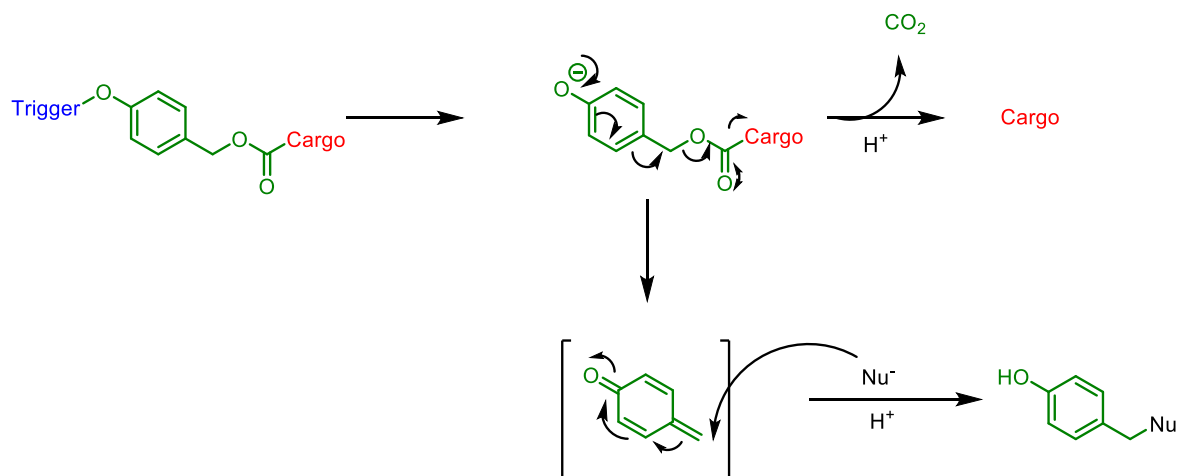
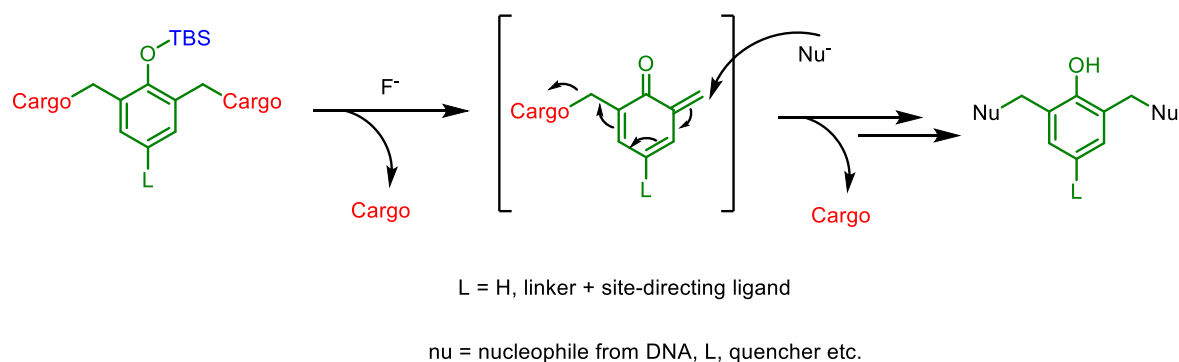


Figure 4.1 Quinone Methide



Scheme 4.3 A general scheme for the quinone methide linker based self-immolative linkers.

In the work done by Rokita *et al.*,³³ quinone methide based linker system was conjugated to a hairpin pyrrole-imidazole polyamide for controlling of DNA Cross-Linking. In their studies, they used a single quinone methide linker to deliver more than one cargo (**Scheme 4.4**). They used fluoride sensitive TBS group as the trigger for the linker system.



Scheme 4.4 Quinone methide based multiple cargo delivery system synthesized by Rokita *et al.*³³

The scope was vastly increased by incorporating multiple quinone methide systems in a dendrimeric chain by Shabat *et al.*² **Figure 4.2** represents one of the dendrimers studied by Shabat *et al.* A single trigger can undergo a chemical cascade reaction which would result in the eventual release of 8 cargo units.

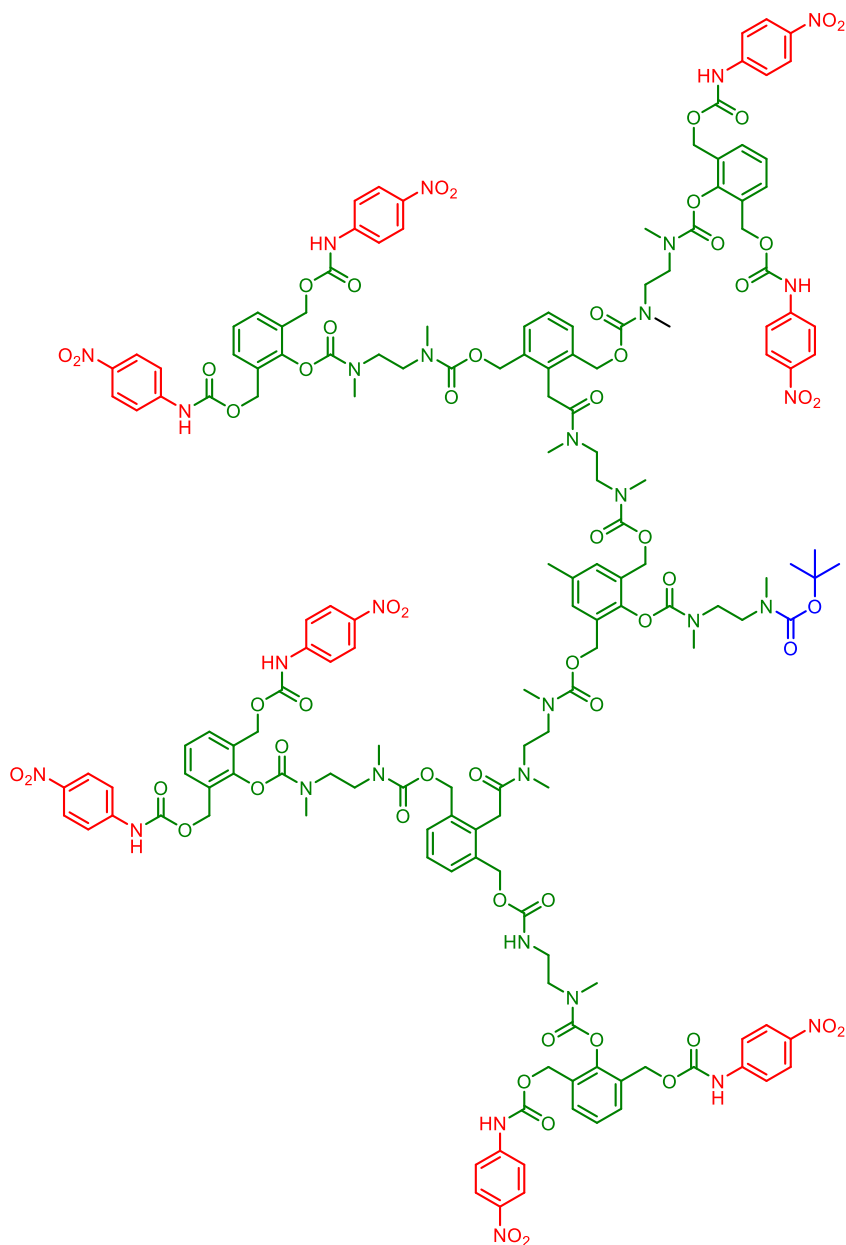
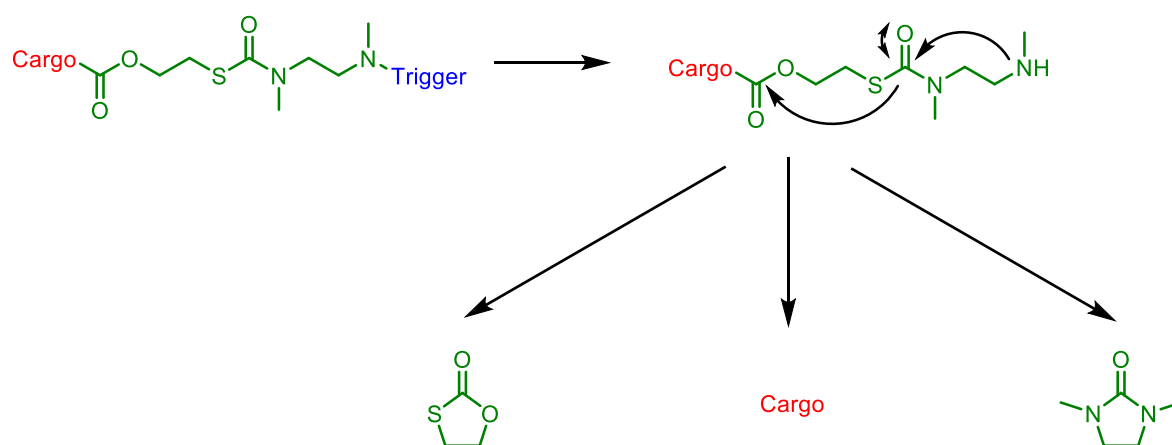


Figure 4.2 Dendrimeric self-immolative linker system

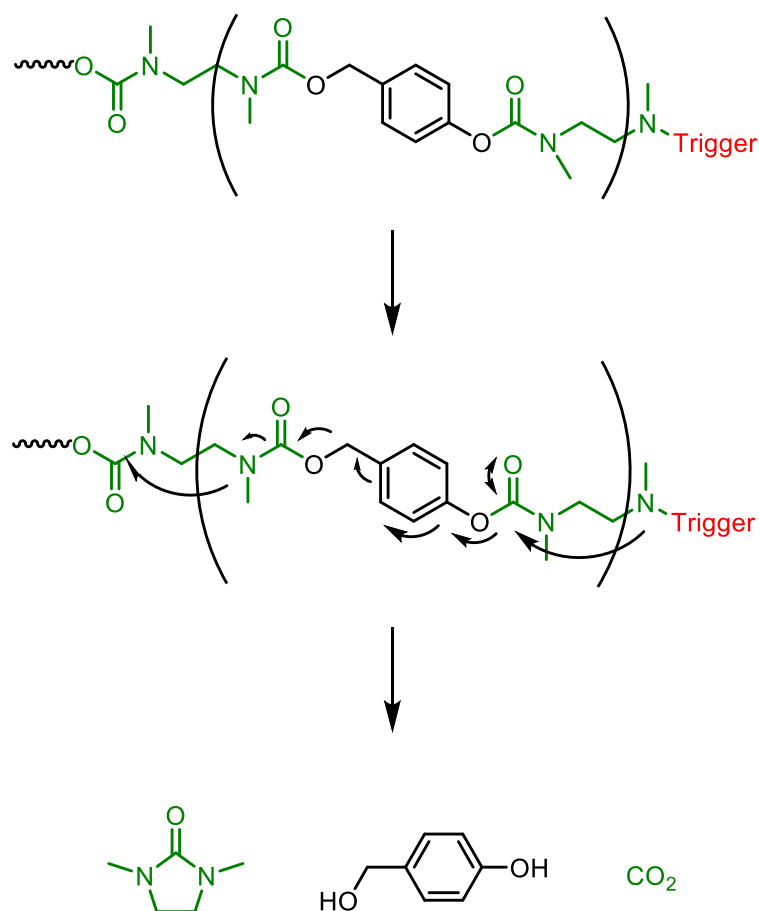
Intramolecular cyclization cascade

A few intramolecular cyclization cascades have been used in self-immolative linker systems. They are generally used in conjunction with other self-immolative linker system like the quinone methide system. A common example of intramolecular cyclization cascade system is given in **Scheme 4.5**. The formation of the five membered heterocyclic rings is the driving force for the reaction. Linkers forming more than five membered heterocyclic rings are also known.¹⁴



Scheme 4.5 A general scheme for the intramolecular cyclization cascade based self-immolative linkers.

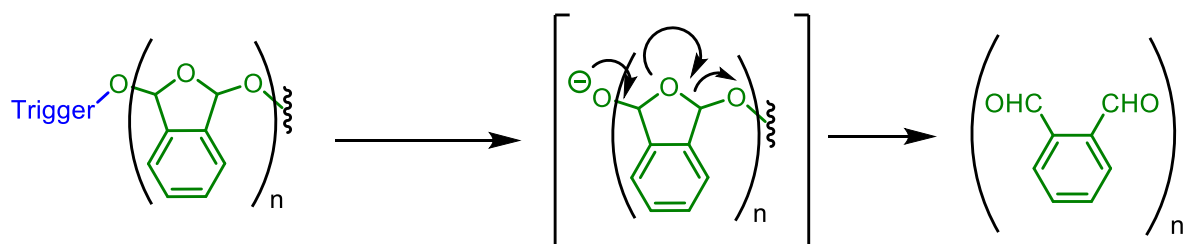
These intramolecular cyclization moieties are added to other linker systems to increase the scope of the overall linker system. An example of this would be the work done by Gillies *et al.* to make a cascade biodegradable polymer (**Scheme 4.6**).²⁶ The cascade polymer consisted of a polycarbamate backbone based on 4-aminobenzyl alcohol derivatives, which degrades entirely by intramolecular 1,6-elimination reactions via iminoquinone methide intermediates. An enzyme trigger was used to initiate the cascade event and release the cargo.



Scheme 4.6 An intramolecular cyclization cascade based self-immolative linkers with a quinone methide backbone

Hemiacetal cascade

Hemiacetals cascade event has been used recently as polymeric self-immolative linkers. Phillips *et al.* was able to use this linker unit to make polymers (plastic) which underwent physical changes in response to a chemical input (**Scheme 4.7**).³⁴ In their molecule, they were able to install palladium and fluoride sensitive triggers, which when cleaved led an entire polymer to depolymerize. The resulting structural change in the plastic was much larger than otherwise would be expected for a single reaction between two functional groups.



Scheme 4.7 A general scheme for the hemiacetal cascade based self-immolative linkers.

Triggers

Various kinds of triggers for self-immolative linker systems have been used. They may be broadly divided into:

Chemical triggers

A number of chemo-sensitive triggers have been used with self-immolative linkers.³⁵ (**Figure 4.3**) Fluoride sensitive triggers are the most common in this field. Silicon based protecting groups are employed as the fluoride sensitive triggers. Since fluoride overdose in human body can promote tooth and skeletal fluorosis, self-immolative linkers based on fluoride triggers can also be used as fluoride sensors. Another chemo-sensitive trigger used is a peroxide sensitive trigger. Peroxide has been identified to be important as a bio signaling molecule and various chemical sensors have been developed to monitor it. Work done by Kuivila *et al.*^{36,37} in the 1950s showed the susceptibility of boronic esters to oxidation when reacted with peroxides. Thus, boronic esters (**Figure 4.3**) have been used as sensors for peroxides and subsequently also been used in self-immolative linker systems.³⁸ Other chemoselective triggers include palladium sensitive allylic linkers,³⁹ piperidine/morpholine sensitive triggers that involve β -elimination reaction,²⁷ etc.

Light sensitive triggers

Light sensitive triggers are of particular interest as it involves cleavage with a remote activation without the need of any additional chemical reagent (**Figure 4.3**). The trigger

only requires light at the particular wavelength of its absorbance to initiate the self-immolative linker system. The high spatial and temporal resolution of the release of cargo makes light a very effect trigger especially in biological systems. *o*-nitrobenzyl based photocages, being the most commonly used photo cleavable linker, have been used as a light sensitive trigger for self-immolative linker systems.^{2,39} A near IR photocage based on the coumarinyl system has also been recently used as a red light sensitive trigger.⁴⁰

Enzyme sensitive triggers

Enzyme cleavable functional groups have been widely studied due to its potential application in biological systems. Since the kinetics of enzyme mediated cleavage is relatively well known, these triggers can find application which require fine-tuning of initiation kinetics. Some of the biological agents used in self-immolative linker systems include plasmin,⁴¹ antibody 38C2,² penicillin G amidase,⁴² cathepsin B,⁴³ β -glucuronidase⁴⁴ etc.

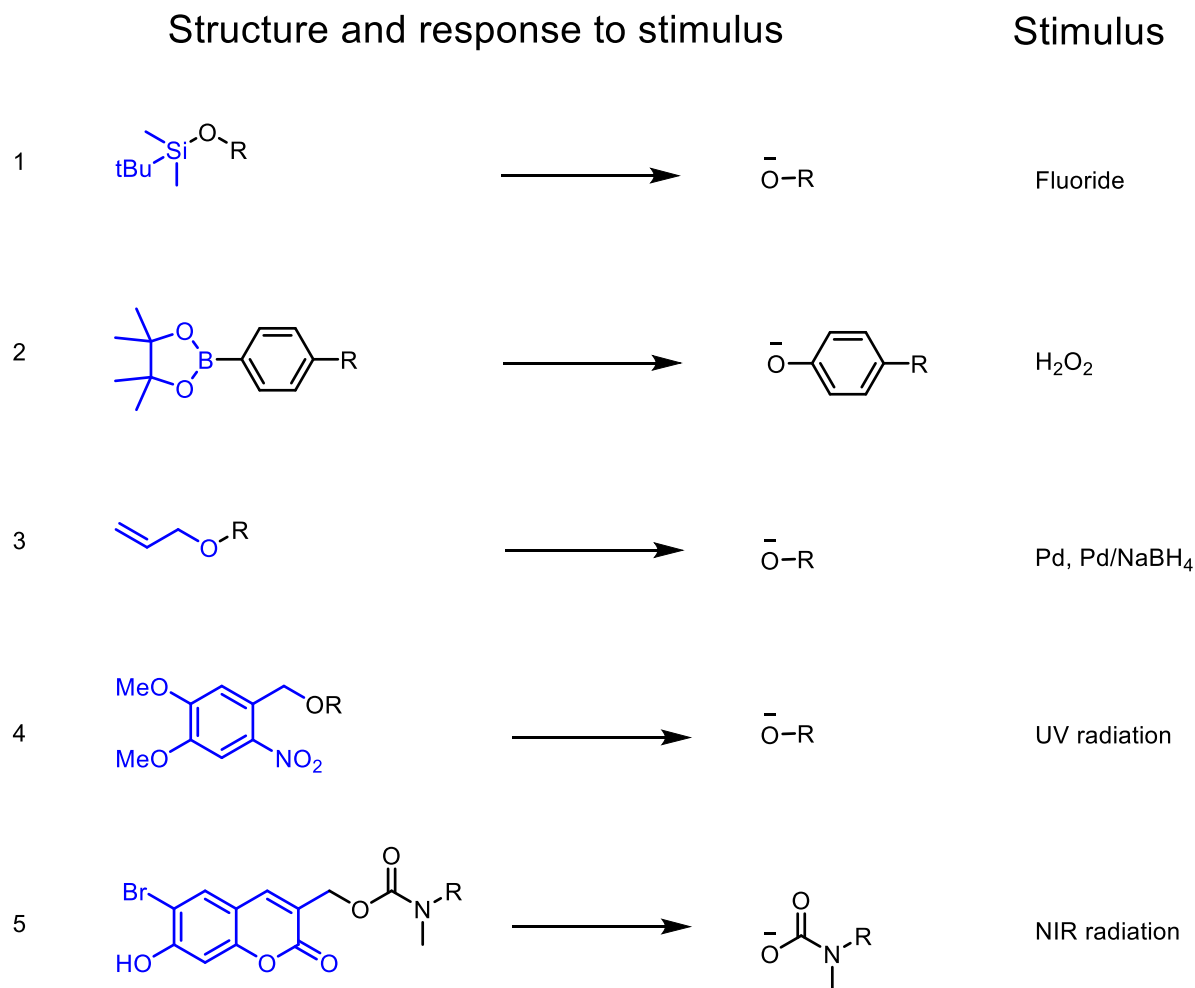


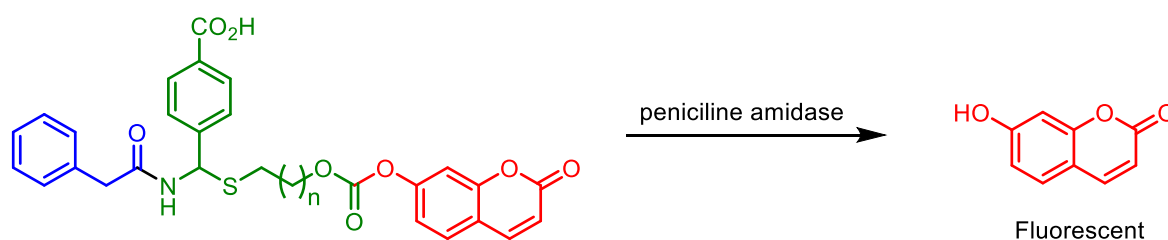
Figure 4.3 The common trigger units with the corresponding stimulus needed to cleave it

Cargos

Self-immolative linkers can be used to deliver different cargos including biomolecules, pro-drugs or reporter molecules like fluorescent dyes. Many recent studies have been focused on the amplification of the cargo molecules. In these systems, the single triggering moiety can be used for a cascade event that results in the release of a number of cargo molecules. This is of particular interest for a drug delivery system as well as in building highly sensitive chemical sensors.

Reporter molecules used as cargos are generally compounds that can be easily quantified, either through their fluorescence or other analytical methods like LC. Coumarin

and its derivatives being robust fluorescent laser dyes have been extensively used as reporter molecules. They absorb light strongly in the UV region. An example of its use as a reporter cargo in a self-immolative linker system would be the one synthesized by Romieu *et al.*¹⁴ (**Scheme 4.8**). They used an enzyme labile trigger and an intramolecular cascade linker system that had the coumarin (a fluorescent dye) as the cargo. The compound was non-fluorescent initially but upon activation with enzyme, the linker breaks down and releases the coumarin, which in turn becomes fluorescent.



Scheme 4.8. The starting compound is non fluorescent and made up of an enzyme sensitive trigger, an intramolecular cascade unit and a coumarin reporter unit. An addition of the enzyme penicilline amidase leads to the release of fluorescent 7-hydroxycoumarin.

Pro-drugs as cargos are one of the most important use of self-immolative linker systems. Drug delivery may be made much efficient by increasing specificity when it is linked to a self-immolative linker system. After activation of the linker by the stimulation of the trigger, the drug is released and becomes active. An example of this approach would be the studies done by Scheeren *et al.*⁴¹, wherein they release doxorubicin and paclitaxel. Doxorubicin is a drug used in cancer chemotherapy including hematological malignancies (blood cancers, like leukaemia and lymphoma), many types of carcinoma (solid tumours) and soft tissue sarcomas.⁴⁵ Paclitaxel is also a drug used to treat a number of cancer types including lung cancer, ovarian cancer, breast cancer and lung cancer amongst others.⁴⁶ The primary structure of their self-immolative linker with a doxorubicin cargo is given in

Figure 4.4. Plasmin, an enzyme sensitive trigger was used for cleaving the linker which was based on the iminoquinone methide system.

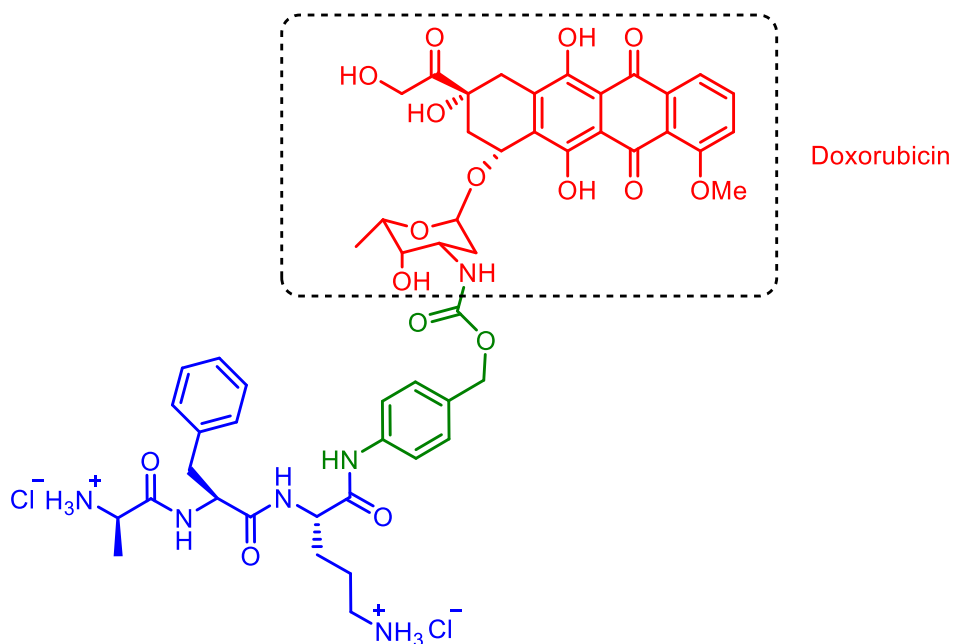


Figure 4.4 An example of a pro-drug based on self-immolative linker system. The enzyme sensitive trigger is linked to Doxorubicin (drug), via an iminoquinone methide linker

Phenyl Hydrogen Phthalate system

Phthalic Anhydride

Phthalic anhydride or, isobenzofuran-1,3-dione, is the anhydride of phthalic acid. (**Figure 4.5**) It was the first anhydride of a dicarboxylic acid to be used commercially. The company BASF using naphthalene oxidation process did the first commercial production of phthalic anhydride in 1872. It is an important chemical used in the synthesis of plasticizers and, to a lesser degree, polyester resins and dyes. About 3 million tons of phthalic anhydride is produced per year for commercial purposes making it as important as acetic acid.⁴⁷

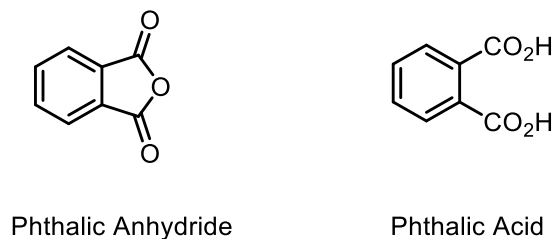
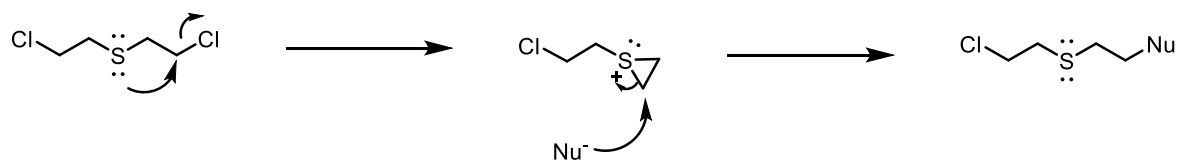


Figure 4.5. Structures of phthalic anhydride and phthalic acid

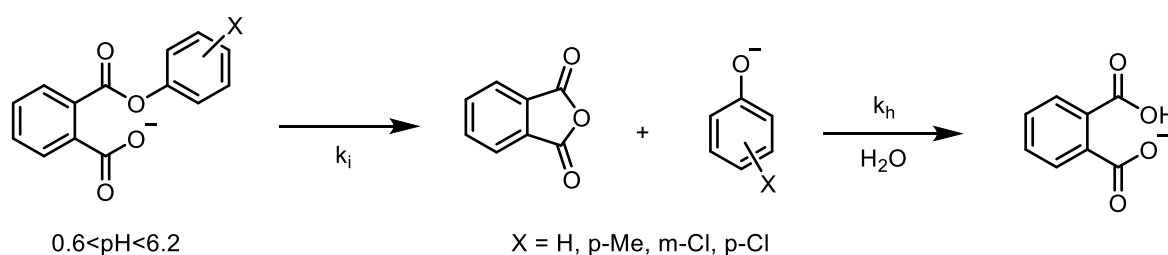
Phthalic anhydride is a self-stable compound but undergoes rapid hydrolysis in water due to neighboring group participation. IUPAC defines neighboring group participation as *the direct interaction of the reaction centre (usually, but not necessarily, an incipient carbenium centre) with a lone pair of electrons of an atom or with the electrons of a σ - or π -bond contained within the parent molecule but not conjugated with the reaction centre. A distinction is sometimes made between n -, σ - and π -participation. A rate increase due to neighbouring group participation is known as 'anchimeric assistance'.⁴⁸ A common example of neighboring group participation is the release of chlorine atom from mustard gas (Scheme 4.9). The lone pair assistance for sulfur significantly increases the rate of reaction with a nucleophile than it would be for a primary alkyl chloride without a heteroatom.*



Scheme 4.9 Common example of neighboring group participation. The presence of lone pair of electrons in sulfur greatly enhances the rate of reaction

The neighboring group participation for phthalic anhydride has been studied in detail. In 1969, Thomas C. Bruice⁴⁹ and A. Turner studied the intramolecular nucleophilic attack of carboxyl anion on phenyl esters.⁴⁹ In their subsequent study, they concluded that

neighboring carboxyl group was responsible for the hydrolysis of monoesters of phthalic acid. They also did studies on how the mechanism was dependent on the leaving group. The effective molarity (which is defined as the ratio between the first-order rate constant of an intramolecular reaction and the second-order rate constant of the corresponding intermolecular reaction) for various leaving groups attached as monoesters of phthalic acid was reported by Kirby.⁵⁰ In depth studies on the kinetics of the hydrolysis of phthalic anhydride and aryl hydrogen phthalates was done by Rita de Rossi *et al.*⁵¹ They were able to study the dependence of the kinetics on different bases, with few bases like phosphate, DABCO etc. actually acting as nucleophiles and reacting with the phthalate system. For the hydrolysis of phenyl hydrogen phthalate ester systems, they proposed a mechanism which involved the formation of phthalic anhydride, which is then hydrolyzed to phthalic acid (**Scheme 4.10**). This mechanism was studied at pH below 6.2 and it was noted by the authors that above this value, the phenoxide ion which has a very high rate constant for the reaction with phthalic anhydride, competes with the hydrolysis of the anhydride. The effect of substitution in the phenyl ring on the kinetics of hydrolysis of the phenyl hydrogen phthalate ester was also studied by the authors.



Scheme 4.10 Proposed mechanism for the hydrolysis of phenyl hydrogen phthalate esters in buffered solution $0.6 < \text{pH} < 6.2$. It involves a phthalic anhydride intermediate which can undergo further hydrolysis to phthalic acid.

Conclusion:

Self-immolative linkers can be used with a variety of different triggers and cargos. As such, they can be indispensable as chemical delivery systems. Phenyl hydrogen phthalate systems with fast kinetics and low toxicity make them ideal choice to explore their use as self-immolative linker unit.

References

- (1) Carl, P. L.; Chakravarty, P. K.; Katzenellenbogen, J. A. *J. Med. Chem.* **1981**, *24*, 479.
- (2) Amir, R. J.; Popkov, M.; Lerner, R. A.; Barbas, C. F.; Shabat, D. *Angew. Chem., Int. Ed.* **2005**, *44*, 4378.
- (3) Dubowchik, G. M.; Firestone, R. A.; Padilla, L.; Willner, D.; Hofstead, S. J.; Mosure, K.; Knipe, J. O.; Lasch, S. J.; Trail, P. A. *Bioconjugate Chem.* **2002**, *13*, 855.
- (4) Gopin, A.; Pessah, N.; Shamis, M.; Rader, C.; Shabat, D. *Angew. Chem., Int. Ed.* **2003**, *42*, 327.
- (5) Kim, Y. C.; Park, H. J.; Yang, J. G.; Kolon Ind. Inc., S. Korea . 2003, p No pp. given.
- (6) Niculescu-Duvaz, D.; Niculescu-Duvaz, I.; Friedlos, F.; Martin, J.; Spooner, R.; Davies, L.; Marais, R.; Springer, C. J. *J. Med. Chem.* **1998**, *41*, 5297.
- (7) Redy, O.; Shabat, D. *J. Controlled Release* **2012**.
- (8) Sáez, J. A.; Escuder, B.; Miravet, J. F. *Tetrahedron* **2010**, *66*, 2614.
- (9) Weinstain, R.; Baran, P. S.; Shabat, D. *Bioconjugate Chem.* **2009**, *20*, 1783.
- (10) Yang, J. J.; Kularatne, S. A.; Chen, X.; Low, P. S.; Wang, E. *Mol. Pharm.* **2012**, *9*, 310.
- (11) Chandran, S. S.; Dickson, K. A.; Raines, R. T. *J. Am. Chem. Soc.* **2005**, *127*, 1652.
- (12) Wang, R. E.; Costanza, F.; Niu, Y.; Wu, H.; Hu, Y.; Hang, W.; Sun, Y.; Cai, J. J. *Controlled Release* **2012**, *159*, 154.
- (13) Richard, J.-A.; Meyer, Y.; Jolivel, V.; Massonneau, M.; Dumeunier, R.; Vaudry, D.; Vaudry, H.; Renard, P.-Y.; Romieu, A. *Bioconjugate Chem.* **2008**, *19*, 1707.

- (14) Meyer, Y.; Richard, J.-A.; Massonneau, M.; Renard, P.-Y.; Romieu, A. *Org. Lett.* **2008**, *10*, 1517.
- (15) Lo, L.-C.; Chu, C.-Y. *Chem. Commun.* **2003**, 2728.
- (16) Ding, S.; Gray, N. S.; Ding, Q.; Schultz, P. G. *J. Org. Chem.* **2001**, *66*, 8273.
- (17) Horton, J. R.; Stamp, L. M.; Routledge, A. *Tetrahedron Lett.* **2000**, *41*, 9181.
- (18) Stieber, F.; Grether, U.; Waldmann, H. *Angew. Chem., Int. Ed.* **1999**, *38*, 1073.
- (19) Hulme, C.; Peng, J.; Morton, G.; Salvino, J. M.; Herpin, T.; Labaudiniere, R. *Tetrahedron Lett.* **1998**, *39*, 7227.
- (20) Antczak, C.; Jaggi, J. S.; LeFave, C. V.; Curcio, M. J.; McDevitt, M. R.; Scheinberg, D. A. *Bioconjugate Chem.* **2006**, *17*, 1551.
- (21) Duimstra, J. A.; Femia, F. J.; Meade, T. J. *J. Am. Chem. Soc.* **2005**, *127*, 12847.
- (22) Jeffrey, S. C.; Torgov, M. Y.; Andreyka, J. B.; Boddington, L.; Cerveny, C. G.; Denny, W. A.; Gordon, K. A.; Gustin, D.; Haugen, J.; Kline, T.; Nguyen, M. T.; Senter, P. *D. J. Med. Chem.* **2005**, *48*, 1344.
- (23) Leu, Y.-L.; Chen, C.-S.; Wu, Y.-J.; Chern, J.-W. *J. Med. Chem.* **2008**, *51*, 1740.
- (24) Esser-Kahn, A. P.; Sottos, N. R.; White, S. R.; Moore, J. S. *J. Am. Chem. Soc.* **2010**, *132*, 10266.
- (25) Sella, E.; Shabat, D. *J. Am. Chem. Soc.* **2009**, *131*, 9934.
- (26) DeWit, M. A.; Gillies, E. R. *J. Am. Chem. Soc.* **2009**, *131*, 18327.
- (27) Weinstain, R.; Sagi, A.; Karton, N.; Shabat, D. *Chem. Eur. J.* **2008**, *14*, 6857.
- (28) Warnecke, A.; Kratz, F. *J. Org. Chem.* **2008**, *73*, 1546.
- (29) Sagi, A.; Weinstain, R.; Karton, N.; Shabat, D. *J. Am. Chem. Soc.* **2008**, *130*, 5434.

- (30) Gingras, M.; Raimundo, J.-M.; Chabre, Y. M. *Angew. Chem., Int. Ed.* **2007**, *46*, 1010.
- (31) Shabat, D. *J. Polym. Sci., Part A: Polym. Chem* **2006**, *44*, 1569.
- (32) Ping Wang, Y. S., Lixia Zhang, Hanping He, Xiang Zhou *Curr. Med. Chem.*, *12*, 2893.
- (33) Kumar, D.; Veldhuyzen, W. F.; Zhou, Q.; Rokita, S. E. *Bioconjugate Chem.* **2004**, *15*, 915.
- (34) Seo, W.; Phillips, S. T. *J. Am. Chem. Soc.* **2010**, *132*, 9234.
- (35) Peterson, G. I.; Larsen, M. B.; Boydston, A. J. *Macromolecules* **2012**, *45*, 7317.
- (36) Kuivila, H. G.; Armour, A. G. *J. Am. Chem. Soc.* **1957**, *79*, 5659.
- (37) Kuivila, H. G.; Wiles, R. A. *J. Am. Chem. Soc.* **1955**, *77*, 4830.
- (38) Jourden, J. L. M.; Daniel, K. B.; Cohen, S. M. *Chem. Commun.* **2011**, *47*, 7968.
- (39) Kevitch, R. M.; Shanahan, C. S.; McGrath, D. V. *New J. Chem.* **2012**, *36*, 492.
- (40) de Gracia Lux, C.; McFearin, C. L.; Joshi-Barr, S.; Sankaranarayanan, J.; Fomina, N.; Almutairi, A. *ACS Macro Letters* **2012**, *1*, 922.
- (41) de Groot, F. M. H.; Loos, W. J.; Koekkoek, R.; van Berkom, L. W. A.; Busscher, G. F.; Seelen, A. E.; Albrecht, C.; de Bruijn, P.; Scheeren, H. W. *J. Org. Chem.* **2001**, *66*, 8815.
- (42) Erez, R.; Shabat, D. *Org. Biomol. Chem.* **2008**, *6*, 2669.
- (43) Erez, R.; Segal, E.; Miller, K.; Satchi-Fainaro, R.; Shabat, D. *Bioorg. Med. Chem.* **2009**, *17*, 4327.
- (44) Grinda, M.; Clarhaut, J.; Renoux, B.; Tranoy-Opalinski, I.; Papot, S. *Med. Chem. Comm.* **2012**, *3*, 68.

- (45) Tacar, O.; Sriamornsak, P.; Dass, C. R. *J. Pharm. Pharmacol.* **2013**, *65*, 157.
- (46) Saville, M. W.; Lietzau, J.; Pluda, J. M.; Wilson, W. H.; Humphrey, R. W.; Feigel, E.; Steinberg, S. M.; Broder, S.; Yarchoan, R.; Odom, J.; Feuerstein, I. *The Lancet*, *346*, 26.
- (47) Lorz, P. M.; Towae, F. K.; Enke, W.; Jäckh, R.; Bhargava, N.; Hillesheim, W. In *Ullmann's Encyclopedia of Industrial Chemistry*; Wiley-VCH Verlag GmbH & Co. KGaA: 2000.
- (48) McNaught, A. D.; Wilkinson, A. In *XML on-line corrected version*; 2nd ed.; Nic, M., Jirat, J., Kosata, B., Eds.; Blackwell Scientific Publications: Oxford, 1997; Vol. 2014.
- (49) Bruice, T. C.; Turner, A. *J. Am. Chem. Soc.* **1970**, *92*, 3422.
- (50) Kirby, A. J. *Adv. Phys. Org. Chem.* **1980**, *17*, 183.
- (51) Andres, G. O.; Granados, A. M.; de Rossi, R. H. *J. Org. Chem.* **2001**, *66*, 7653.

CHAPTER 5

SELF-IMMOLATIVE ARYL PHTHALATE ESTERS

Taken in part from: Mahoney, K. M.; **Goswami, P. P.**; Winter, A. H., *J. Org. Chem.*, 2013, **78**, 702.

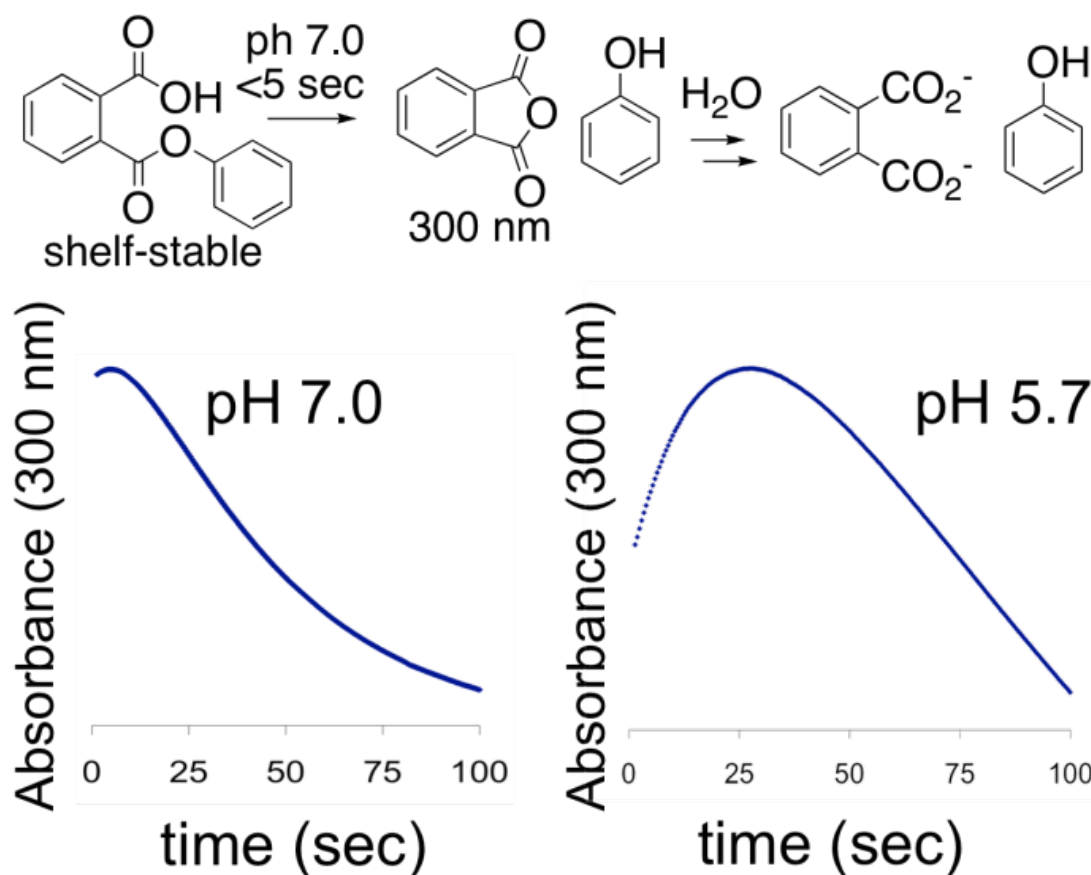
INTRODUCTION

Self-immolative linkers have become indispensable molecules for connecting a cleavable mask to an output cargo molecule.¹⁻³ Upon an input reaction that cleaves the mask, self-immolative linkers release their output cargo. Despite their unsavory moniker, self-immolative linkers have proven to be extremely useful in enzyme-activated prodrugs,⁴⁻¹² chemical sensors,^{2,13-16} traceless linkers,¹⁷⁻²⁰ biological probes,²¹⁻²⁴ and degradable polymers.^{1,25-33} Released chemical cargoes are often biomolecules, drugs, or reporters such as fluorescent dyes. Linker structure can aid prodrugs by improving stability, solubility, biodistribution, pharmacokinetics, bioavailability and activation.

The ideal self-immolative linker does not impose: It is simple, stable, compatible with water, and transforms into a benign byproduct upon releasing the output cargo. Furthermore, such linkers should be easy to conjugate, readily adaptable to a variety of inputs and outputs, and quickly release the output cargo upon the input reaction. In particular, some common self-immolative linkers suffer from slow release of their output cargo. New linkers that incorporate these desirable features would be highly useful.

The hydrolysis of phenyl hydrogen phthalate is a classic case of neighboring group participation, the mechanism of which has seen extensive investigation.³⁴⁻³⁷ Phenyl hydrogen phthalate is a shelf-stable compound when stored away from moisture, but this

compound hydrolyzes rapidly in water (**Scheme 5.1**). It has been determined that the fast ester hydrolysis of this compound is a case of intramolecular catalysis wherein the neighboring carboxylate group displaces the phenol to generate a water-unstable anhydride that in turn spontaneously hydrolyzes to phthalic acid. In neutral water, release of phenol is too fast to obtain accurate rate constants using standard UV-vis studies ($\tau < 5$ s), but the rate of release is slowed in more acidic water ($\tau = 23$ s, pH 5.7). The known favorable kinetics of this hydrolysis led us to test aryl phthalate esters for use as self-immolative linkers.



Scheme 5.1. Fast hydrolysis of the classic phenyl hydrogen phthalate hydrolysis in water followed by monitoring growth and decay of phthalic anhydride

Incorporating a classic reaction into a self-immolative linker. The hydrolysis of phenyl hydrogen phthalate is a classic case of neighboring group participation.³¹⁻³⁴ Phenyl hydrogen phthalate is a shelf-stable compound when stored away from moisture, but this compound hydrolyzes rapidly in water (**Scheme 5.1**). The astounding fast ester hydrolysis of this compound is an exemplary case of intramolecular catalysis wherein the neighboring carboxylate group displaces the phenol to generate a water-unstable anhydride that in turn spontaneously hydrolyzes to phthalic acid. In neutral water, release of phenol is too fast to obtain reliable rate constants using standard UV-Vis studies ($t < 5$ sec), but the rate of release is slowed in more acidic water ($t = 23$ sec, pH 5.7). The favorable kinetics of this hydrolysis led us to test aryl phthalate esters for use as self-immolative linkers.

Using a fluoride-sensitive 2-(trimethylsilyl)ethyl ether to mask the catalytic carboxyl group, in combination with three phenolic cargos (phenol **1** plus the fluorescent dyes 7-hydroxycoumarin **2** and 3-(2-Benzothiazolyl)-7-hydroxycoumarin **3**), we find that aryl phthalate esters can indeed be exploited as self-immolative linkers. We show that these linkers can be conjugated easily starting from phthalic anhydride, a cheap industrial starting material in the manufacture of plastics, and “self-immolate” to ultimately yield phthalic acid as a biologically benign byproduct upon release of the phenolic output.

RESULTS AND DISCUSSION

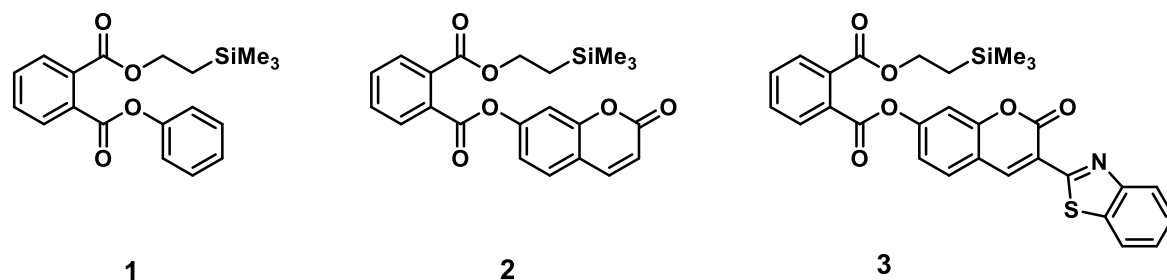


Figure 5.1. Aryl phthalate esters described in this study.

Fluoride titrations studies and product analysis.

Compounds **1-3** were synthesized and titrated with fluoride ion (**Scheme 5.2**) in pH 7 buffer. The titration of **1** was followed by ^1H NMR spectroscopy and titrations of **2** and **3** were followed with fluorescence spectroscopy. The titration of compound **2** is remarkable because we observe a 730-fold increase in fluorescence upon complete fluoride deprotection as a consequence of the release of the highly fluorescent 7-hydroxycoumarin dye. Thus, compound **2** is an exquisite fluoride sensor. Curiously, compound **3** shows a decrease in fluorescence during the titration even though the highly fluorescent free coumarin dye is released. This decrease in fluorescence is due to the starting ester **3** being highly fluorescent, whereas ester **2** is essentially non-fluorescent.

Chemical stability, product analysis, and release mechanism.

Compounds **1-3** are stable in water in the absence of fluoride, with no decomposition observed after 1 day at room temperature. Additionally, NMR product analysis after fluoride deprotection indicates that the organic end products are the free phenolic compound and phthalic acid. These results lead us to postulate the mechanism of release shown in **Scheme 5.2**. Surprisingly, our titrations indicate that compounds **2, 3** require

three equivalents of fluoride to achieve complete deprotection, while **1** requires the expected 1 equiv. of fluoride. This “excess” F⁻ required is puzzling since the presumed mechanism for TMSE deprotection involves a single fluoride ion adding to the silicon to eliminate ethane gas and trimethylsilyl fluoride. Possibly, deprotection of **2** and **3** proceed through a hypervalent silicon mechanism, although further work would be needed to verify this mechanistic possibility.

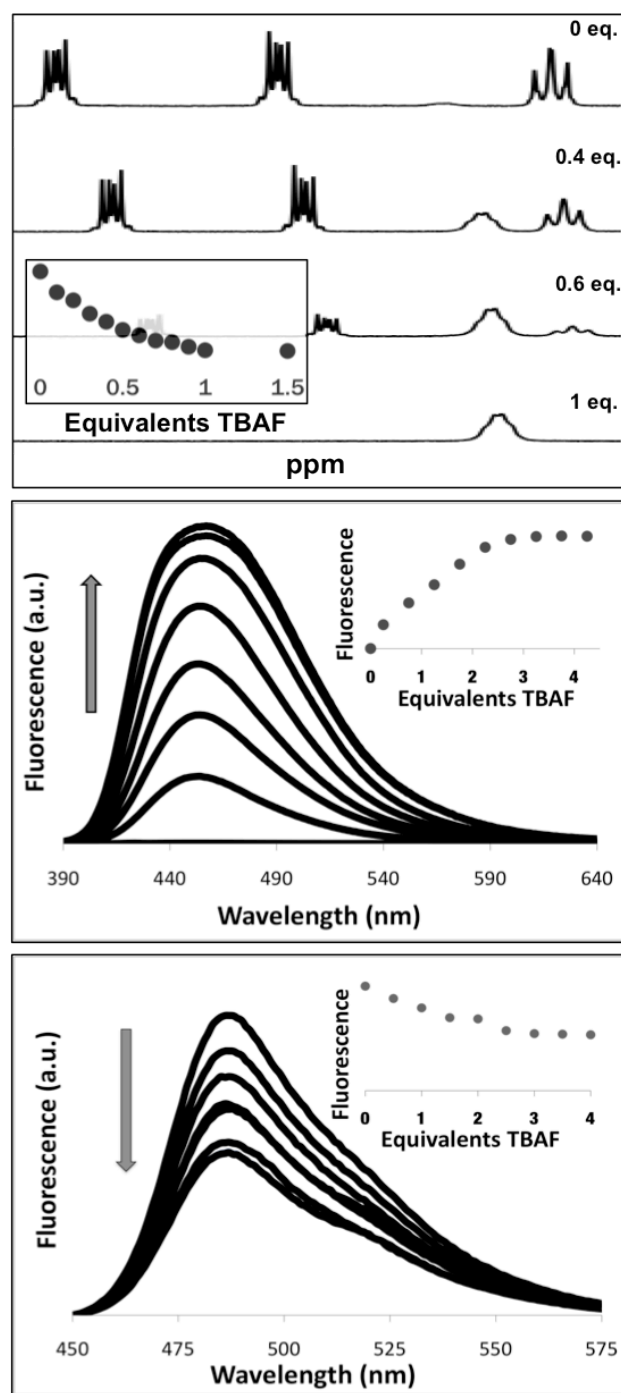
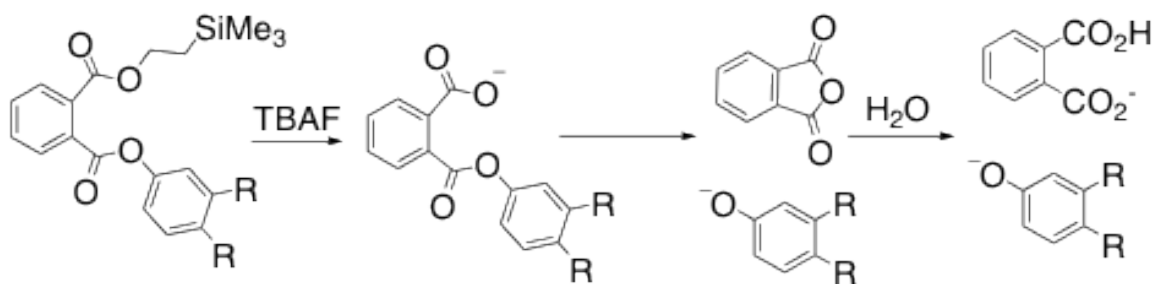
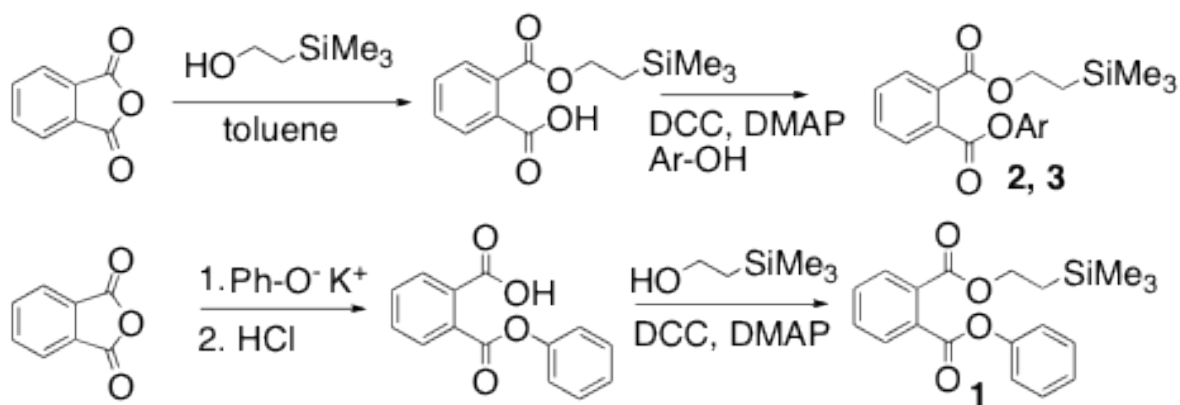


Figure 5.2. Fluoride titrations by NMR for **1** (top) and by fluorescence detection for **2** (middle) and **3** in pH 7.0 buffer. Plot inserts depict fluorescence (or NMR integration) at the emission maxima vs. equivalents of tetrabutyl ammonium fluoride.



Scheme 5.2. Putative mechanism of decomposition of **1-3** with F^- ion.

Compounds **1-3** were prepared from phthalic anhydride (See **Scheme 5.3**). Addition of TMSE to phthalic anhydride yields the TMSE-protected acid ester, which was further converted to aryl esters **2,3** using the Stieglich DCC/DMAP coupling procedure. For **1**, esterification of phenyl hydrogen phthalate was accomplished in a similar way using DCC/DMAP conditions.



Scheme 5.3. Synthesis of **1-3**.

EXPERIMENTAL

Phenyl hydrogen phthalate,³⁴ 2-(trimethylsilyl)ethyl hydrogen phthalate,³⁵ and 3-(2-benzothiazolyl)-7-hydroxycoumarin³⁶ were prepared by published procedures. All NMR matched the known spectra.

Synthesis of phenyl 2-(trimethylsilyl)ethyl phthalate 1. Phenyl hydrogen phthalate (1.50 g, 6.21 mmol), 2-trimethylsilylethanol (1 mL, 6.98 mmol) and 4-*N,N*-dimethylaminopyridine (0.085 g, 0.69 mmol) were dissolved in dry DMF (4 mL), followed by continuous stirring of the solution. *N,N*-dicyclohexylcarbodiimide (1.54 g, 7.45 mmol), dissolved in dry DMF (2 mL), was next added to the reaction mixture and the reaction was stirred under an argon atmosphere overnight. The dicyclohexylurea byproduct was filtered off as a white solid. The solvent was then removed under reduced pressure to yield the crude product as a yellow oil. Flash chromatography (Hex/EtOAc, 90:10) gave the pure final product (0.595 g, 28%) as a colorless oil. (¹H NMR, CD₃OD, 400 MHz) δ 7.90 (m, 1H), 7.83 (m, 1H), 7.70 (m, 2H), 7.46 (m, 2H), 7.29 (m, 3H), 4.44-4.40 (m, 2H), 1.09 (m, 2H), 0.04 (s, 9H); (¹³C NMR, CD₃OD, 100MHz) δ 169.1, 167.9, 152.5, 133.9, 133.1, 132.9, 132.7, 130.7, 130.4, 130.2, 127.3, 122.7, 65.4, 18.3, -1.4; High-res MS(ESI) calculated for formula C₁₉H₂₃O₄Si (M+1) requires 343.1287; found 343.1360.

Synthesis of 7-hydroxycoumarinyl 2-(trimethylsilyl)ethyl phthalate 2. 2-(trimethylsilyl)ethyl hydrogen phthalate (1.29 g, 4.83 mmol), 7-hydroxycoumarin (1.21 g, 4.83 mmol), and 4-dimethylaminopyridine (0.65 g, 5.3 mmol) were dissolved in a mixture of anhydrous methylene chloride (15 mL) and anhydrous DMF (9 mL). *N,N*-dicyclohexylcarbodiimide was quickly added to the reaction mixture and stirred under argon overnight. Dicyclohexyl urea was filtered off and the filtrate was diluted 10 mL of methylene chloride. The solution was washed with brine and then dried over anhydrous MgSO₄. The crude product was collected by evaporation under reduced pressure and then purified by flash chromatography on silica gel (Hex/EtOAc, 70:30) to yield **2** (0.65g, 33%) as a white solid: (¹H NMR CDCl₃, 400 MHz) δ 7.87, (m, 2H), 7.73 (d, 1H, J = 8 Hz), 7.64

(m, 2H), 7.57 (d, 1H, J = 8 Hz), 7.34 (s, 1H), 7.30 (s, 1H), 6.43 (d, 1H, J = 8 Hz), 4.43 (t, 2H, J = 8 Hz), 1.11 (t, 2H, J = 8 Hz), 0.06 (s, 9H); (^{13}C NMR CDCl_3 , 100 MHz) δ 167.2, 166.2, 160.7, 155.1, 153.7, 143.2, 132.0, 131.8, 131.7, 129.6, 129.4, 128.9, 118.7, 117.2, 116.5, 110.8, 64.7, 17.7, -1.1. High-res MS (ESI) calcd. for formula $\text{C}_{22}\text{H}_{22}\text{O}_6\text{Si}$ (M+1) requires 411.1186; found, 411.1258.

Synthesis of 3-(benzo[d]thiazol-2-yl)-7-hydroxycoumarinyl-2-(trimethylsilyl)ethyl phthalate 3. 2-(trimethylsilyl)ethyl hydrogen phthalate (50 mg, 0.34 mmol), 3-(2-benzothiazolyl)-7-hydroxycoumarin (99 mg, 0.34 mmol), and 4-dimethylaminopyridine (4 mg, 0.034 mmol) were dissolved in DMF (5 mL). N,N-dicyclohexylcarbodiimide (69 mg, 0.34 mmol) was quickly added to the reaction mixture and was stirred under argon for 12 h. The white solid was filtered off and the DMF was removed by evaporation under reduced pressure. The crude mixture was purified by preparatory thin-layer chromatography (200 microns) using a (Hex/EtOAc, 70:30) eluent followed by an additional prep TLC purification using (Hexane/EtOAc, 50:50) to yield the product **3** (37 mg, 20%) as a yellow solid: (^1H NMR CDCl_3 , 400 MHz) δ 9.11 (s, 1H), 8.12 (d, 1H, J=8 Hz), 8.01 (d, 1H, J = 8 Hz), 7.89 (m, 2H), 7.81 (d, 1H, J = 8 Hz), 7.66 (m, 2H), 7.56 (t, 1H, J = 8 Hz), 7.48 (s, 1H), 7.45 (s, 1H), 7.40 (dd, 2H, J = 4 Hz), 4.45 (t, 2H, J = 8 Hz), 1.12 (t, 2H, J = 8 Hz), 0.07 (s, 9H); (^{13}C NMR CDCl_3 , 100 MHz) δ 167.1, 166.2, 160.0, 159.9, 154.9, 152.7, 141.24, 137.2, 132.3, 132.1, 131.9, 131.8, 130.6, 129.7, 129.5, 126.9, 125.8, 123.3, 122.1, 120.1, 119.7, 117.3, 110.68, 64.8, 17.7, -1.1. High-res MS (ESI) calcd. for formula $\text{C}_{29}\text{H}_{26}\text{NO}_6\text{SSi}$ (M+1) requires 544.1172; found, 544.1245.

¹H NMR titration of 1. A stock solution of **1** was prepared (9.05×10^{-2} M) in DMSO-D₆ and distributed equally (97 μL) into 12 vials. To these vials was added varying equivalents of a second stock solution made of 1M TBAF/THF (7.44×10^{-2} M) in DMSO-D₆. 0.5 ml D₂O was then added to each vial. ¹H NMR spectra of each was then recorded. The titration was repeated three times and the results were averaged. Conversion was calculated by measuring the ratio of DMSO-D₆ signal integration with the integration of the -CH₂ peak (δ 4.42 ppm) in **1**.

Fluorescence titration of 2 and 3. A stock solution of **2** was prepared (7.68×10^{-5} M) in acetonitrile and distributed equally (52 μL) into vials. These samples were titrated using varying equivalents of a 1 M TBAF in THF solution. The samples were then diluted with 1 mM phosphate buffered (pH = 7.0) water to 3.0 mL. Excitation was carried out at 370 nm with all excitation and emission slit widths at 2 nm. The titration was repeated three times and the data were averaged. The same experimental procedure was used in the titration of compound **3** except the stock solution (2.3×10^{-6} M) was prepared in DMF, and the excitation of these scans was carried out at 440 nm.

CONCLUSION

In conclusion, we have shown that aryl phthalate esters are robust self-immolative linkers in water using a fluoride sensitive mask as a test case and phenolic outputs. The phthalate scaffold also appears to be highly promising for latent fluorophores, given the $\sim 10^3$ fluorescence enhancement upon releasing 7-hydroxycoumarin. Ester **2** represents an exquisite water-compatible fluoride sensor. The advantages of this linker include a simple synthesis from inexpensive starting materials, aqueous stability and compatibility, but most importantly very fast release kinetics that lead to a biologically benign byproduct. The

possibility of tuning the rate of release by chemical substitutions to the phthalate ring system, as well as the scope of this linker for different masking groups and output cargos, is currently under investigation in our laboratory. These phthalate esters appear to be highly promising for use in biological and materials applications.

REFERENCES

- (1) Amir, R. J.; Pessah, N.; Shamis, M.; Shabat, D. *Angew. Chem. Int. Ed.* **2003**, *42*, 4494-4499.
- (2) Chandran, S. S.; Dickson, K. A.; Raines, R. T. *J. Amer. Chem. Soc.* **2005**, *127*, 1652-1653.
- (3) Schmid, K. M.; Jensen, L.; Phillips, S. T. *J. Org. Chem.* **2012**, *77*, 4363-4374.
- (4) Amir, R. J.; Popkov, M.; Lerner, R. A.; Barbas, C. F.; Shabat, D. *Angew. Chem. Int. Ed.* **2005**, *44*, 4378-4381.
- (5) Dubowchik, G. M.; Firestone, R. A.; Padilla, L.; Willner, D.; Hofstead, S. J.; Mosure, K.; Knipe, J. O.; Lasch, S. J.; Trail, P. A. *Bioconjugate Chem.* **2002**, *13*, 855-869.
- (6) Gopin, A.; Pessah, N.; Shamis, M.; Rader, C.; Shabat, D. *Angew. Chem. Int. Ed.* **2003**, *42*, 327-332.
- (7) Kim, Y. C.; Park, H. J.; Yang, J. G.; Kolon Ind. Inc. Patent No. KR2003068955A, 2003.
- (8) Niculescu-Duvaz, D.; Niculescu-Duvaz, I.; Friedlos, F.; Martin, J.; Spooner, R.; Davies, L.; Marais, R.; Springer, C. J. *J. Med. Chem.* **1998**, *41*, 5297-5309.
- (9) Redy, O.; Shabat, D. *J. Control. Release* **2012**.
- (10) Saez, J. A.; Escuder, B.; Miravet, J. F. *Tetrahedron* **2010**, *66*, 2614-2618.
- (11) Weinstein, R.; Baran, P. S.; Shabat, D. *Bioconjugate Chem.* **2009**, *20*, 1783-1791.
- (12) Yang, J. J.; Kularatne, S. A.; Chen, X.; Low, P. S.; Wang, E. *Mol. Pharm.* **2011**, *9*, 310-317.
- (13) Wang, R. E.; Costanza, F.; Niu, Y.; Wu, H.; Hu, Y.; Hang, W.; Sun, Y.; Cai, J. *J. Control. Release* **2012**, *159*, 154-163.
- (14) Richard, J.-A.; Meyer, Y.; Jolivel, V.; Massonneau, M.; Dumeunier, R. I.; Vaudry, D.; Vaudry, H.; Renard, P.-Y.; Romieu, A. *Bioconjugate Chem.* **2008**, *19*, 1707-1718.
- (15) Meyer, Y.; Richard, J. A.; Massonneau, M.; Renard, P.-Y.; Romieu, A. *Org. Lett.* **2008**, *10*, 1517-1520.
- (16) Lo, L. C.; Chu, C. Y. *Chem. Commun.* **2003**, 2728-2729.
- (17) Ding, S.; Gray, N. S.; Ding, Q.; Schultz, P. G. *J. Org. Chem.* **2001**, *66*, 8273-8276.

- (18) Horton, J. R.; Stamp, L. M.; Routledge, A. *Tetrahedron Lett.* **2000**, *41*, 9181-9184.
- (19) Stieber, F.; Grether, U.; Waldmann, H. *Angew. Chem., Int. Ed.* **1999**, *38*, 1073-1077.
- (20) Hulme, C.; Peng, J.; Morton, G.; Salvino, J. M.; Herpin, T.; Labaudiniere, R. *Tetrahedron Lett.* **1998**, *39*, 7227-7230.
- (21) Antczak, C.; Jaggi, J. S.; LeFave, C. V.; Curcio, M. J.; McDevitt, M. R.; Scheinberg, D. A. *Bioconjugate Chem.* **2006**, *17*, 1551-1560.
- (22) Duimstra, J. A.; Femia, F. J.; Meade, T. J. *J. Amer. Chem. Soc.* **2005**, *127*, 12847-12855.
- (23) Jeffrey, S. C.; Torgov, M. Y.; Andreyka, J. B.; Boddington, L.; Cerveny, C. G.; Denny, W. A.; Gordon, K. A.; Gustin, D.; Haugen, J.; Kline, T.; Nguyen, M. T.; Senter, P. D. *J. Med. Chem.* **2005**, *48*, 1344-1358.
- (24) Leu, Y.-L.; Chen, C.-S.; Wu, Y.-J.; Chern, J.-W. *J. Med. Chem.* **2008**, *51*, 1740-1746.
- (25) Esser-Kahn, A. P.; Sottos, N. R.; White, S. R.; Moore, J. S. *J. Am. Chem. Soc.* **2010**, *132*, 10266-10268.
- (26) Sella, E.; Shabat, D. *J. Am. Chem. Soc.* **2009**, *131*, 9934-9936.
- (27) DeWit, M. A.; Gillies, E. R. *J. Am. Chem. Soc.* **2009**, *131*, 18327-18334.
- (28) Weinstain, R.; Sagi, A.; Karton, N.; Shabat, D. *Chem. Eur. J.* **2008**, *14*, 6857-6861.
- (29) Warnecke, A.; Kratz, F. *J. Org. Chem.* **2008**, *73*, 1546-1552.
- (30) Sagi, A.; Weinstain, R.; Karton, N.; Shabat, D. *J. Am. Chem. Soc.* **2008**, *130*, 5434-5435.
- (31) Gingras, M.; Raimundo, J.-M.; Chabre, Y. M. *Angew. Chem. Int. Ed.* **2007**, *46*, 1010-1017.
- (32) Shabat, D. *Bulletin of Israel Chemical Society* **2006**, *22*, 11-18.
- (33) Shabat, D. *J. Poly. Sci. Part A: Poly. Chem.* **2006**, *44*, 1569-1578.
- (34) Bruice, T. C.; Turner, A. *J. Am. Chem. Soc.* **1970**, *92*, 3422-3428.
- (35) Thanassi, J. W.; Bruice, T. C. *J. Am. Chem. Soc.* **1966**, *88*, 747-752.
- (36) Kirby, A. J. *Adv. Phys. Org. Chem.* **1980**, *17*, 183.

- (37) Andres, G. O.; Granados, A. M.; de Rossi, R. H. *J. Org. Chem.* **2001**, *66*, 7653-7657.
- (38) Barrett, A. G. M.; Gross, T.; Hamprecht, D.; Ohkubo, M.; White, A. J. P.; Williams, D. J. *Synthesis-Stuttgart* **1998**, 490-494.
- (39) Lin, W.; Long, L.; Tan, W. *Chem. Commun.* **2010**, *46*, 1503-1505.

CHAPTER 6

SELF-IMMOLATIVE PHTHALATE ESTERS SENSITIVE TO HYDROGEN

PEROXIDE AND LIGHT

Taken in part from: Mahoney, K. M.; **Goswami, P. P.**; Syed, A.; Kolker, P.; Shannan, B; Smith, E. A.; Winter, A. H., *J. Org. Chem.* 2014, **79**, 11740.

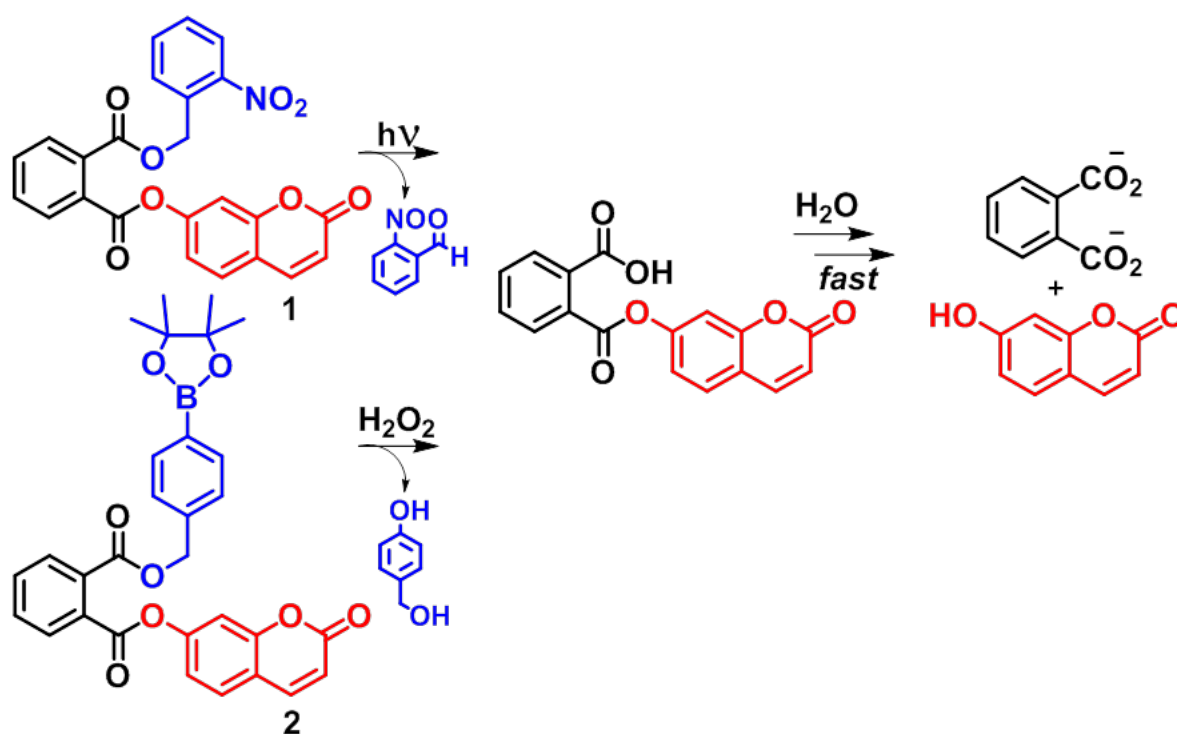
INTRODUCTION

Self-immolative linkers have proven to be useful for connecting a cleavable masking molecule to an output cargo molecule.^{24,26,37-39} Upon exposure to an input stimulus that cleaves the mask, self-immolative linkers release their cargo. Self-immolative linkers have found applications in enzyme-activated prodrugs,^{10,20,40-46} chemical sensors,^{26,47} traceless linkers,⁴⁸⁻⁵¹ biological probes,⁵²⁻⁵⁵ and degradable polymers.^{3,56,57} Released chemical cargos are often biomolecules, drugs, or reporters such as fluorescent dyes. Ideally, self-immolative linkers should be simple in design, stable, compatible with water, and transformed into a benign byproduct upon releasing the output cargo. Additionally, they should be easy to conjugate, readily adaptable to a variety of inputs and outputs, and quickly release the output cargo. A drawback to known self-immolative linkers is that cargo release rates can be slow,⁵⁸ leading to loss of temporal resolution.

Our group has recently reported aryl phthalate esters as fast-releasing self-immolative linkers.³⁸ In this previous work, we demonstrated that a fluoride-sensitive masking group could release cargo phenols and phenolic-based fluorescent dyes. Phthalate self-immolative linkers exploit the rapid hydrolysis of esters with adjacent catalytic carboxylate moieties, a classic case of neighboring group participation^{32,59,60} (phenyl hydrogen phthalate releases phenol in < 5 sec in neutral water³⁸). Here, we demonstrate that

phthalate esters masked with light- and peroxide-sensitive groups can release a coumarin dye upon exposure to light or peroxide. Peroxide is an important biological signaling molecule, whereas light-releasable fluorescent dyes (pro-fluorophores) have found application in monitoring dynamic events in real time⁶¹⁻⁶⁶ as well as recording images with sub-diffraction resolution at the nanometer level.⁶⁷⁻⁷⁰

RESULTS AND DISCUSSION



Scheme 6.1. General unmasking scheme

Both **1** and **2** were synthesized by the addition of the trigger molecule to phthalic anhydride followed by the addition of 7-hydroxycoumarin by either a DCC/DMAP or EDC/DMAP coupling.

Compounds **1** and **2** were synthesized and exposed to UV light and hydrogen

peroxide, respectively. The reactions were monitored using fluorescence and ^1H NMR spectroscopy. The titration of Compound **1** resulted in an 18-fold increase in fluorescence intensity and Compound **2** showed an 8-fold increase as a result of releasing the free fluorescent dyes.

The titrations of **1** and **2** were followed by fluorescence spectroscopy (**Figure 6.1**). To aid with solubility, experiments with **1** were carried out by first dissolving the compound in DMF and exposing the resulting solution to 350 nm light. A small aliquot (7 μL) of the solution was then injected into buffered water (3.0 mL, pH 7.0, 1 mM phosphate buffer) and fluorescence was followed as a function of time. Experiments for **2** were carried out by first dissolving the compound in DMF and titrating with increasing amounts of hydrogen peroxide. This procedure was followed by injection of a small aliquot of the DMF/ H_2O_2 solutions into buffered water for the fluorescence analysis.

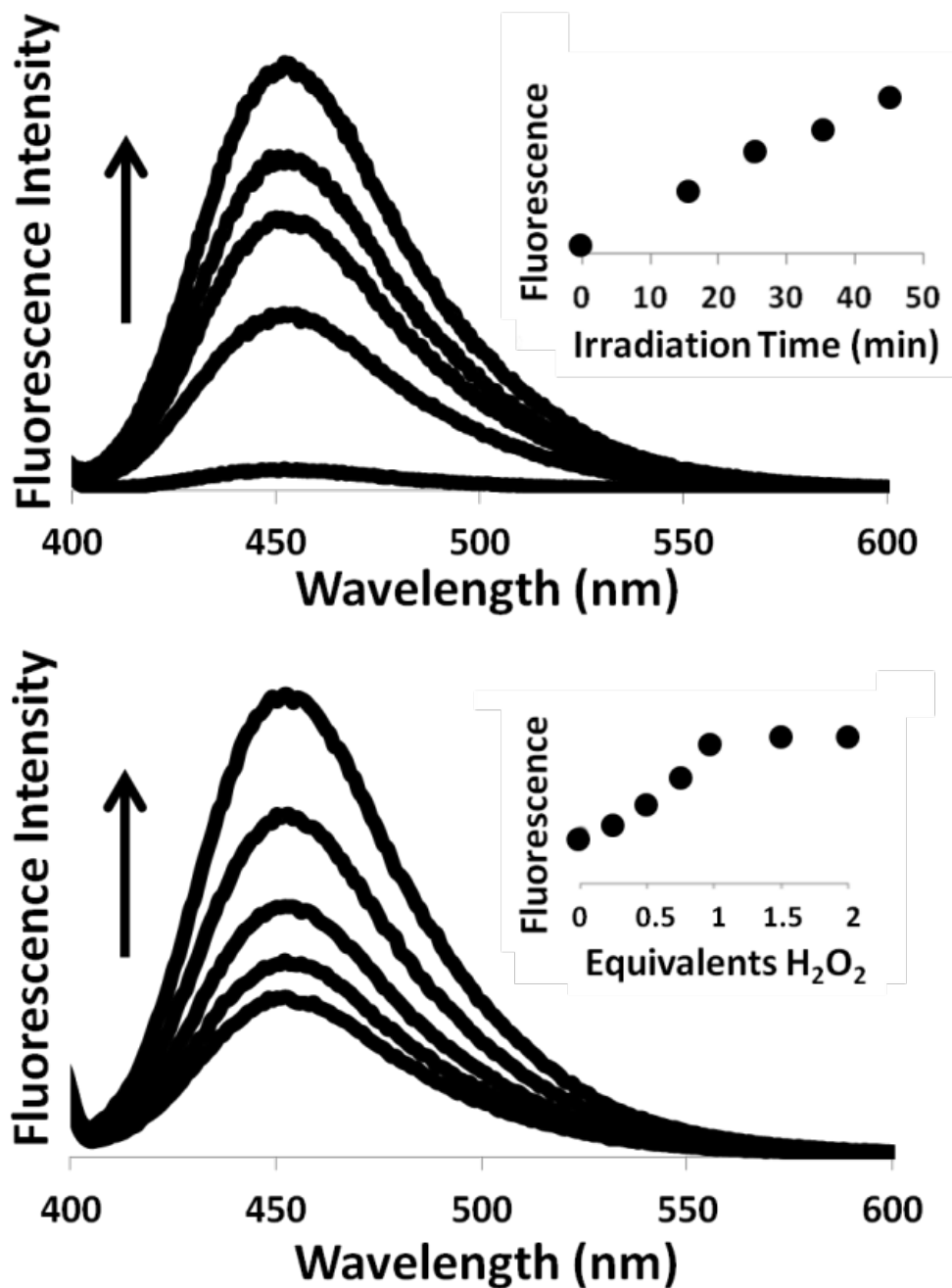


Figure 6.1. Fluorescence of compound **1** as a function of irradiation time (top); fluorescence of **2** as a function of peroxide (bottom) in pH 7.0 buffer. Plot inserts depict fluorescence at the emission maxima (453 nm) vs. time of irradiation or equivalents of hydrogen peroxide.

Compound **1** was stable in water/DMF mixtures in the absence of light for at least 1 day at room temperature. Compound **2** did show some instability, as seen by a small increase in fluorescence after a 16-hour period in a water/DMF mixture in the absence of hydrogen peroxide. Additionally, it is noteworthy that this structure **2** is quite unstable under the seemingly mild conditions required to synthesize it (e.g. DCC/DMAP ester coupling), possibly the result of the boronate ester under the reaction conditions catalyzing a spontaneous ester hydrolysis (**2** is stable as a solid or dissolved in a solution void of hydrogen peroxide, however). Additionally, NMR product studies after exposure to light and hydrogen peroxide indicate that the organic products are the expected free 7-hydroxy coumarin as well as phthalic acid. The toxicity of phthalic acid has been studied due to its industrial use in the synthesis of phthalate plastics and esters; it has not been found to be very toxic in mice [LD_{50} (mouse) is 2.53 g/kg].^{71,72}

Because **1** showed the largest increase in fluorescence intensity and the greatest stability during *in vitro* studies, we chose to use it for cellular experiments. Compound **1** was incubated with *Drosophila S2* cells and dye release was monitored using fluorescence microscopy. See **Figure 6.2**.

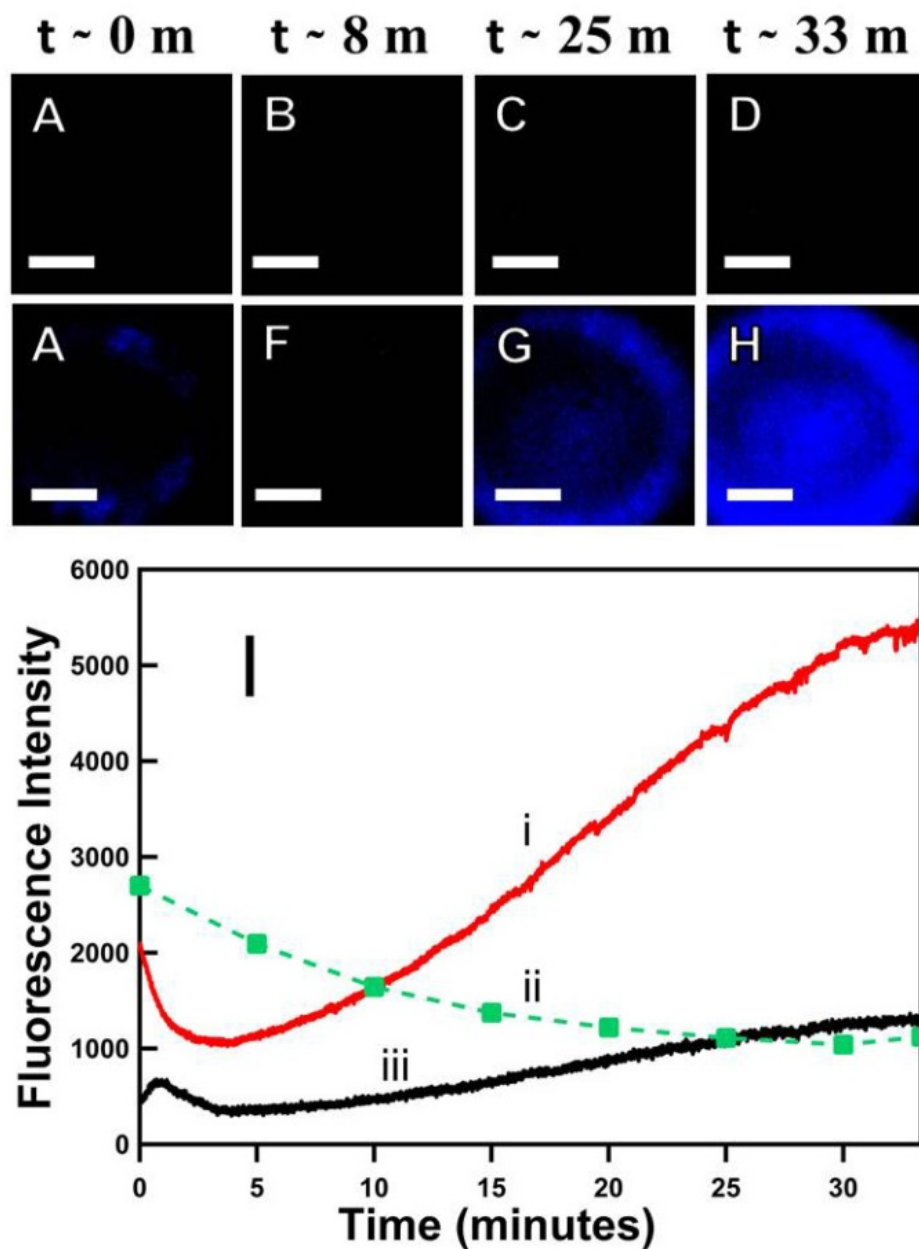


Figure 6.2. Fluorescence images of a cell with no compound 1 (A-D) and cell incubated with compound 1 (50 μ M) (E-H) as function of irradiation time. I) average fluorescence intensity as a function of time for i) four cells incubated with compound 1 and exposed to continuous irradiation for 35 minutes ii) four cells incubated with compound 1 and only exposed to irradiation briefly every 5 minutes to obtain an image iii) a cell without compound 1 and exposed to continuous irradiation for 35 minutes. Scale bar represents 5 μ m in all images.

The *Drosophila* S2 cells were loaded with **1** and subjected to continuous irradiation with 335 nm light. Fluorescence images were collected every 500 ms for a total of 33

minutes (**Figure 6.2**). Fluorescence emission was observed at 450 nm. Fluorescence intensity for **Figure 6.2**, i-iii, was taken from the periphery of the cell where the concentration of **1** was highest. As shown in **Figure 6.2 E-H**, at the beginning of the experiment there was minimal fluorescence; however, after exposure to light a gradual increase in fluorescence is seen for up to 33 minutes. The initial fluorescence seen at time zero can be attributed to cellular auto fluorescence, which undergoes initial bleaching prior to significant release of the free coumarin dye. Control studies were performed to make sure the fluorescence was due to the controlled release of 7-hydroxycoumarin by irradiation. **Figure 6.2, A-D** shows that there is minimal change in fluorescence of cells when irradiated without being loaded with **1**. Another control study (**Figure 6.2, ii**) was performed with cells incubated with **1** but not exposed to irradiation. There was an initial fluorescence signal due to cellular auto fluorescence; however, a decrease in fluorescence signal is seen, eventually leveling off to an intensity similar to that of the unloaded cells, indicating that the **1** does not release the dye in the absence of irradiation.

The cytotoxicity of **1** in the cells was determined by incubating the cells (1×10^6 cells/mL) with different dilutions ($100 \mu\text{M}$, $50 \mu\text{M}$, $25 \mu\text{M}$, $12.5 \mu\text{M}$, $6.25 \mu\text{M}$ and $3.125 \mu\text{M}$) of **1** in phosphate buffer saline (PBS, pH=7.1) for an hour. At a compound concentration of $50 \mu\text{M}$, 83% of the cells remained viable after an hour and this concentration was used in all fluorescence imaging cell studies.

EXPERIMENTAL

Synthesis of 2-(Nitrobenzyl) Hydrogen Phthalate. Phthalic acid (0.100 g, 0.675 mmol) and 2-nitrobenzyl alcohol (0.103 g, 0.675 mmol) were refluxed in toluene under argon

overnight. The crude product was collected by evaporation under reduced pressure. The resulting mixture was dissolved in ethyl acetate and the product was extracted with aqueous sodium bicarbonate followed by acidification with 1 M aqueous hydrogen chloride. Final collection of a white solid was performed by vacuum filtration. The product was dried under vacuum and used without any further purification (0.203 g, 36%); ^1H NMR (400 MHz, DMSO- d_6) δ 13.35 (s, 1H), 8.15 (dd, J = 8.1, 1.2 Hz, 1H), 7.85 – 7.60 (m, 7H), 5.63 (s, 2H). δ ; ^{13}C (DMSO- d_6 , 100 MHz) ^{13}C NMR (100 MHz) δ 168.4, 167.6, 147.8, 134.6, 132.1, 131.9, 131.9, 131.5, 129.9, 129.8, 129.4, 128.8, 125.3, 64.1; mp 142–145°C; HRMS (ESI) m/z : $[\text{M} + \text{Na}]^+$ for $\text{C}_{15}\text{H}_{11}\text{NNaO}_6$ requires 324.0479, found 324.0480

Synthesis of 7-Hydroxycoumarinyl 2-(Nitrobenzyl) Hydrogen Phthalate (1).

2-(nitrobenzyl) hydrogen phthalate (0.200 g, 0.664 mmol), *N*-(3-Dimethylaminopropyl)-*N'*-ethylcarbodiimide hydrochloride (0.126 g, 0.657 mmol), and 4-*N,N*-dimethylaminopyridine (0.089 g, 0.728 mmol) were dissolved in dry DCM (10 mL), followed by continuous stirring of the solution. 7-hydroxycoumarin potassium salt (0.132 g, 0.660 mmol) and 18-crown-6 (0.174 g, 0.660 mmol) were added next to the reaction mixture, and the reaction was stirred under an argon atmosphere for 12 h. The product was washed with an aqueous saturated sodium bicarbonate solution. The solvent was then removed under reduced pressure to yield the crude product as a white solid. Flash chromatography (Hex/EtOAc, 30:70 \rightarrow Chloroform/MeOH 95:5) gave the pure final product (0.123 g, 42%). ^1H NMR (DMSO- d_6 , 400 MHz) δ 8.16 – 8.08 (m, 2H), 8.06 – 7.91 (m, 2H), 7.90 – 7.72 (m, 5H), 7.67 – 7.56 (m, 1H), 7.34 (d, J = 2.2 Hz, 1H), 7.23 (dd, J = 8.4, 2.2 Hz, 1H), 6.53 (d, J = 9.6 Hz, 1H), 5.74 – 5.69 (m, 2H), 1.24 (s, 1H), 0.84 (t, J = 6.8 Hz, 1H); ^{13}C (DMSO- d_6 , 100 MHz) δ 166.3, 165.7, 160.0, 154.5, 153.0, 148.0, 144.2, 134.5, 132.8, 131.0, 130.3,

130.0, 129.9, 129.8, 125.3, 118.6, 117.4, 116.2, 110.2, 79.6, 79.4, 79.1, 64.4; mp >260°C; HRMS (ESI) calcd for formula $C_{24}H_{15}NO_8 [M + H]^+$ requires 446.0870, found 446.0872.

Synthesis of 4-(Hydroxymethyl)benzeneboronic Acid Pinacol Hydrogen Phthalate.

Phthalic anhydride (0.049 g, 0.294 mmol), 4-(hydroxymethyl)benzeneboronic acid pinacol (0.077 g, 0.329 mmol) were refluxed in toluene overnight. The crude product was collected by evaporation under reduced pressure. The resulting mixture was dissolved in ethyl acetate and the product was extracted with aqueous sodium bicarbonate followed by acidification with hydrogen chloride. Vacuum filtration was used to collect the white solid. The product was dried under vacuum and used without any further purification (0.045 g, 40%); 1H NMR (DMSO- d_6 , 400 MHz) δ 7.85 (s, 1H), 7.72 (m, 6H), 7.52 (d, 1H, $J = 0.8$ Hz), 1.36 (s, 12H); ^{13}C (DMSO- d_6 , 100 MHz) δ 168.4, 167.9, 139.4, 137.0, 135.0, 134.7, 132.6, 131.9, 129.4, 128.8, 127.8, 127.4, 84.2, 67.1, 25.1; mp 121-123°C; HRMS(ESI) calcd for formula $C_{21}H_{23}BO_6 (M - H)^+$ requires 380.1551, found 380.1550 (mass calculated using boron isotope ^{10}B).

Synthesis of 7-Hydroxycoumarinyl 2-(4-Hydroxymethyl)benzeneboronic Phthalate

(2). 4-(hydroxymethyl)benzeneboronic acid pinacol hydrogen phthalate (0.100 g, 0.262 mmol), *N,N*-dicyclohexylcarbodiimide (0.068 g, 0.314 mmol), and 4-*N,N*-dimethylaminopyridine (0.011 g, 0.087 mmol) and 18-crown-6 ether (0.069 g, 0.262 mmol) were dissolved in dry DMF (3 mL), followed by continuous stirring of the solution. 7-hydroxy coumarin potassium salt (0.052 g, 0.262 mmol) was next added to the reaction mixture, and the reaction was stirred under an argon atmosphere overnight. The dicyclohexylurea byproduct was filtered off as a white solid. The solvent was then

removed under reduced pressure to yield the crude product as a white solid. Flash chromatography (Hex/EtOAc, 50:50) gave the pure final product (5.6 mg, 4.1%). ¹H NMR (400 MHz, DMSO-d₆) δ 8.10 (d, *J* = 9.6 Hz, 1H), 8.02 – 7.90 (m, 2H), 7.87 – 7.75 (m, 3H), 7.62 (dd, *J* = 7.0, 1.3 Hz, 2H), 7.43 (d, *J* = 7.6 Hz, 2H), 7.32 (d, *J* = 2.1 Hz, 1H), 7.18 (ddd, *J* = 8.5, 2.2, 0.8 Hz, 1H), 6.52 (dd, *J* = 9.6, 0.8 Hz, 1H), 5.40 (s, 2H), 1.27 (d, *J* = 0.8 Hz, 12H); ¹³C (DMSO-d₆, 100 MHz) δ 166.6, 165.8, 160.3, 154.7, 153.3, 142.8, 138.2, 135.1, 131.8, 131.6, 131.5, 129.5, 129.2, 128.6, 127.5, 118.4, 116.8, 116.2, 110.4, 80.9, 67.6, 24.9; mp; HRMS(ESI) calcd for formula C₃₀H₂₇BO₈ (M + H)⁺ requires 526.1904, found 526.1908. (mass calculated using boron isotope ¹⁰B).

CONCLUSION

In conclusion, we have shown that aryl phthalate self-immolative linkers are easily conjugated with the light sensitive 2-nitrobenzyl ethanol group and the hydrogen peroxide sensitive group 4-(hydroxymethyl)phenylboronic acid pinacol ester. Compound **2** could be potentially useful as a hydrogen peroxide sensor. Compound **1** is of interest because it is able to deliver cargo in a temporally and spatially controlled manner using irradiation. Release of caged 7-hydroxycoumarin occurs upon irradiation within *S2* cells. We note finally that the fast rates of hydrolysis of phthalate self-immolative linkers may make these structures good candidates for domino self-immolative linkers,^{17,18,73-75} wherein a single input reaction results in the spontaneous release of numerous cargo molecules. Current domino self-immolative linkers tend to have slow kinetics of release.⁵⁸ A recent method to synthesize aryl mellitic acid esters⁷⁶ may enable these structures to be used within fast-releasing domino self-immolative systems.

REFERENCES

- (1) Amir, R. J.; Pessah, N.; Shamis, M.; Shabat, D. *Angew. Chem. Int. Ed.* **2003**, 42, 4494-4499.
- (2) Chandran, S. S.; Dickson, K. A.; Raines, R. T. *J. Am. Chem. Soc.* **2005**, 127, 1652-1653.
- (3) Mahoney, K. M.; Goswami, P. P.; Winter, A. H. *J. Org. Chem.* **2012**, 78, 702-705.
- (4) Schmid, K. M.; Jensen, L.; Phillips, S. T. *J. Org. Chem.* **2012**, 77, 4363-4374.
- (5) Sella, E.; Shabat, D. *Chem. Comm.* **2008**, 5701-5703.
- (6) Amir, R. J.; Popkov, M.; Lerner, R. A.; Barbas, C. F.; Shabat, D. *Angew. Chem. Int. Ed.* **2005**, 44, 4378-4381.
- (7) Dubowchik, G. M.; Firestone, R. A.; Padilla, L.; Willner, D.; Hofstead, S. J.; Mosure, K.; Knipe, J. O.; Lasch, S. J.; Trail, P. A. *Bioconjugate Chem.* **2002**, 13, 855-869.
- (8) Gopin, A.; Pessah, N.; Shamis, M.; Rader, C.; Shabat, D. *Angew. Chem. Int. Ed.* **2003**, 42, 327-332.
- (9) Grinda, M.; Legigan, T.; Clarhaut, J.; Peraudeau, E.; Tranoy-Opalinski, I.; Renoux, B.; Thomas, M.; Guilhot, F.; Papot, S. *Org. Biomol. Chem.* **2013**, 11, 7129-7133.
- (10) Niculescu-Duvaz, D.; Niculescu-Duvaz, I.; Friedlos, F.; Martin, J.; Spooner, R.; Davies, L.; Marais, R.; Springer, C. J. *J. Med. Chem.* **1998**, 41, 5297-5309.
- (11) Redy, O.; Shabat, D. *J. Control. Release* **2012**, 164, 276-282.
- (12) Saez, J. A.; Escuder, B.; Miravet, J. F. *Tetrahedron* **2010**, 66, 2614-2618.
- (13) Weinstein, R.; Baran, P. S.; Shabat, D. *Bioconjugate Chem.* **2009**, 20, 1783-1791.
- (14) Yang, J. J.; Kularatne, S. A.; Chen, X.; Low, P. S.; Wang, E. *Mol. Pharm.* **2011**, 9, 310-317.
- (15) Meyer, Y.; Richard, J.-A.; Delest, B.; Noack, P.; Renard, P.-Y.; Romieu, A. *Org. Biomol. Chem.* **2010**, 8, 1777-1780.
- (16) Ding, S.; Gray, N. S.; Ding, Q.; Schultz, P. G. *J. Org. Chem.* **2001**, 66, 8273-8276.
- (17) Horton, J. R.; Stamp, L. M.; Routledge, A. *Tetrahedron Lett.* **2000**, 41, 9181-9184.

- (18) Hulme, C.; Peng, J.; Morton, G.; Salvino, J. M.; Herpin, T.; Labaudiniere, R. *Tetrahedron Lett.* **1998**, 39, 7227-7230.
- (19) Stieber, F.; Grether, U.; Waldmann, H. *Angew. Chem. Int. Ed.* **1999**, 38, 1073-1077.
- (20) Antczak, C.; Jaggi, J. S.; LeFave, C. V.; Curcio, M. J.; McDevitt, M. R.; Scheinberg, D. A. *Bioconjugate Chem.* **2006**, 17, 1551-1560.
- (21) Duimstra, J. A.; Femia, F. J.; Meade, T. J. *J. Am. Chem. Soc.* **2005**, 127, 12847-12855.
- (22) Jeffrey, S. C.; Torgov, M. Y.; Andreyka, J. B.; Boddington, L.; Cervený, C. G.; Denny, W. A.; Gordon, K. A.; Gustin, D.; Haugen, J.; Kline, T.; Nguyen, M. T.; Senter, P. D. *J. Med. Chem.* **2005**, 48, 1344-1358.
- (23) Leu, Y.-L.; Chen, C.-S.; Wu, Y.-J.; Chern, J.-W. *J. Med. Chem.* **2008**, 51, 1740-1746.
- (24) Shabat, D. *J. Polym. Sci. A Polym. Chem.* **2006**, 44, 1569-1578.
- (25) Weinstain, R.; Sagi, A.; Karton, N.; Shabat, D. *Chem. Eur. J.* **2008**, 14, 6857-6861.
- (26) Blencowe, C. A.; Russell, A. T.; Greco, F.; Hayes, W.; Thornthwaite, D. W. *Polym. Chem.* **2011**, 2, 773-790.
- (27) Amir, R.; Shabat, D. Polymer Therapeutics I; Satchi-Fainaro, R., Duncan, R., Eds.; Springer Berlin Heidelberg: **2006**; Vol. 192, p 59-94.
- (28) Pasto, D. J.; Serve, M. P. *J. Am. Chem. Soc.* **1965**, 87, 1515-1521.
- (29) Andres, G. O.; Granados, A. M.; de Rossi, R. H. *J. Org. Chem.* **2001**, 66, 7653-7657.
- (30) Thanassi, J. W.; Bruice, T. C. *J. Am. Chem. Soc.* **1966**, 88, 747-752.
- (31) Dirks, R. W.; Molenaar, C.; Tanke, H. J. *Histochem. Cell Biol.* **2001**, 115, 3-11.
- (32) Xu, Y.; Melia, T. J.; Toomre, D. K. *Curr. Opin. Chem. Biol.* **2011**, 15, 822-830.
- (33) Zaitsev, S.; Zaitsev, S. Y. *World Appl. Sci. J.* **2013**, 26, 712.
- (34) Agasti, S. S.; Kohler, R. H.; Liong, M.; Peterson, V. M.; Lee, H.; Weissleder, R. *Small* **2013**, 9, 222-227.
- (35) Adams, S. R.; Tsien, R. Y. *Annu. Rev. Physiol.* **1993**, 55, 755-784.
- (36) Politz, J. C. *Trends Cell Biol.* **1999**, 9, 284-287.

- (37) Fernandez-Suarez, M.; Ting, A. Y. *Nat. Rev. Mol. Cell Biol.* **2008**, 9, 929-943.
- (38) Huang, B.; Bates, M.; Zhuang, X. *Annu. Rev. Biochem.* **2009**, 78, 993-1016.
- (39) Toomre, D.; Bewersdorf, J. *Annu. Rev. Cell Dev. Biol.* **2010**, 26, 285-314.
- (40) van de Linde, S.; Heilemann, M.; Sauer, M. *Annu. Rev. Phys. Chem.* **2012**, 63, 519-540.
- (41) Lin, V. S.; Dickinson, B. C.; Chang, C. J. In *Methods in Enzymology*; Enrique, C., Lester, P., Eds.; Academic Press: **2013**; Vol. Volume 526, p 19-43.
- (42) National Cancer Institute Carcinogenesis Technical Report Series. **1979**, 1-123.
- (43) Turan, I. S.; Akkaya, E. U. *Org. Lett.* **2014**, 16, 1680-1683.
- (44) Shamis, M.; Shabat, D. *Chem. Eur. J.* **2007**, 13, 4523-4528.
- (45) Amir, R. J.; Danieli, E.; Shabat, D. *Chem. Eur. J.* **2007**, 13, 812-821.
- (46) Sagi, A.; Segal, E.; Satchi-Fainaro, R.; Shabat, D. *Bioorg. Med. Chem.* **2007**, 15, 3720-3727.
- (47) Karton-Lifshin, N.; Shabat, D. *New J. Chem.* **2012**, 36, 386-393.
- (48) Geraskina, M. R.; Juetten, M. J.; Winter, A. H. *J. Org. Chem.* **2014**, 79, 5334-5337.

GENERAL CONCLUSIONS FOR PART II

A phenyl hydrogen phthalate based self-immolative linker system was synthesized. UV/Vis and NMR experiments demonstrated the fast rate of hydrolysis of this system in aqueous solution. The release of phenol takes less than 5s when the compound is monitored in pH =7 buffer. Silicon based mask triggered by fluoride was used to release phenol based cargo molecules which included coumarin based fluorescent dyes. Titration studies were done using NMR and fluorescence to verify the amount of fluoride needed to completely release the reporter cargos.

Peroxide and light sensitive triggers were linked to the phenyl hydrogen phthalate linker system to demonstrate the wider applicability of the phenyl hydrogen phthalate linker. Phenyl boronic ester was used as the peroxide sensitive trigger while the popular photocage *o*-nitrobenzyl alcohol was used as the light sensitive trigger. 7-hydroxy coumarin was used as cargo that was monitored using fluorescence. The light-sensitive aryl phthalate ester was also demonstrated as a pro-fluorophore in cultured *S2* cells.

APPENDIX A: CHAPTER 2

I. TD-DFT computations

All TD-DFT computations were done using the Gaussian 09¹ software. The geometries were first optimized using RB3LYP with a 6-31G(d) basis set and found to have no imaginary frequencies. The iodine atom in 6 was computed with the 6-311G(d) basis set. All the singlet species computed possess R->U instabilities. Thus, an unrestricted broken-symmetry approach was used for the calculation. To negate the spin contamination for low-energy triplet state for such broken-symmetry singlet calculations in DFT, the energy of singlet state was corrected using equation 1.²⁻⁵

$$E_{\text{singlet}} = \frac{2E_{\langle S_z \rangle=0} - \langle S^2 \rangle E_{\langle S_z \rangle=1}}{2 - \langle S^2 \rangle}$$

Equation 1

Where E_{singlet} is the corrected singlet energy, $E_{\langle S_z \rangle=0}$ is the broken-symmetry energy, $\langle S^2 \rangle$ is the expectation value of the total-spin operator for the broken-symmetry calculation (anywhere from about 0-1), and $E_{\langle S_z \rangle=1}$ is the energy of the triplet state at the singlet geometry.

The TD-DFT computation was done using RTD-B3LYP with a 6-311G(2d,p) basis set. For TD-DFT computation of compound 6, iodine was done with 6-311G**.

Table A1: TD-DFT computed S₀-S₁ vertical gap for cations derived from heterolysis of 1-

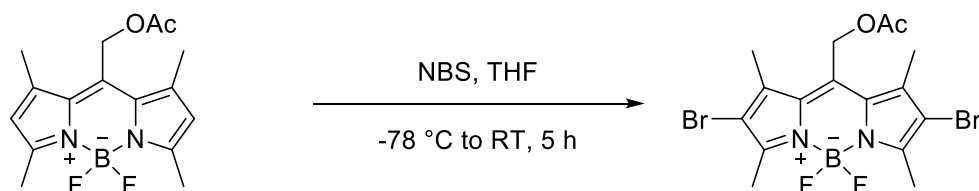
6

Cation derived from Compound	TD-DFT Vertical S ₀ -S ₁ Energy (kcal/mol)
1	11.8
2	8.3
3	3.8
4	3.6
5	4.3
6	3.8

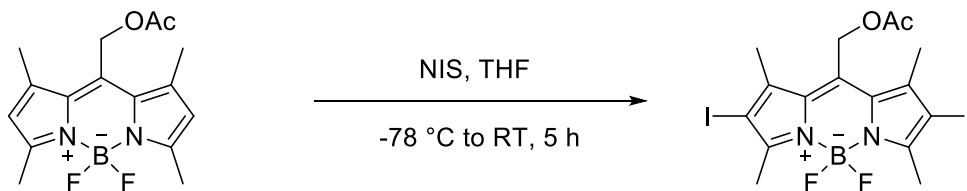
Table A2: Singlet-triplet energy gaps for cations derived from C-O heterolysis of 1-6. A large difference between restricted ΔE_{ST} and unrestricted corrected singlet ΔE_{ST} suggest an open-shell diradical singlet structure for the singlet configuration. A positive value for ΔE_{ST} indicates a triplet ground state.

Cation derived from Compound	ΔE_{ST} (restricted singlet) kcal/mol	ΔE_{ST} (corrected singlet) kcal/mol
1	+14.9	+5.1
2	+15.9	+5.4
3	+17.4	+5.2
4	+16.4	+5.0
5	+16.2	+5.2
6	+15.8	+5.0

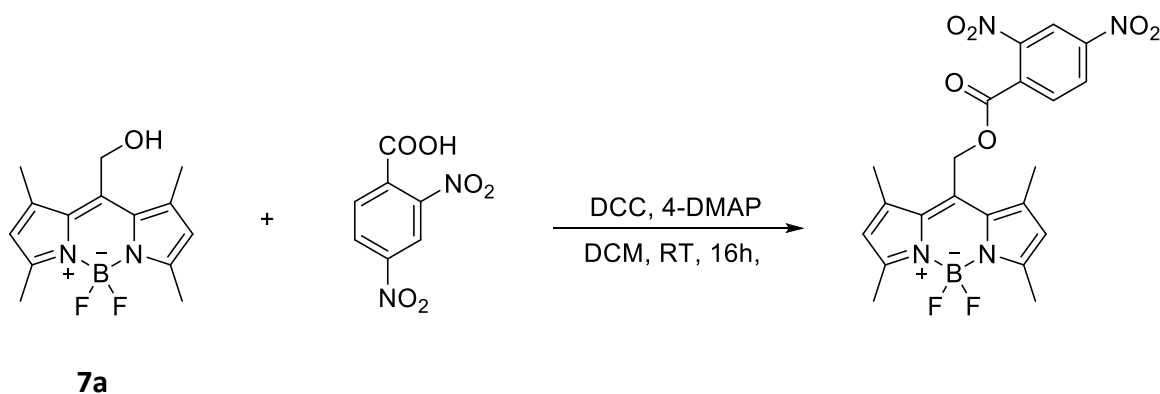
II. Synthetic procedures



(1) **Synthesis of 5:** Compound **2** (0.1 g, 0.31 mmol, 1 equiv.), was dissolved in 3 mL of dry THF under argon and cooled to $-78\text{ }^{\circ}\text{C}$. *N*-Bromosuccinimide (0.23 g, 1.25 mmol, 4 equiv.) dissolved in 2 mL of dry THF was added dropwise to the solution. The reaction mixture was stirred for 15 min at $-78\text{ }^{\circ}\text{C}$, after which it was warmed to room temperature and stirred for an additional 5 h. The solvent was evaporated under reduced pressure. The solid residue was loaded onto a silica gel flash column and eluted with hexane-ethyl acetate 90:10 vol/vol to give **5** as dark red crystals (0.14 g, 95% yield). Mp 230°C (decomp); ^1H NMR (600MHz, CDCl_3): δ 5.32 (s, 2H), 2.63 (s, 6H), 2.40 (s, 6H), 2.15 (s, 3H); ^{13}C NMR (150MHz, CDCl_3) δ 170.45, 155.29, 138.93, 133.85, 131.87, 113.10, 58.04, 20.69, 14.94, 14.08; High-res MS (ESI) for formula $\text{C}_{16}\text{H}_{17}\text{BBr}_2\text{F}_2\text{N}_2\text{O}_2\text{Na}^+$, Calc. 497.9646, Found 497.9646



(2) **Synthesis of 6:** Compound **2** (0.1 g, 0.31 mmol, 1 equiv.), was dissolved in 3 mL of dry THF under argon and cooled to $-78\text{ }^{\circ}\text{C}$. N-Iodosuccinimide (0.18 g, 2.5 mmol, 4 equiv.) dissolved in 2 mL of dry THF was added dropwise to the solution. The reaction mixture was stirred for 15 min at $-78\text{ }^{\circ}\text{C}$, after which it was warmed to room temperature and stirred for an additional 5 h. The solvent was evaporated under reduced pressure. The solid residue was loaded onto a silica gel flash column and eluted with dichloromethane to give **6** as dark purple crystals (0.07 g, 39% yield). Mp 210°C ; $^1\text{H NMR}$ (600MHz, CDCl_3): δ 5.31(s,2H), 2.59(s, 6H), 2.38(s, 6H), 2.14(s, 3H); $^{13}\text{C NMR}$ (150MHz, CDCl_3) δ 170.43, 158.06, 143.60, 132.92, 132.70, 87.38, 58.35, 20.68, 18.29, 16.47; MS (ESI) for formula $\text{C}_{16}\text{H}_{17}\text{BI}_2\text{F}_2\text{N}_2\text{O}_2\text{Na}^+$, Calc. 593.9369, Found 593.9378

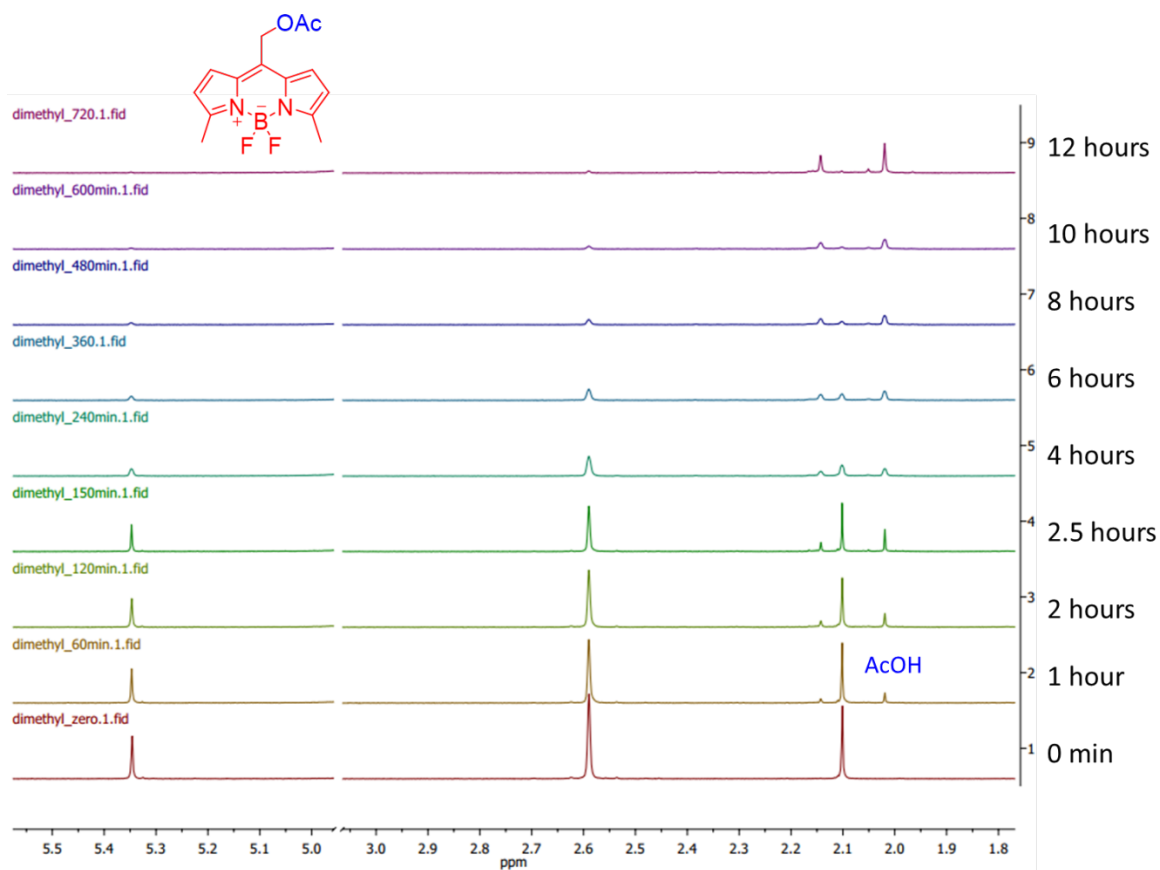


(3) **Synthesis of 7:** 2,4 dinitrobenzoic acid (0.054 g, 0.194 mmol, 1 equiv.) was dissolved in 3 ml of dry DCM under argon in room temperature. DCC (*N,N'*-Dicyclohexylcarbodiimide) (0.048 mg, 0.233 mmol, 1.2 equiv.) dissolved in 3 ml of dry DCM was added dropwise to the solution. 4-DMAP (4-Dimethylaminopyridine) (0.001 g, 0.007 mmol, 0.04 equiv.) was added to this solution. Next, **7a** (0.049 g, 0.233 mmol, 1.2

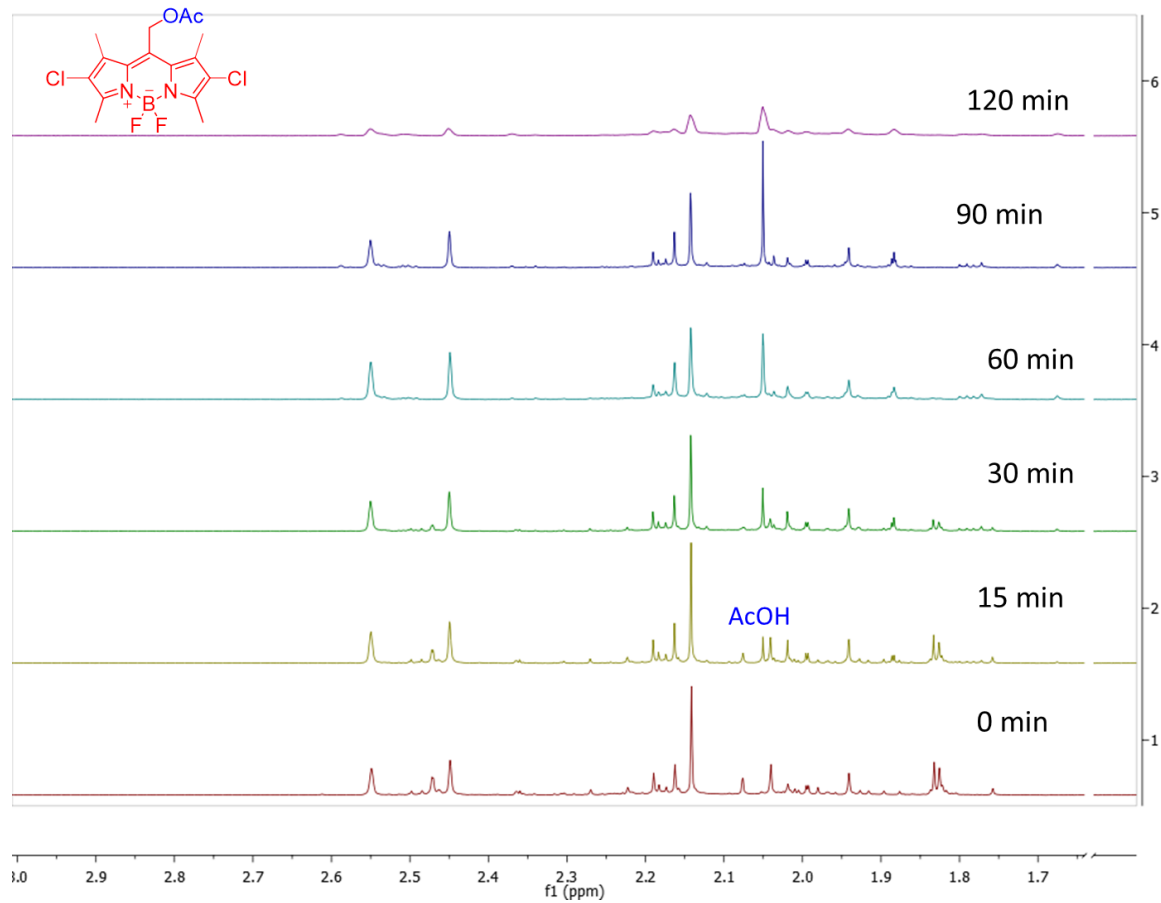
equiv.) dissolved in 3 ml of dry DCM was slowly added to the solution. The reaction mixture was stirred for 16 h until its completion. The reaction mixture was filtered to get rid of DCU (Dicyclohexyl Urea) by-product. The filtrate was evaporated under reduced pressure. The solid residue was loaded onto a silica gel flash column and eluted with hexane-ethyl acetate 80:20 vol/vol to give 7 as a dark orange crystals (0.08 g, 91% yield). ^1H NMR (600MHz, CDCl_3): δ 8.86(d, $J = 2.2\text{Hz}$, 1H), 8.54(dd, $J = 8.4\text{Hz}$, 1H), 7.86(d, $J = 8.4\text{Hz}$, 1H), 6.11(s, 2H), 5.69(s, 2H), 2.53(s, 6H), 2.44(s, 6H); ^{13}C NMR (150MHz, CDCl_3) δ 163.79, 157.46, 149.27, 141.54, 132.59, 132.72, 131.20, 130.97, 128.07, 122.88, 120.10, 60.28, 15.89, 14.89; MS (ESI) for formula $\text{C}_{21}\text{H}_{19}\text{BF}_2\text{N}_4\text{O}_6\text{Na}^+$, Calc. 495.1258, Found 498.1271

III. Acetic acid growth over time followed by NMR

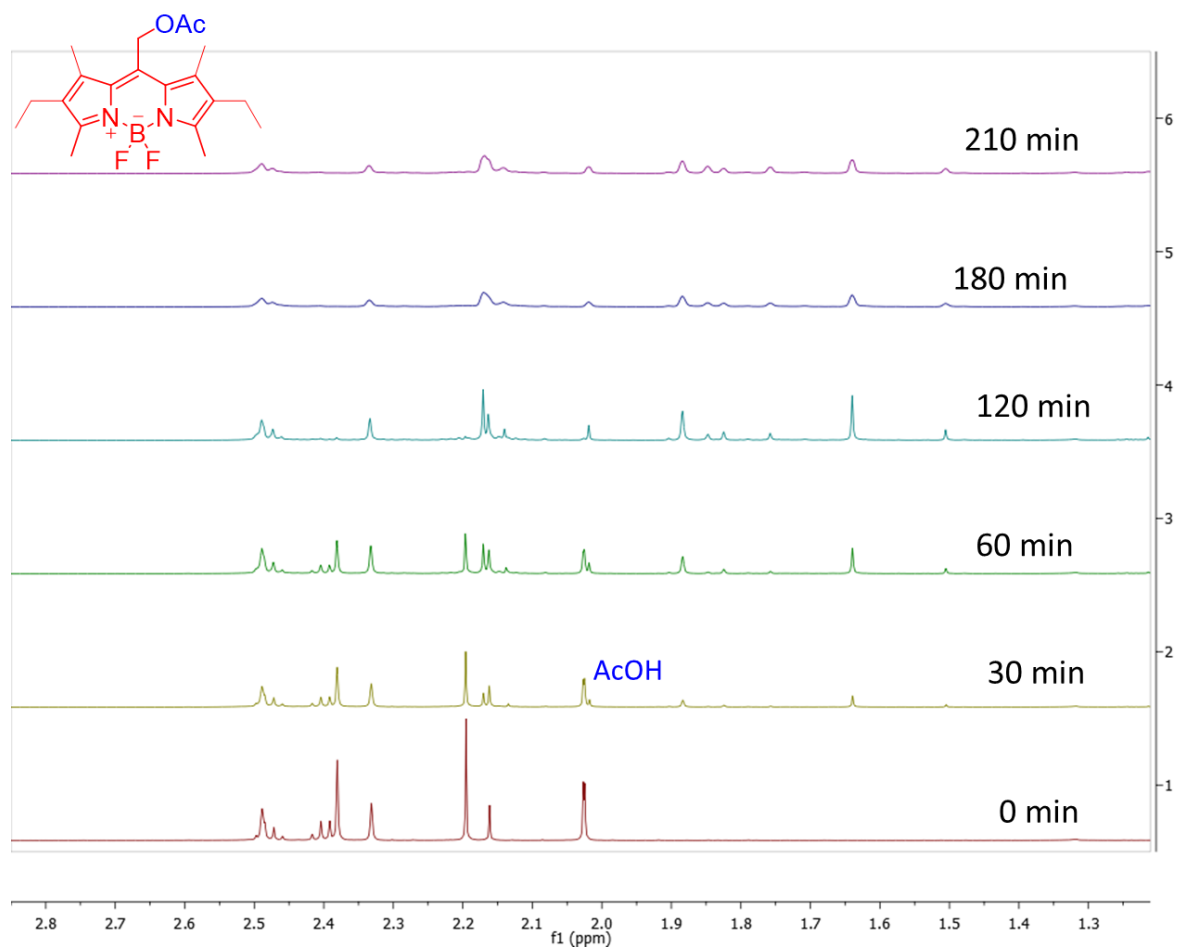
The BODIPY compound was dissolved in minimum amount of CDCl_3 to dissolve and then MeOD was added to it to make a 600 μl of 2 mM solution. A halogen lamp (500W) was used to irradiate the sample and it was followed by NMR over time.



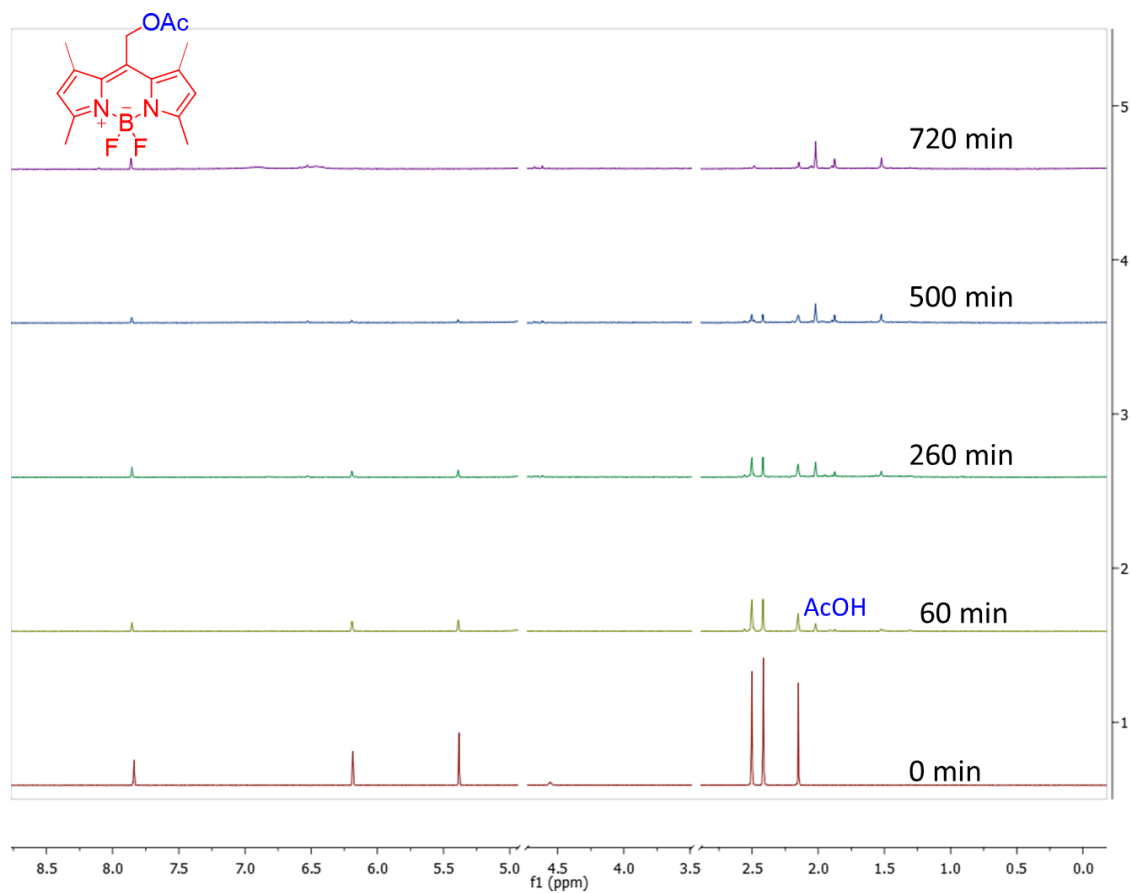
¹H NMR depicting the growth of acetic acid over time upon irradiation with a halogen lamp (500W) for compound 1



^1H NMR depicting the growth of acetic acid over time upon irradiation with a halogen lamp (500W) for compound 4



¹H NMR depicting the growth of acetic acid over time upon irradiation with a halogen lamp (500W) for compound 3

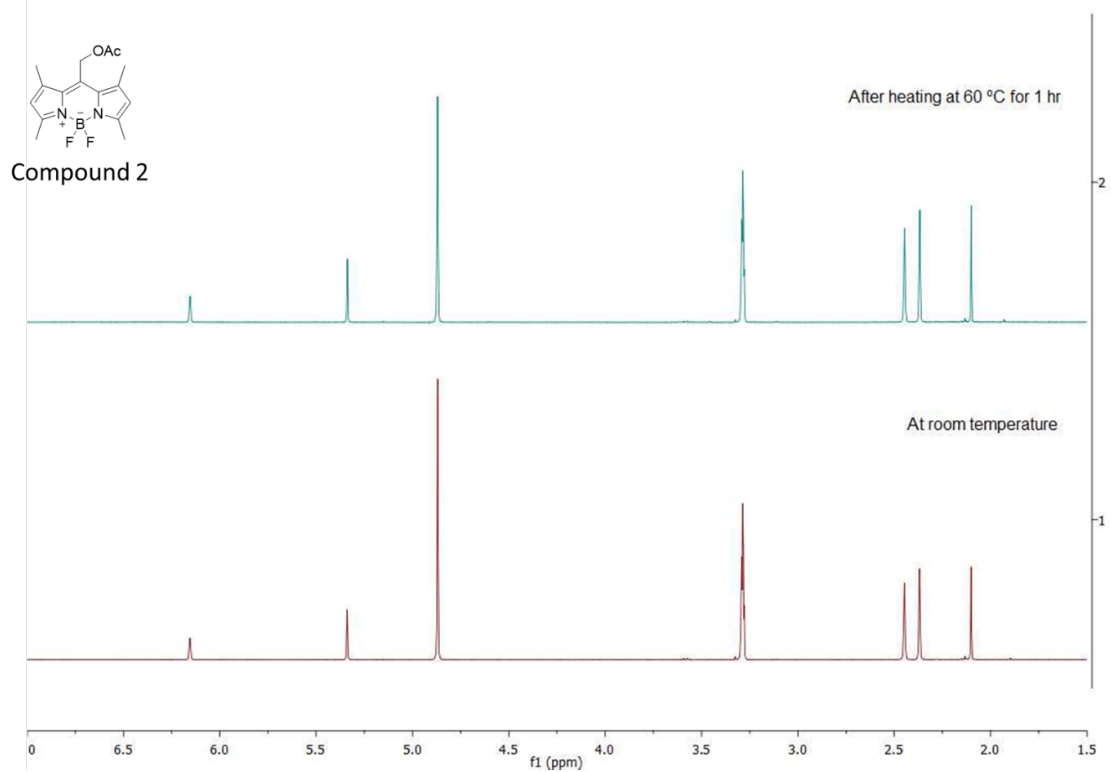
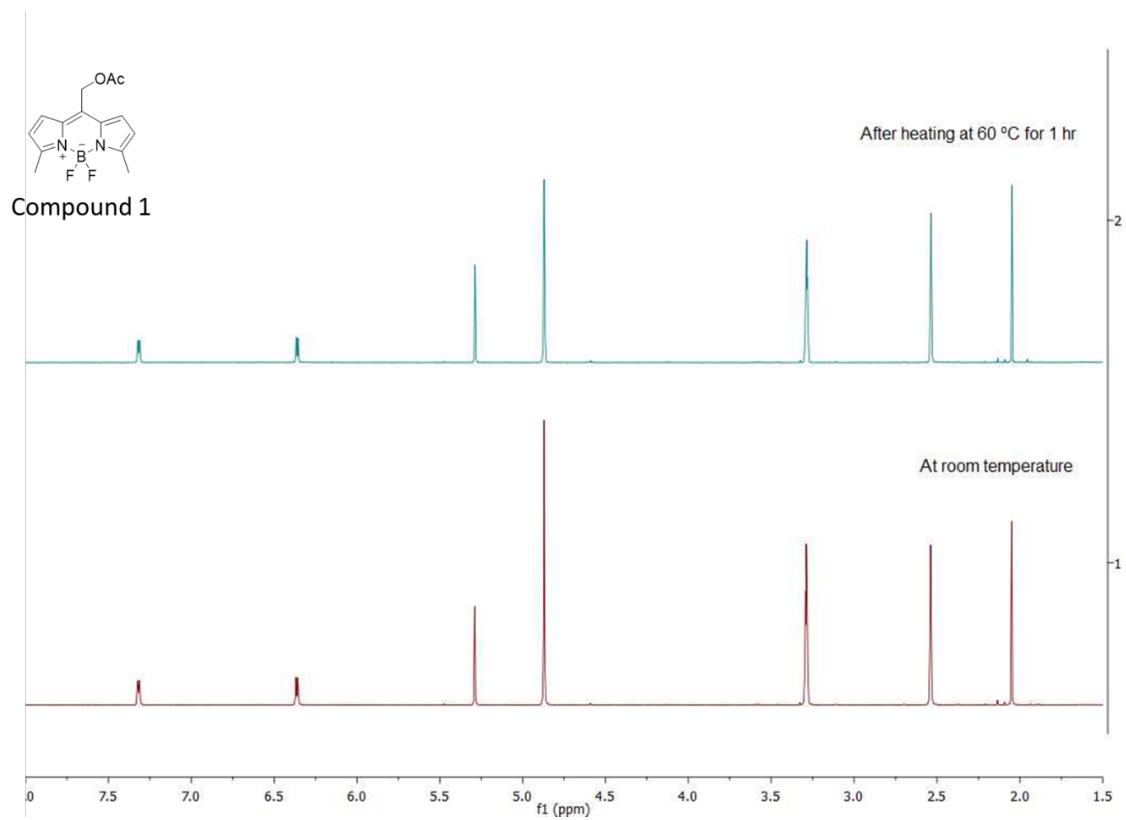


¹H NMR depicting the growth of acetic acid over time upon irradiation with a halogen lamp (500W) for compound 2

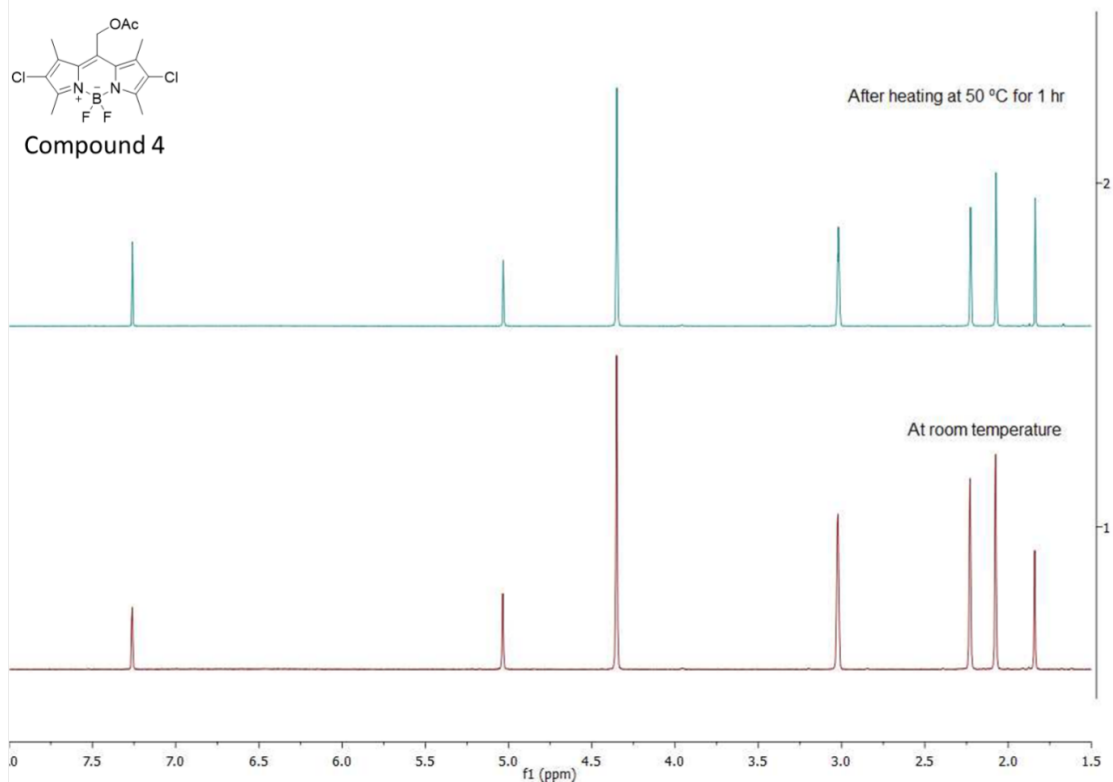
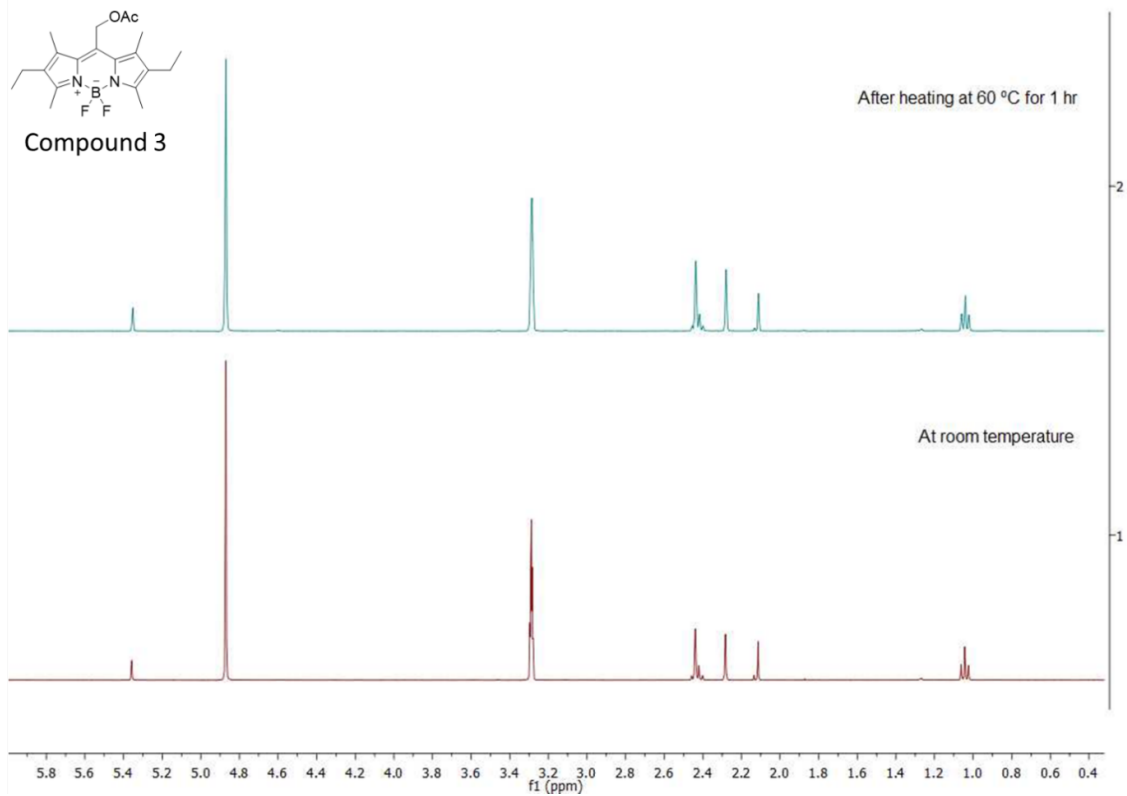
IV. Thermal stability studies

a. 1.7 mg of compounds **1,2** and **3** were dissolved in 650 μL of CD_3OD respectively. ^1H NMR (400 MHz) were recorded for these compounds at room temperature. They were then heated at 60 $^\circ\text{C}$ in the dark for 1 hour. ^1H NMR was then retaken to compare with the earlier NMRs.

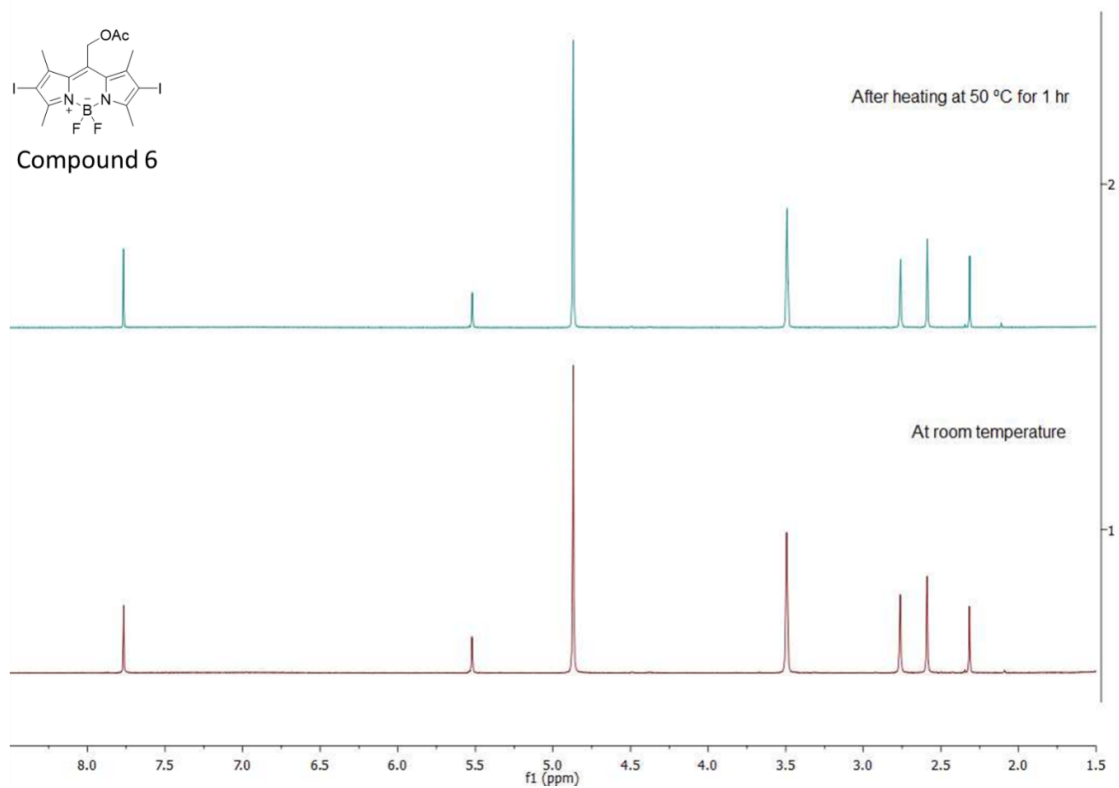
b. 1.7 mg of compounds **4** and **6** were dissolved in a 1:1 650 μL solution of CD_3OD and CDCl_3 (325 μL each) respectively. Addition of chloroform was done to aid in solubility of the compounds (4, 6 are sufficiently soluble for neat photolysis studies in MeOH, but not soluble at concentrations needed for ^1H NMR). ^1H NMR (400 MHz) were taken for both the compounds at room temperature. They were then heated at 50 $^\circ\text{C}$ in the dark for 1 hour. ^1H NMR was retaken to compare with the earlier NMRs.



Thermal studies showing no change in structure over time if heated in the dark



Thermal studies showing no change in structure over time if heated in the dark



Thermal studies showing no change in structure over time if heated in the dark

V. Quantum yield studies

Using LC-UV to determine the quantum yield for cleavage of acetic acid from the Compounds 1-6.

All quantum yields were carried out using a liquid-phase potassium ferrioxalate actinometer. The actinometer was prepared by mixing three volumes of 1.5 M $K_2C_2O_4$ solution with one volume of 1.5 M $FeCl_3$ solution in water, and stirring in complete darkness. The precipitated $K_3Fe(C_2O_4)_3 \cdot 3H_2O$ was then recrystallized three times from hot water and dried in a current of warm air. To prepare 1 L of 0.15M $K_3Fe(C_2O_4)_3 \cdot 3H_2O$ solution, 73.68 g of the precipitate was dissolved in 800 mL water; 100 mL 1.0 N sulfuric acid was added and filled to the mark with water, again in complete darkness. For all quantitative work the preparation and manipulation of the ferrioxalate solutions and samples must be carried out in a darkroom, using a red light. Irradiating the ferrioxalate solution and monitoring the subsequent change in absorbance at 510 nm determines the light intensity. Irradiation was conducted using 532 nm excitation from a ND:YAG laser source (1st harmonic). Autopipettes were used to ensure all volumes were accurately measured.

For each actinometric measurement, a methacrylate cuvette was filled with 3 mL of 0.15 M ferrioxalate solution. The cell was placed in the sample holder, stirred and irradiated for a set period of time (0, 0.25, 0.50, 0.75, 1, 2, 3 minutes). After the allocated irradiation time the solution was transferred into a 25 mL volumetric flask, to which was added in sequence 6 mL of a developer solution (0.05 mol% phenanthroline/0.75 M acetate/0.2 M sulfuric acid), and 5 mL 1M sodium fluoride solution in water. The sample was diluted to 25mL with water, mixed and allowed to incubate for 10 min. After the

incubation period was complete, 3 mL of sample was transferred into 1 cm methacrylate cuvette and the absorbance at 510 nm read using a UV-Vis spectrophotometer.

Using iron sulfate standard solutions between 1.6×10^{-5} M to 9.6×10^{-5} M, a standard curve based on absorbance of the ferrioxalate/phenanthroline complex at 510 nm was compiled and the irradiated samples absorbances were compared to yield the concentration iron (II) cleaved via photolysis within the timescale of experiment.

The flux of the laser was calculated the following equations:

$$I = \frac{\Delta n}{(10^{-3} \cdot \Phi \cdot V_1 \cdot t)}$$

where I is the flux (Einstein/L/s), Δn is the moles of Fe^{2+} photogenerated, ϕ is the quantum yield at 532 nm, V_1 is the irradiated volume (mL), and t = irradiation time (seconds).

$$\Delta n = \frac{10^{-3} \cdot V_1 \cdot V_3 \cdot C_T}{V_2}$$

where V_2 is the volume taken from the irradiated sample (mL), V_3 is the volume after dilution for concentration determination (mL), and C_T is the concentration of Fe^{2+} after dilution (M)

$$C_T = \frac{abs}{\epsilon \cdot l}$$

where abs is the absorbance at 510nm, ϵ is the molar absorptivity ($M^{-1}cm^{-1}$) and l is the path length .

The 0.15 M potassium ferrioxalate solution has only a weak absorbance at 532 nm (<2), so the flux was corrected by the %light transmission through a 1 cm cuvette with the experimentally determined absorption at 532.

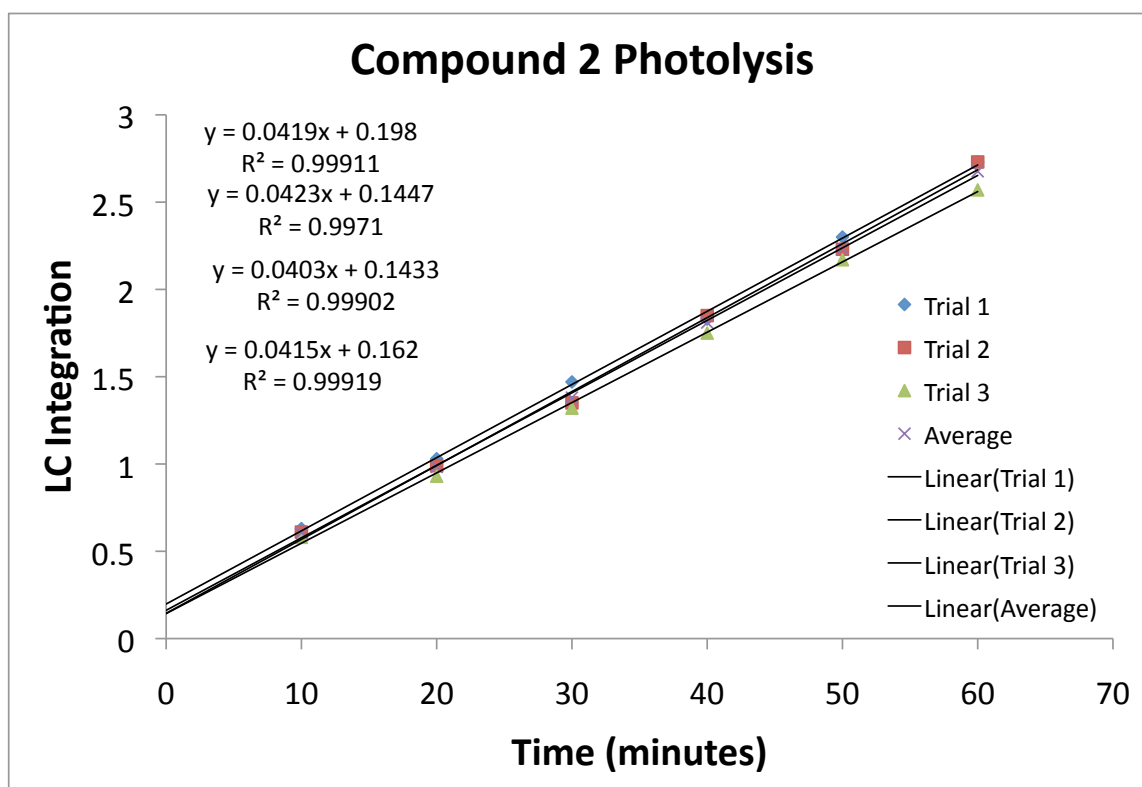
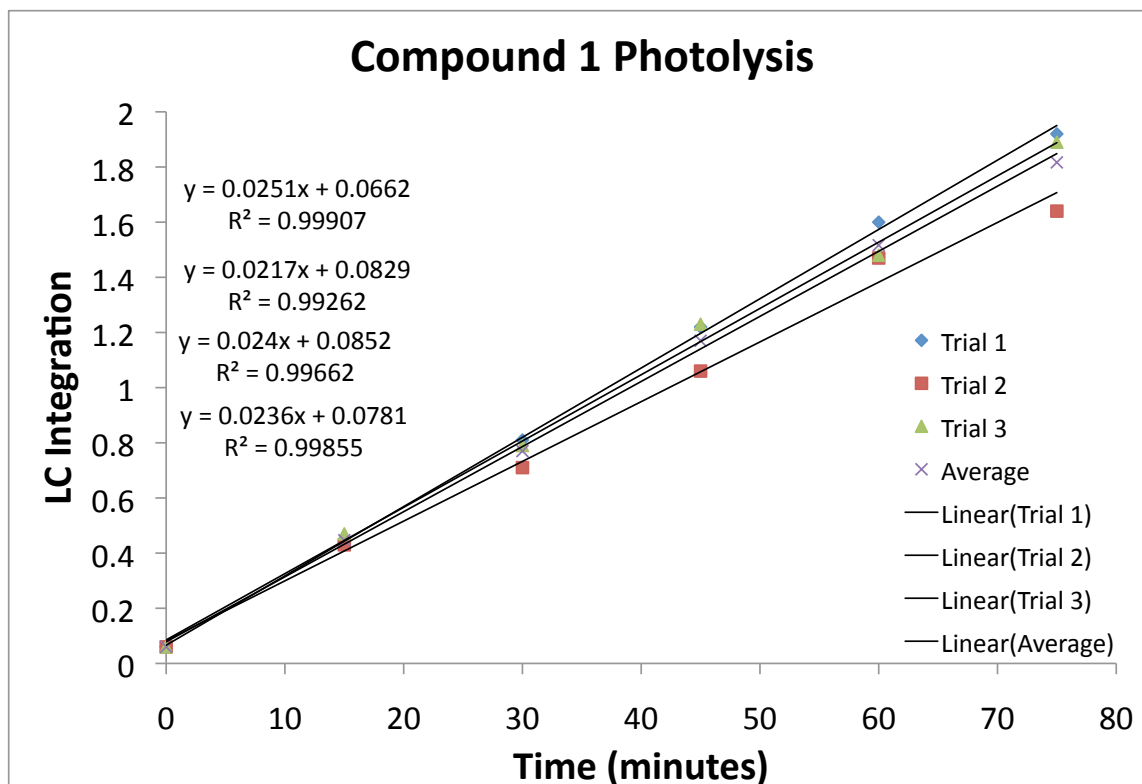
For Compounds 1-6

For each compound, a solution of 1000 ppm was prepared using 1 mg of sample and dissolving in 1 mL methanol. Due to solubility issues, samples were predissolved in 20 μ L of acetonitrile and injected into the 1 mL of methanol (the exception being Compound 4, where tetrahydrofuran was used in place of acetonitrile). Each sample cuvette was placed in the sample holder and irradiated for a specified period of time (so as not to exceed 30% cleavage). At each time point selected, 10 μ L of the irradiated solution was removed and placed into a LC vial fitted with a 250 μ L glass vial insert fitted with polymer feet. Each quantum yield was determined as the average of three independent photolysis runs.

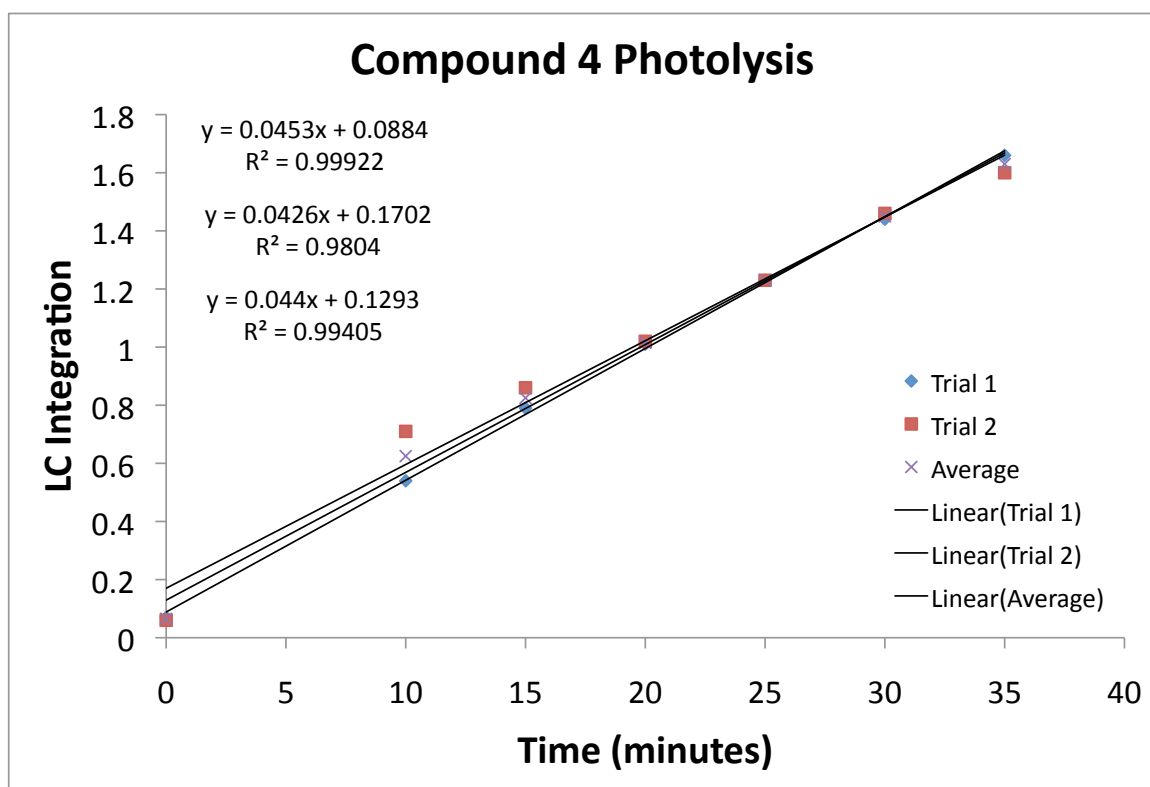
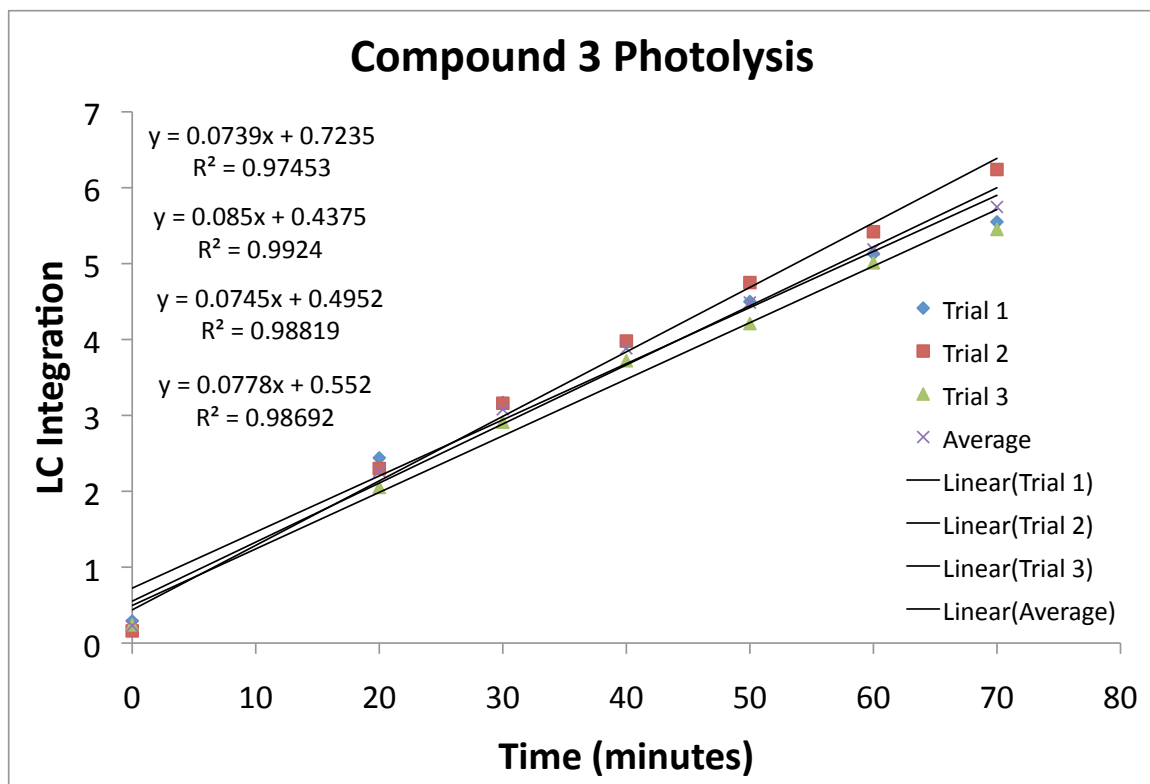
LC-UV was conducted for all samples using an XDB-C18 column and monitoring the absorbance at 210 nm with 2 μ L of sample injected. The eluent system was a 1 mmol/L sulfuric acid:8 mmol/L sodium sulfate (made using 54.3 μ L concentrated sulfuric acid and 1.1370 g sodium sulfate in 1L of water). Column washes between runs were done using either pure acetonitrile or 1:1 acetonitrile:methanol. For Compounds 1-3, a flow rate of 0.8 mL/min was used with were the acidic buffer was ran for 3 minutes with the acetonitrile wash starting at 3.1 minute until 6 minute. This was followed with a post-run of

9 minutes. For Compounds **4-6**, a flow rate of 0.7 mL/min was used with were the acidic buffer was ran for 3 minutes with the acetonitrile:methanol wash starting at 3.1 minute until 6 minute. This was followed with a post-run of 14 minutes.

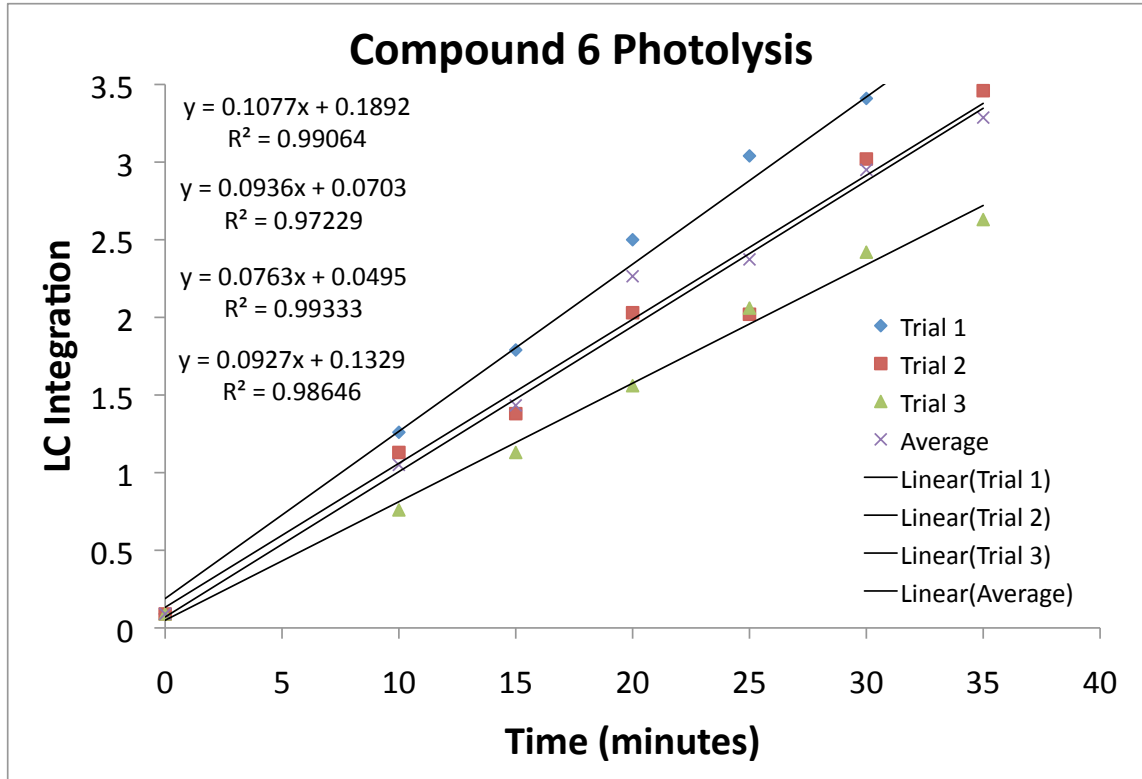
Using acetic acid standard solutions between 5-1000 ppm, a standard curve based on the LC-UV integration of acetic acid was compiled and the irradiated samples peak integrations were compared to yield the concentration of acetic acid cleaved via photolysis within the timescale of experiment.



Growth of acetic acid (measured by LC) over time upon irradiation of the photocage with 532nm LASER



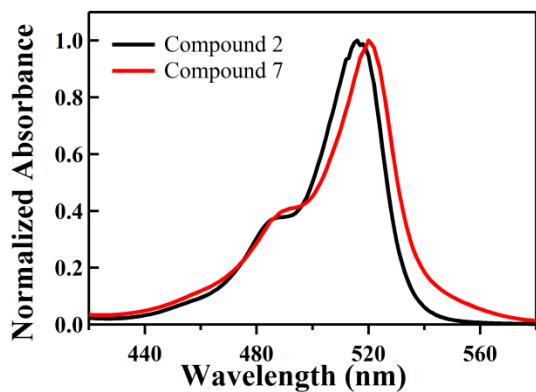
Growth of acetic acid (measured by LC) over time upon irradiation of the photocage with 532nm LASER



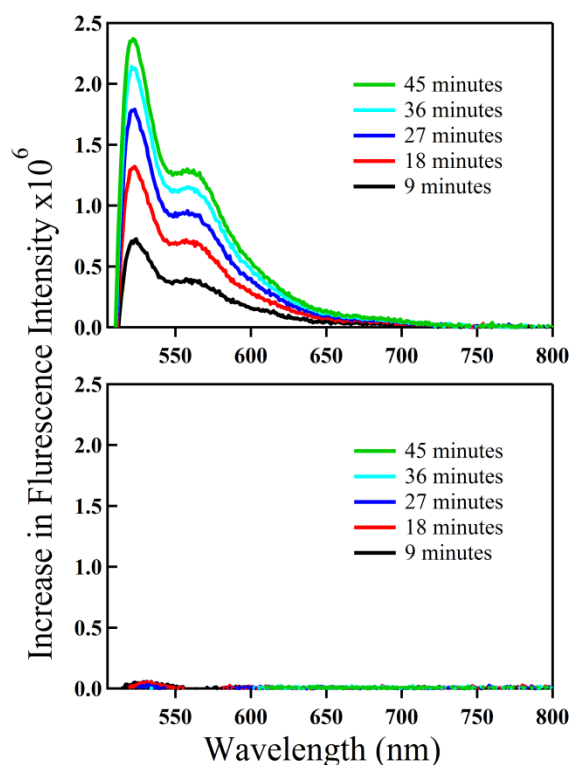
Growth of acetic acid (measured by LC) over time upon irradiation of the photocage with 532nm LASER

VI. Fluorescence studies of compound 7

Steady-state absorption spectra of compound 2 and 7 in methanol were measured using a Hewlett-Packard 8453 UV-Visible spectrometer (Agilent technologies Inc., Santa Carla, CA). Compound 7 contains a fluorescence quencher 2, 4 Dinitrobenzene attached to BODIPY through a photo sensitive ester linkage. A 100 μ M solution of compound 7 in *N,N*-Bis(2-hydroxyethyl) taurine (BES) buffer (pH=7.0, 20 mM BES, 0.14M NaCl, 2.9mM KCl, 0.1 w/v glucose, 0.1 w/v BSA) was excited with a mercury lamp (100% power, X-Cite 120 PC, EXFO Photonic Solutions Inc., Mississauga, Ontario, Canada) through excitation filter (HQ500/20 nm, Chroma Technology Crop. Bellows Falls, VT) and reflected by dichoric mirror (Q515LP, Chroma Technology Crop.) and directed to the cuvette. Quencher release from the compound 7 was monitored by measuring an increase in steady-state fluorescence from released BODIPY using a SPEX Fluoromax (ISA Jobin-Yvon/SPEX, Edison, NJ) with a 5 nm band pass and corrected for lamp spectral intensity and detector response. As a control, similar steady state fluorescence measurements were performed for compound 7 in the dark without any light exposure. For all fluorescence measurements samples were excited at 500 nm.

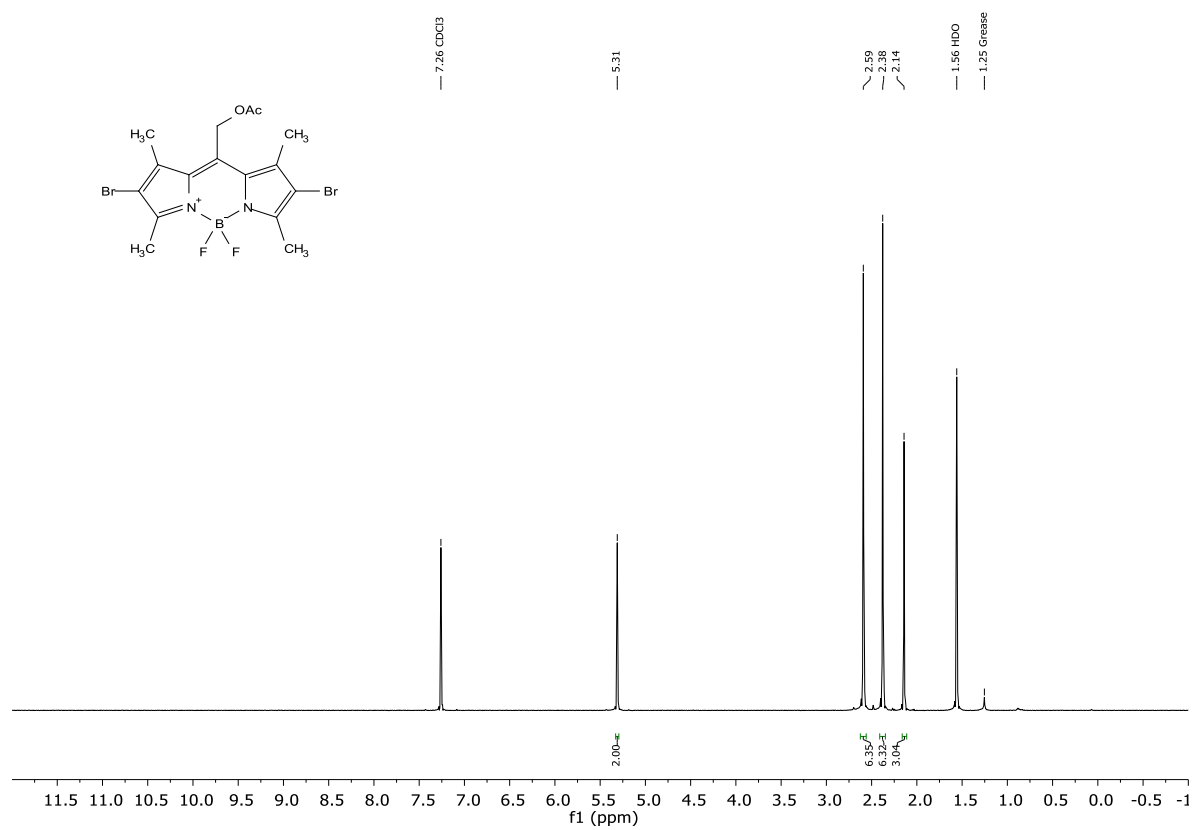


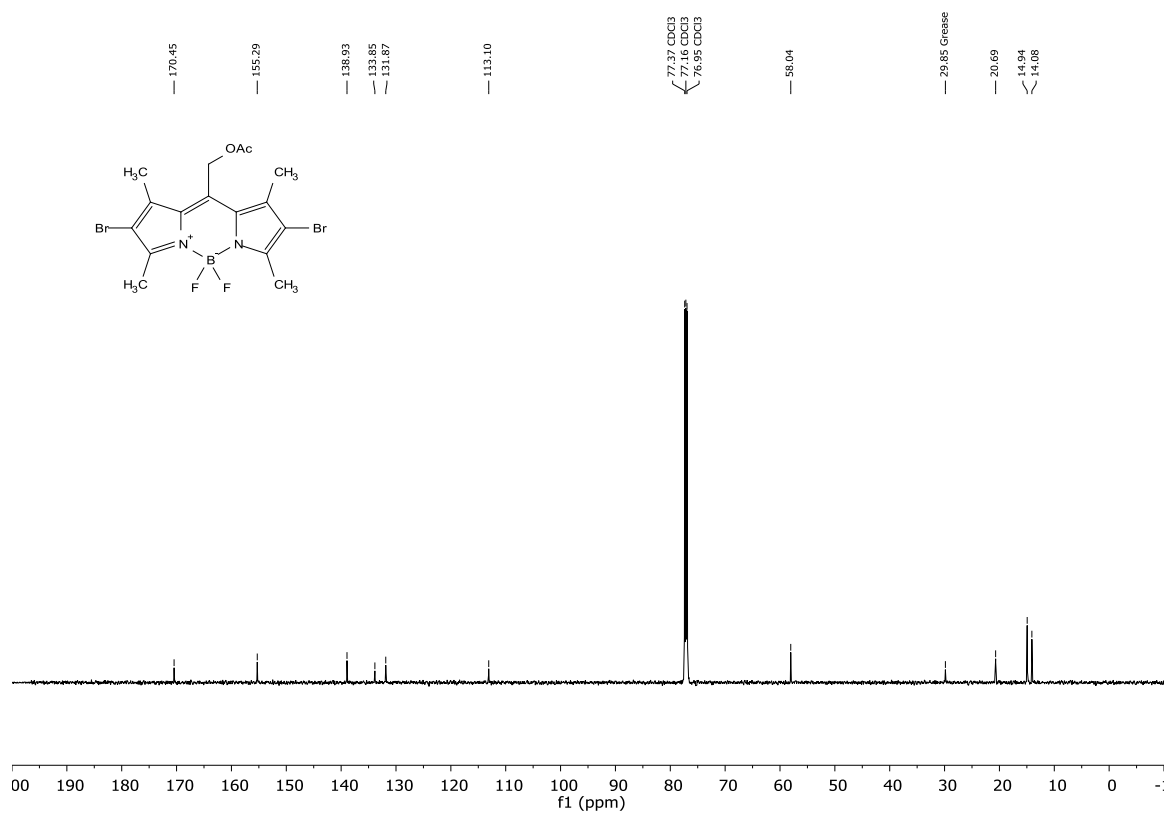
Normalized absorption spectra for compound 2 (black) and 7 (red) in methanol.



Increase in free BODIPY fluorescence signal over time with quencher release from compound 7 in BES buffer. (Upper panel) sample was continuously irradiated with light, and in the (lower panel) the sample was kept in dark without any light irradiation except for brief exposures during spectral measurements.

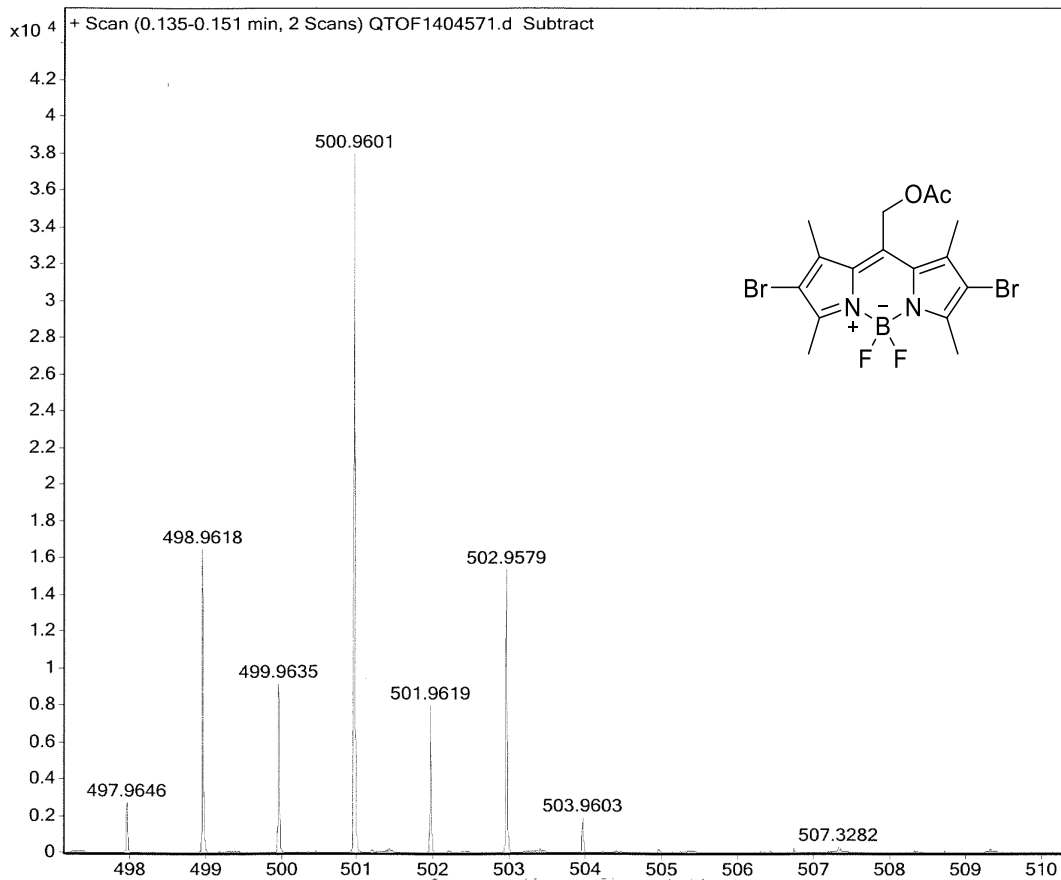
VII. NMR and MS spectra

Compound **5** ^1H NMR of compound **5**



¹³C NMR of compound 5

Sample Name BromoBoDIPY **Position** vial1 **Instrument Name** QTOF **User Name** CIF-PC\admin
Inj Vol 2 **InjPosition** **SampleType** Sample **IRM Calibration Status** Success
Data Filename QTOF1404571.d **ACQ Method** ESI2-pos.m **Comment** **Acquired Time** 8/20/2014 1:34:55 PM

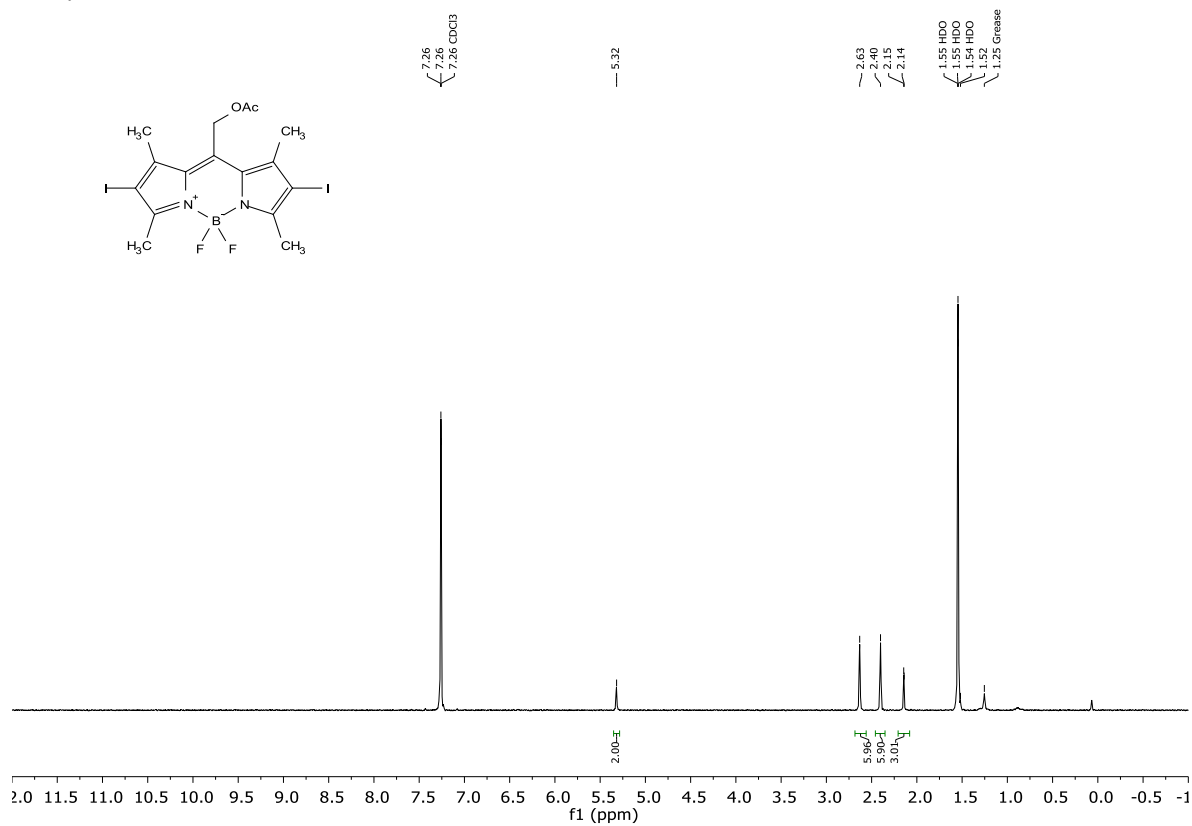


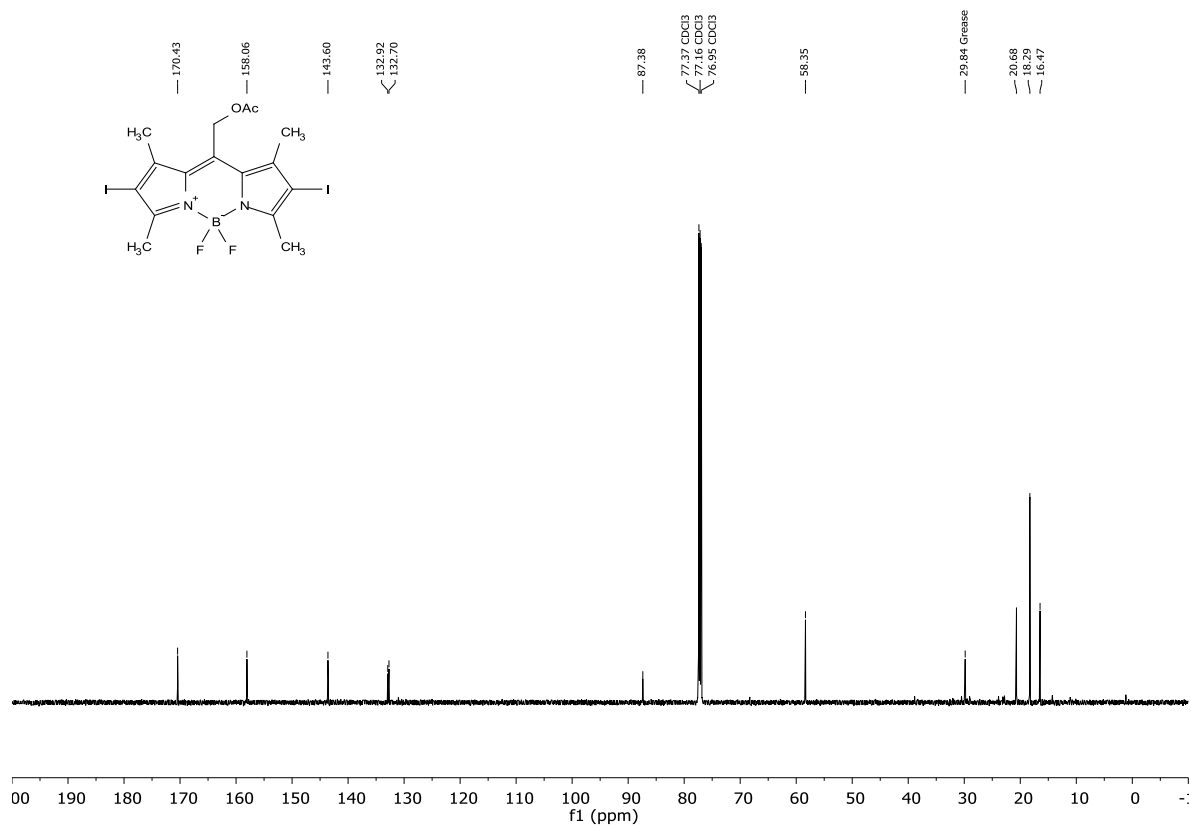
Formula Calculator

Formula (M)	Score (MFG)	Mass	Mass (MFG)	m/z (Calc)	Diff (ppm)	DBE	m/z
C16 H17 B Br2 F2...	100	474.97538	474.97542	497.9646	0.09	8	497.9646

Mass Spec of compound 5

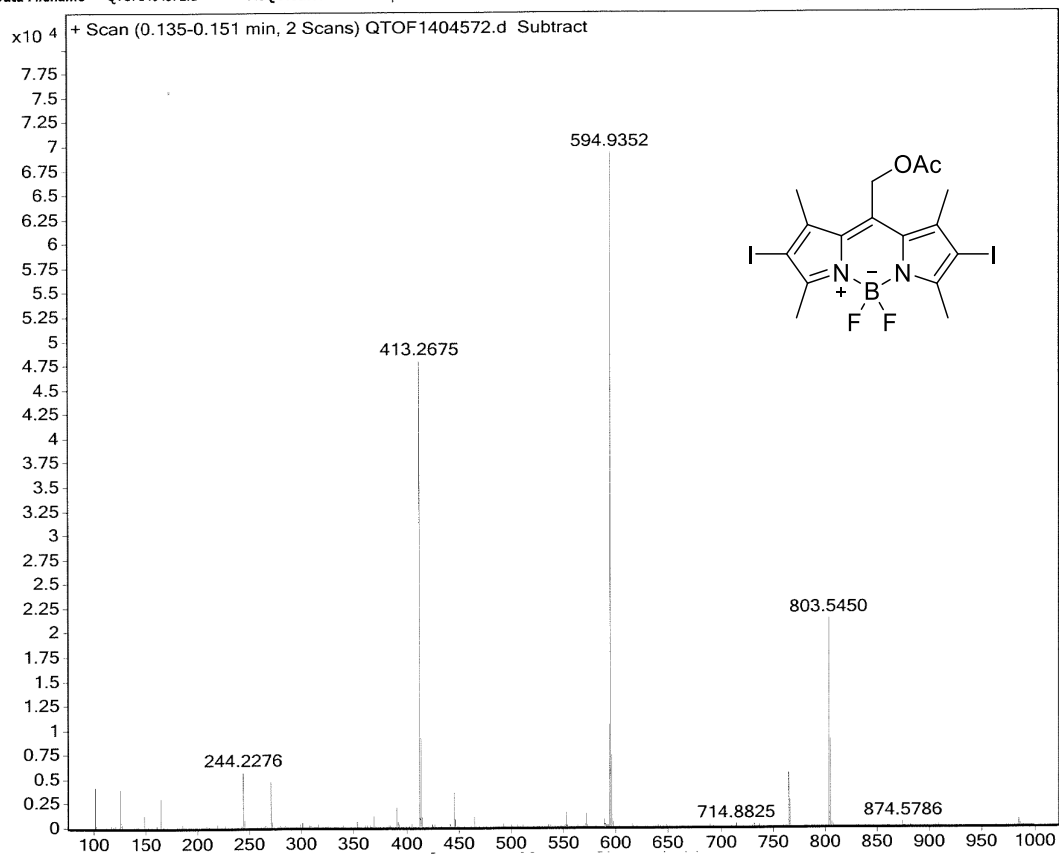
Compound 6

 $^1\text{H-NMR}$ of compound 6



¹³C-NMR of compound 6

Sample Name	IodoBoDIPY	Position	vial1	Instrument Name	QTOF	User Name	CIF-PC/admin
Inj Vol	2	InjPosition		SampleType	Sample	IRM Calibration Status	Success
Data Filename	QTOF1404572.d	ACQ Method	ESI2-pos.m	Comment		Acquired Time	8/20/2014 1:39:32 PM

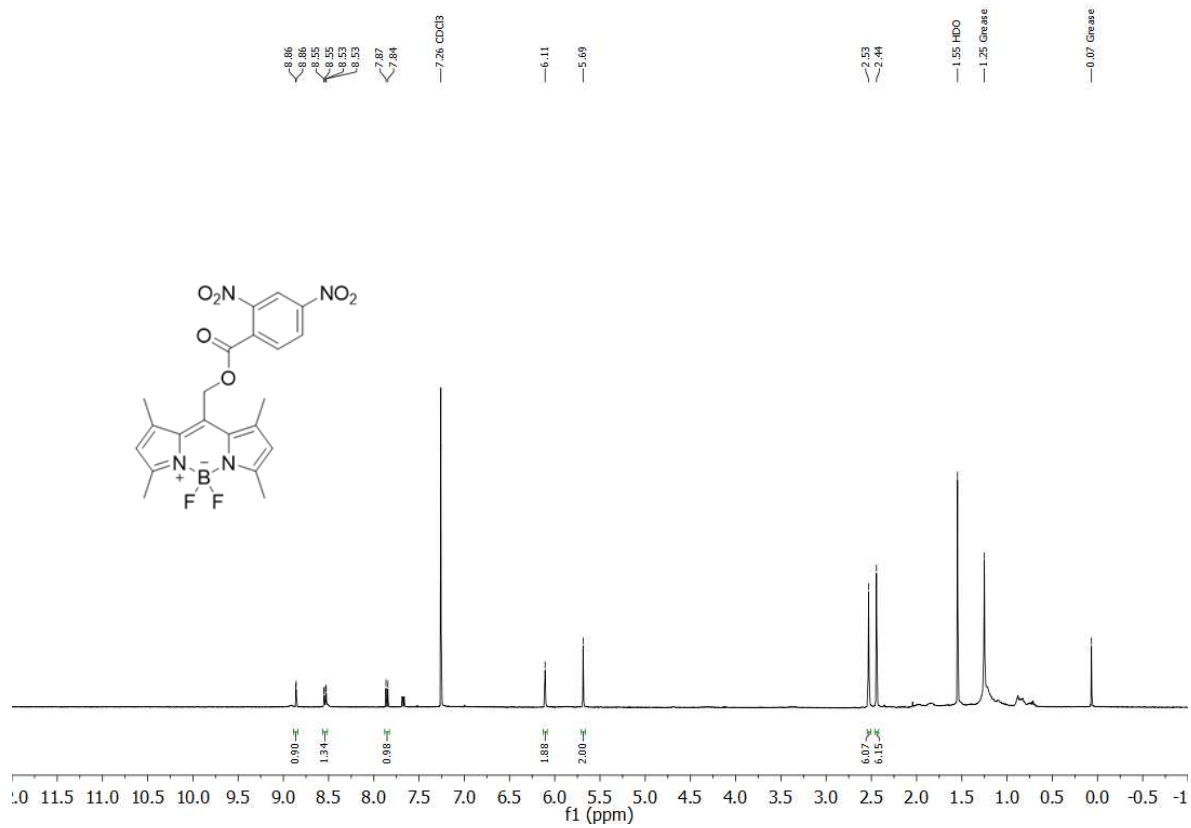


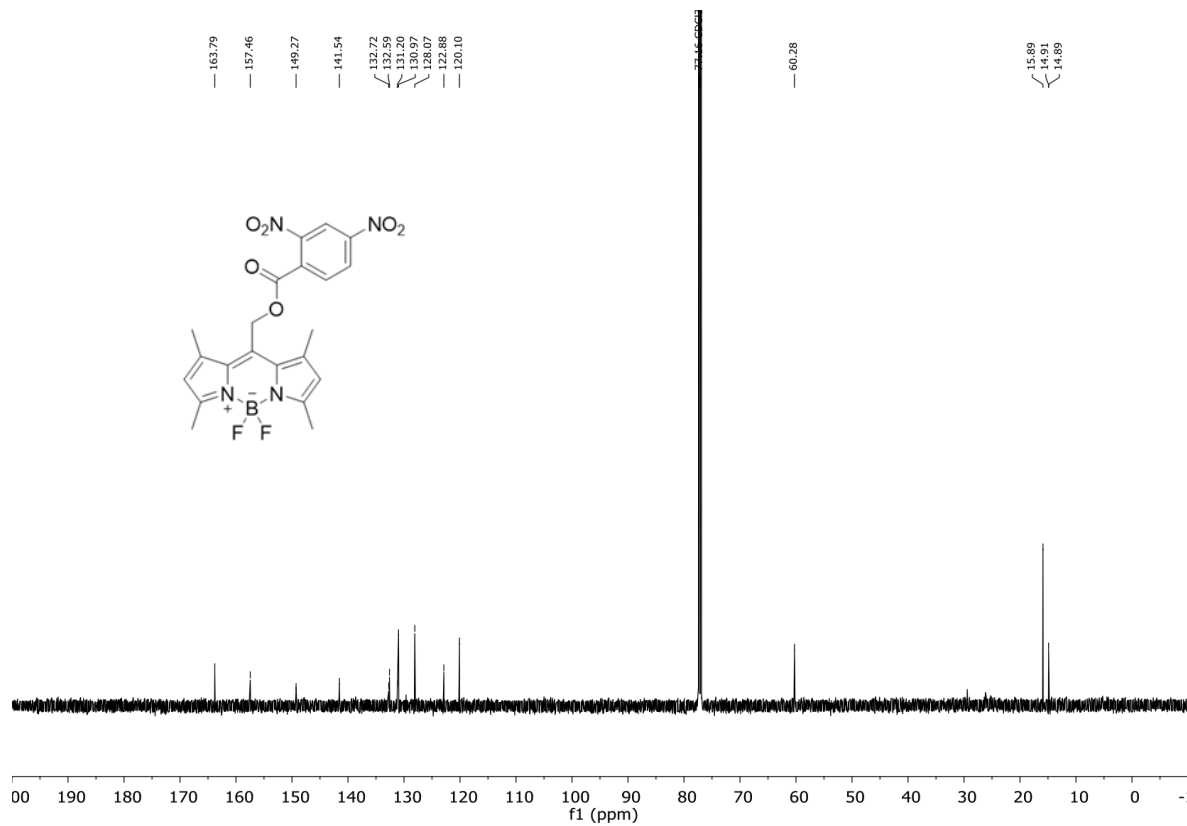
Formula Calculator

Formula (M)	Mass	Mass (MFG)	m/z (Calc)	Diff (ppm)	DBE	m/z
C16 H17 B F2 I2 N...	570.94858	570.94768	593.9369	-1.57	8	593.9378

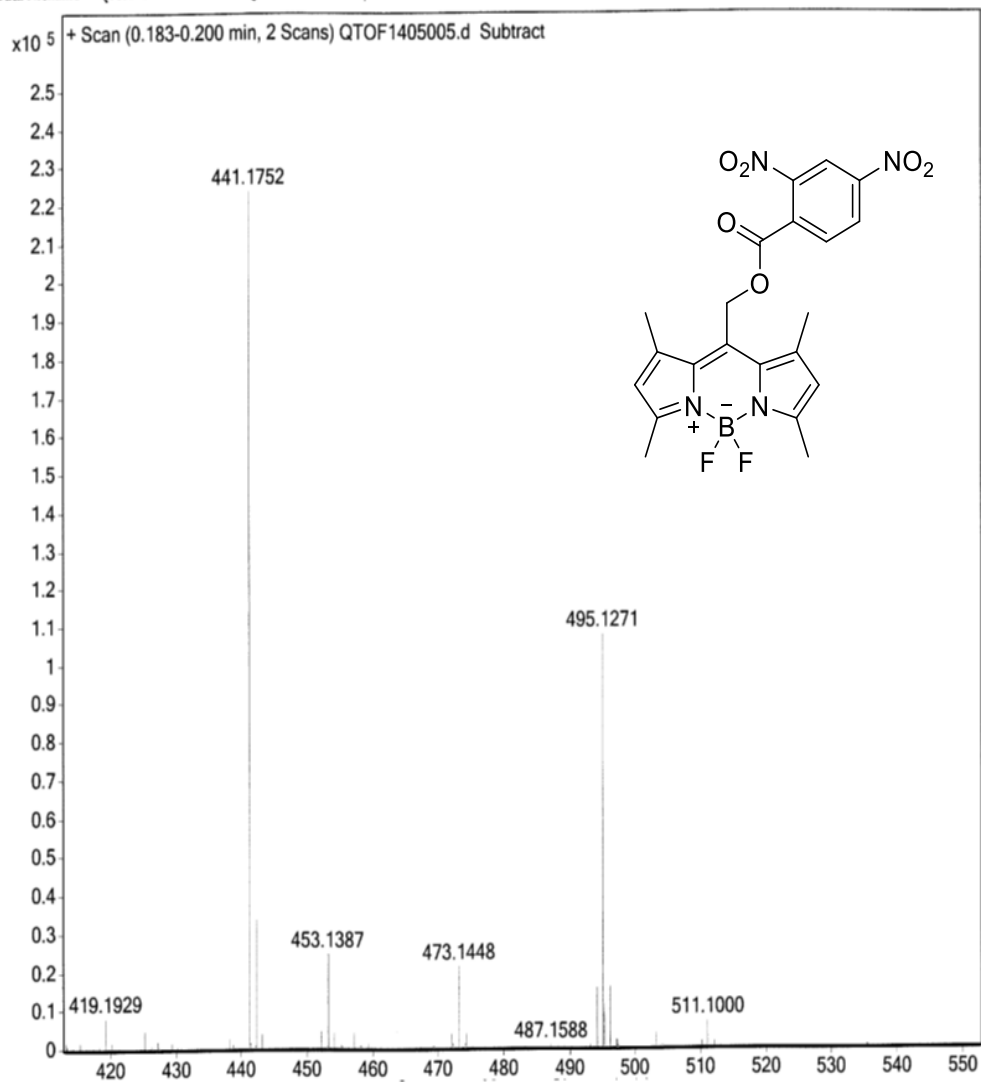
Mass Spec of compound 6

Compound 7

 $^1\text{H-NMR}$ of compound 7

 $^{13}\text{C-NMR}$ of compound 7

Sample Name	blue	Position	Vial 1	Instrument Name	QTOF	User Name	CIF-PC\admin
Inj Vol	1	InjPosition		SampleType	Sample	IRM Calibration Status	Success
Data Filename	QTOF1405005.d	ACQ Method	ESI2-pos.m	Comment		Acquired Time	12/8/2014 4:53:41 PM



Mass Spec of compound 7

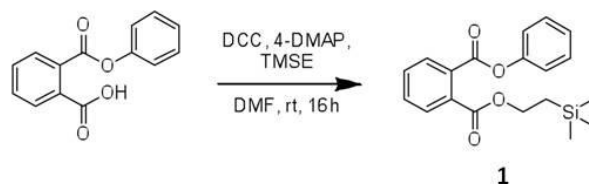
VIII. References

- (1) Frisch, M. J.; Trucks, G. W.; Schlegel, H. B.; Scuseria, G. E.; Robb, M. A.; Cheeseman, J. R.; Scalmani, G.; Barone, V.; Mennucci, B.; Petersson, G. A.; Nakatsuji, H.; Caricato, M.; Li, X.; Hratchian, H. P.; Izmaylov, A. F.; Bloino, J.; Zheng, G.; Sonnenberg, J. L.; Hada, M.; Ehara, M.; Toyota, K.; Fukuda, R.; Hasegawa, J.; Ishida, M.; Nakajima, T.; Honda, Y.; Kitao, O.; Nakai, H.; Vreven, T.; Jr., J. A. M.; Peralta, J. E.; Ogliaro, F.; Bearpark, M.; Heyd, J. J.; Brothers, E.; Kudin, K. N.; Staroverov, V. N.; Kobayashi, R.; Normand, J.; Raghavachari, K.; Rendell, A.; Burant, J. C.; Iyengar, S. S.; Tomasi, J.; Cossi, M.; Rega, N.; Millam, J. M.; Klene, M.; Knox, J. E.; Cross, J. B.; Bakken, V.; Adamo, C.; Jaramillo, J.; Gomperts, R.; Stratmann, R. E.; Yazyev, O.; Austin, A. J.; Cammi, R.; Pomelli, C.; Ochterski, J. W.; Martin, R. L.; Morokuma, K.; Zakrzewski, V. G.; Voth, G. A.; Salvador, P.; Dannenberg, J. J.; Dapprich, S.; Daniels, A. D.; Farkas, O.; Foresman, J. B.; Ortiz, J. V.; Cioslowski, J.; Fox, D. J. *Gaussian 09, Revision A.02* **2009**.
- (2) Isobe, H.; Takano, Y.; Kitagawa, Y.; Kawakami, T.; Yamanaka, S.; Yamaguchi, K.; Houk, K. N. *Mol. Phys.* **2002**, *100*, 717.
- (3) Yamaguchi, K.; Jensen, F.; Dorigo, A.; Houk, K. N. *Chem. Phys. Lett.* **1988**, *149*, 537.
- (4) Noodleman, L.; Case, D. A. *Adv. Inorg. Chem.* **1992**, *38*, 423.
- (5) Lim, M. H.; Worthington, S. E.; Dulles, F. J.; Cramer, C. J. In *Chemical Applications of Density-Functional Theory*; Laird, B. B., Ross, R. B., Ziegler, T., Eds.; Amer Chemical Soc: Washington, 1996; Vol. 629, p 402.

- (6) Whited, M. T.; Patel, N. M.; Roberts, S. T.; Allen, K.; Djurovich, P. I.; Bradforth, S. E.; Thompson, M. E. *Chem. Commun.* **2012**, 48, 284.
- (7) Krumova, K.; Cosa, G. *J. Am. Chem. Soc.* **2010**, 132, 17560.
- (8) Bunch, T. A.; Brower, D. L. *Development* **1992**, 116, 239.
- (9) Bunch, T. A.; Grinblat, Y.; Goldstein, L. S. *Nucleic Acids Res.* **1988**, 16, 1043.
- (10) Zavortink, M.; Bunch, T. A.; Brower, D. L. *Cell Adhes Commun* **1993**, 1, 251.
- (11) Smith, E. A.; Bunch, T. A.; Brower, D. L. *Anal. Chem.* **2007**, 79, 3142.
- (12) Strober, W. In *Current Protocols in Immunology*; John Wiley & Sons, Inc.: 2001.

APPENDIX B: CHAPTER 5

General Information: Phenyl hydrogen phthalate¹, 2-(trimethylsilyl)ethyl hydrogen phthalate², and 3-(2-benzothiazolyl)-7-hydroxycoumarin³ were synthesized as previously described (all spectra for these compounds matched those previously reported).

Experimental procedures.

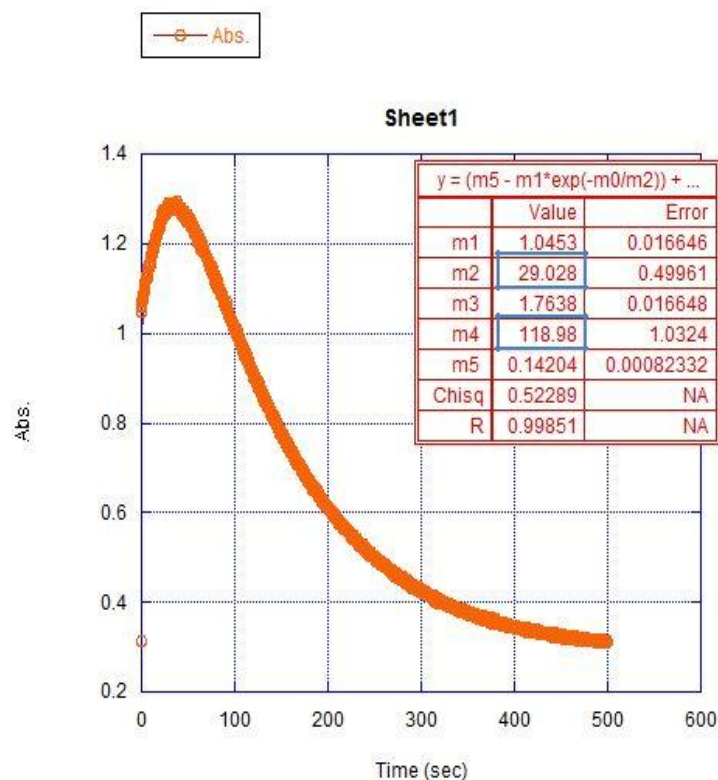
(1) **Synthesis of 1.** Phenyl hydrogen phthalate (1.50 g, 6.21 mmol), 2-trimethylsilylethanol (1 ml, 6.98 mmol) and 4-N,N-dimethylaminopyridine (0.085 g, 0.69 mmol) were dissolved in dry DMF (4 ml), followed by continuous stirring of the solution. N,N-dicyclohexylcarbodiimide (1.54 g, 7.45 mmol), dissolved in dry DMF (2 mL), was next added to the reaction mixture and the reaction was stirred under an argon atmosphere overnight. The dicyclohexylurea byproduct was filtered off as a white solid. The solvent was then removed under reduced pressure to yield the crude product as a yellow oil. Flash chromatography (Hexanes/EtOAc, 90:10) gave the pure final product (0.595 g, 28%) as a colorless oil. (¹H NMR, CD₃OD, 400 MHz) δ 7.90 (m, 1H), 7.83 (m, 1H), 7.70 (m, 2H), 7.46 (m, 2H), 7.29(m, 3H), 4.42 (m, 2H), 1.09 (m, 2H), 0.04 (s, 9H); (¹³C NMR, CD₃OD, 100 MHz) δ 169.1, 167.9, 152.5, 133.9, 133.1, 132.9, 132.7, 130.7, 130.4, 130.2, 127.3,

122.7, 65.4, 18.3, -1.4; High-res MS(ESI) calculated for formula C₁₉H₂₃O₄Si (M+H)⁺ requires 343.1360; found 343.1360.

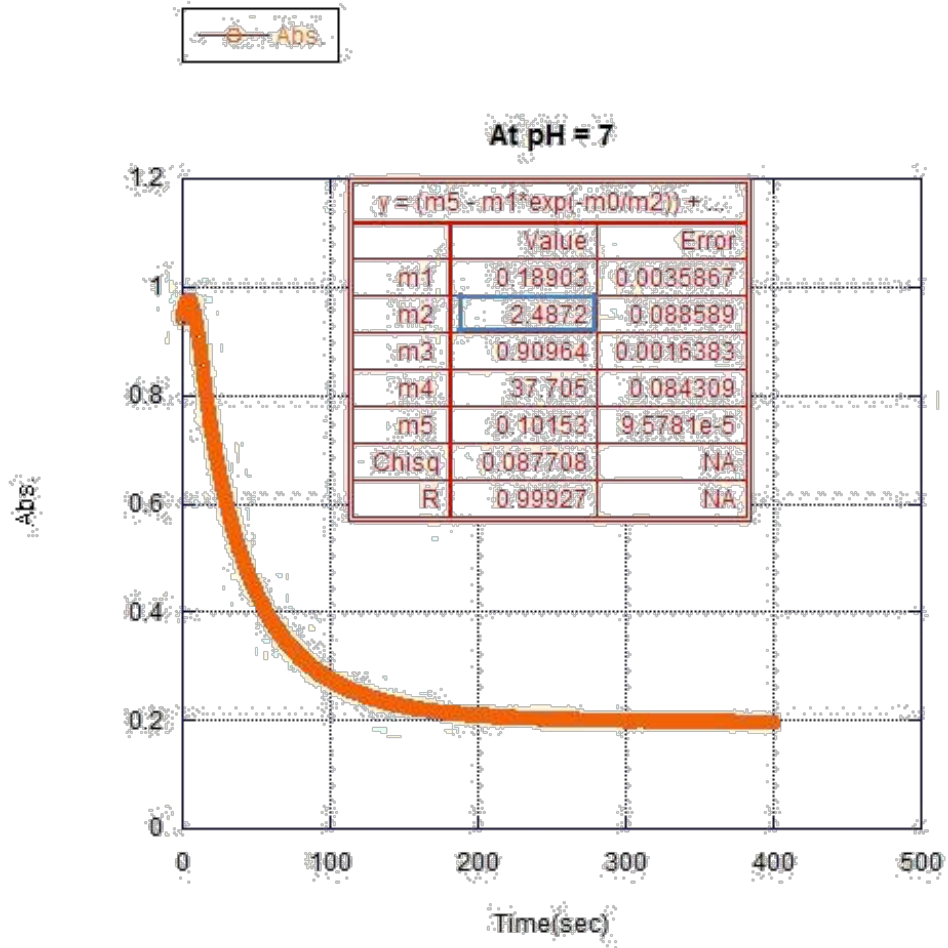
Experimental procedures for titrations of compounds 1-3

A stock solution of **1** was prepared (9.05×10^{-2} M) in DMSO- D₆ and distributed equally (97 μ L) into 12 vials. To these vials was added varying equivalents of a second stock solution made of 1M TBAF/THF (7.44×10^{-2} M) in DMSO-D₆ for 4 h. 0.5 ml D₂ O was then added to each vial. ¹H NMR spectra of each was then recorded. The titration was repeated three times and the results were averaged. Conversion was calculated by measuring the ratio of DMSO-D₆ signal integration with the integration of the –CH₂ peak (δ 4.42 ppm) in **1**.

Kinetic fits of phenyl hydrogen phthalate hydrolysis, following growth and decay of phthalic anhydride at 300 nm.

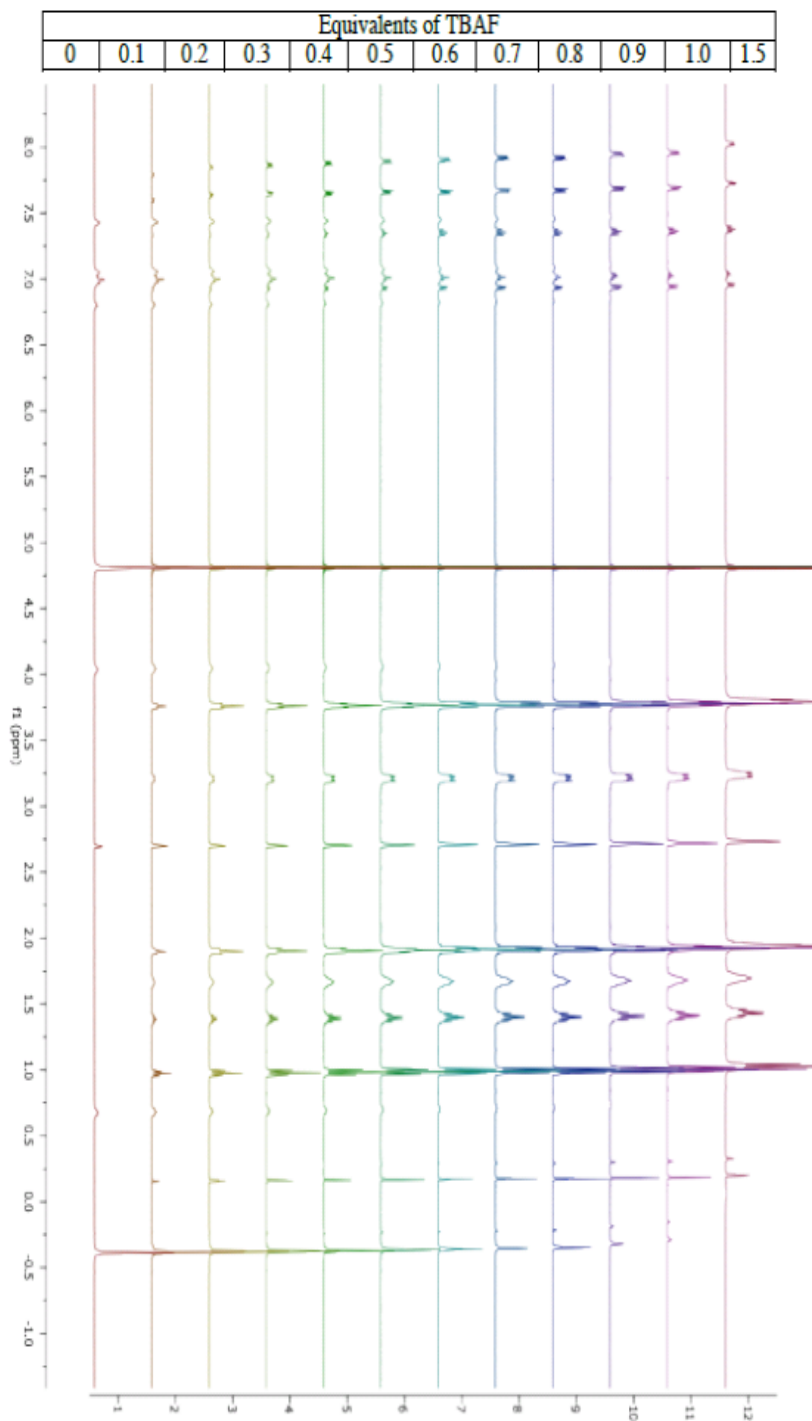


Kinetic fit for the hydrolysis of Phenyl Hydrogen Phthalate at pH = 5.7 buffer
(AcOH/AcO-(0.08M)) using the Kaleidograph software

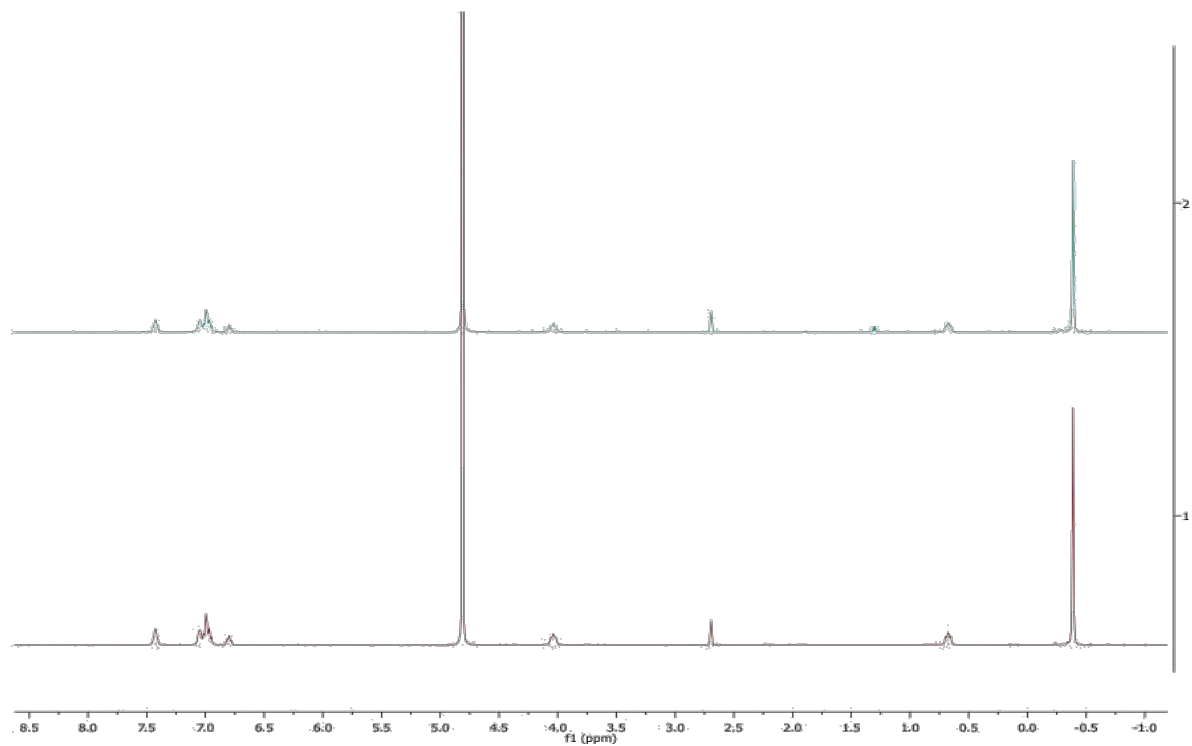


Kinetic fit for the hydrolysis of Phenyl Hydrogen Phthalate at pH = 7.0 buffer
(NaOH/KH₂PO₄(0.1M))

^1H NMR titration of **1** with TBAF

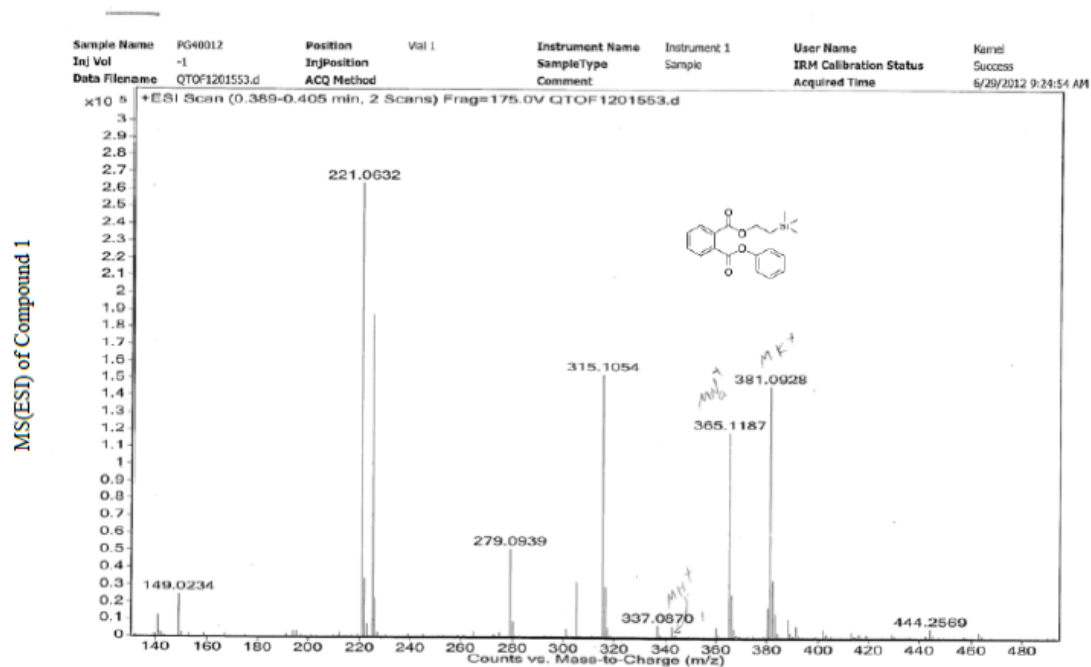


^1H NMR titration of **1** with TBAF

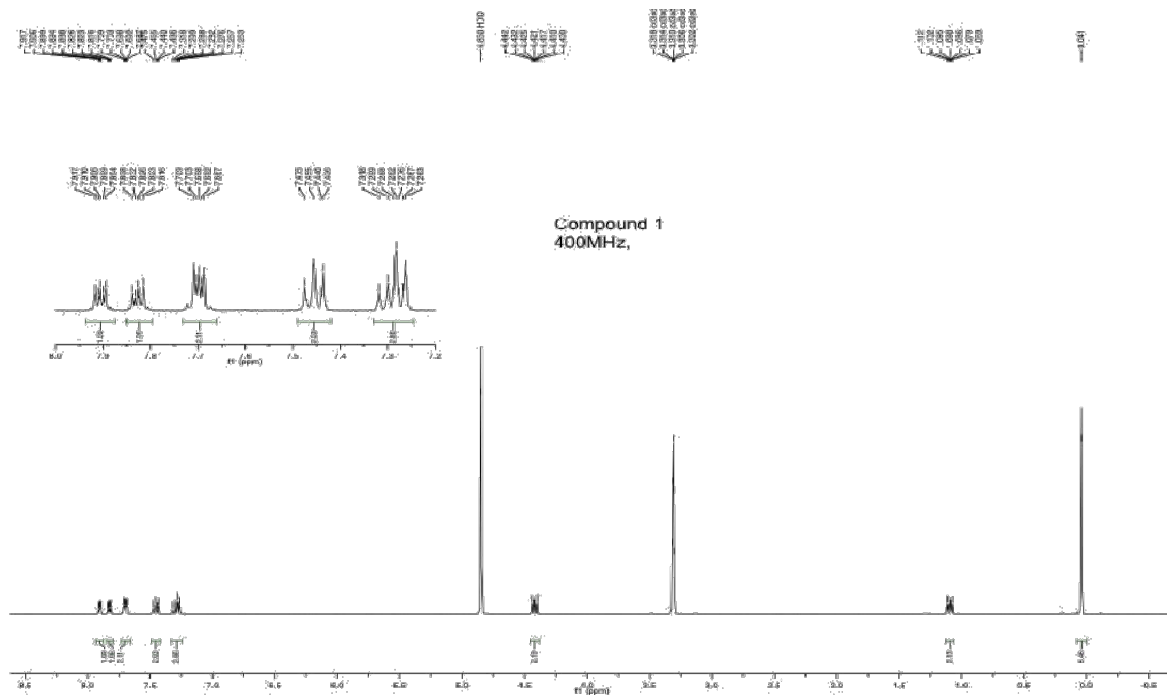


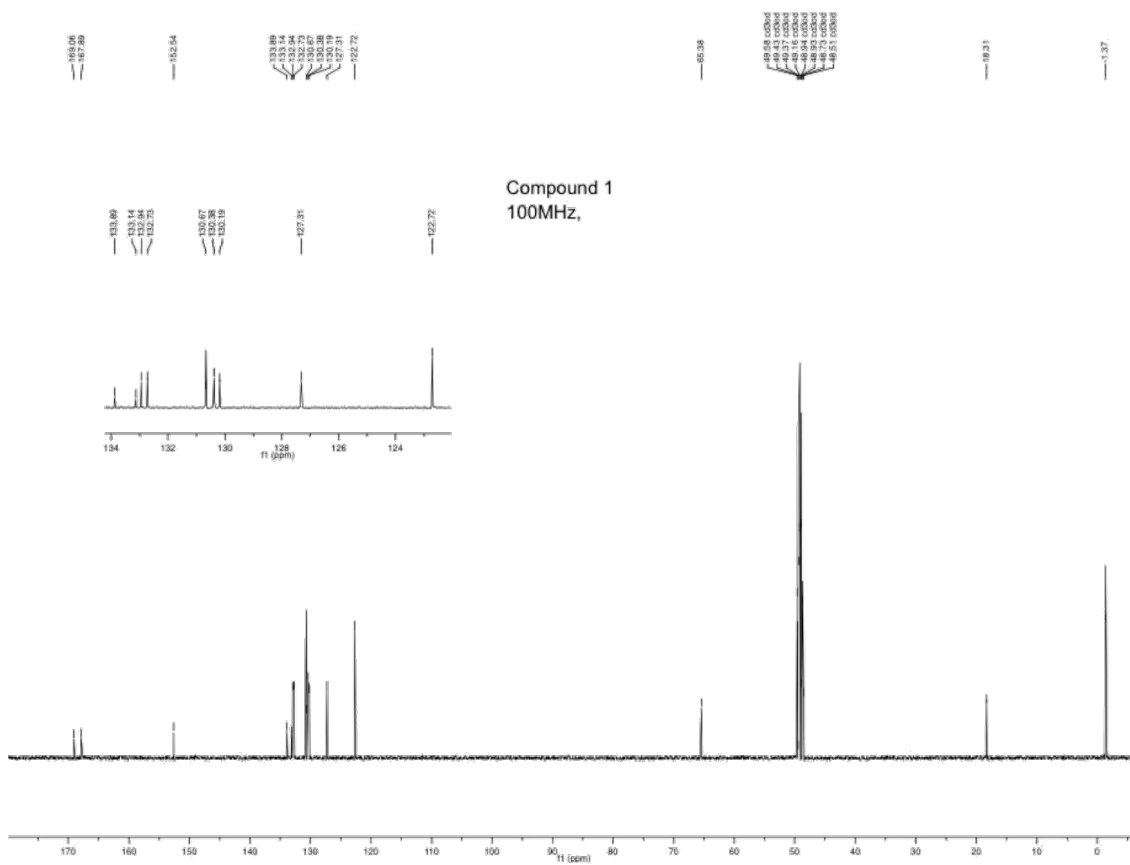
Product stability for compound **1** in D_2O . (bottom plot $t=0$, top plot $t=24\text{h}$)

Characterization of Compound 1



Mass Spec of compound 1

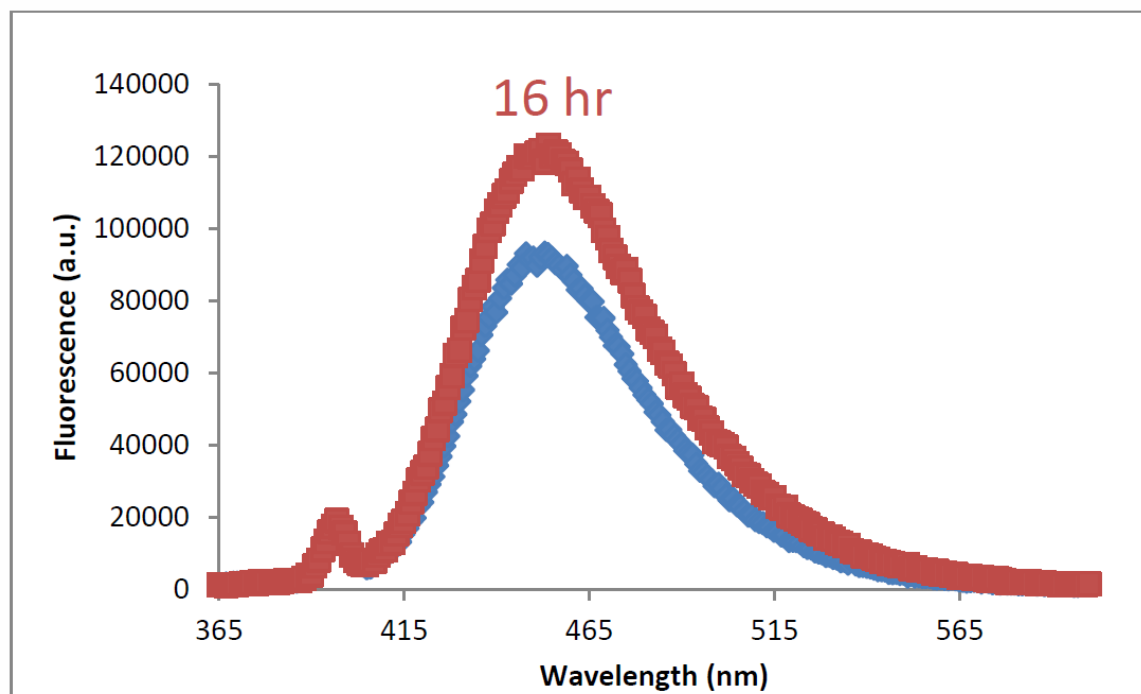
 ^1H NMR of compound 1

 ^{13}C NMR of compound 1

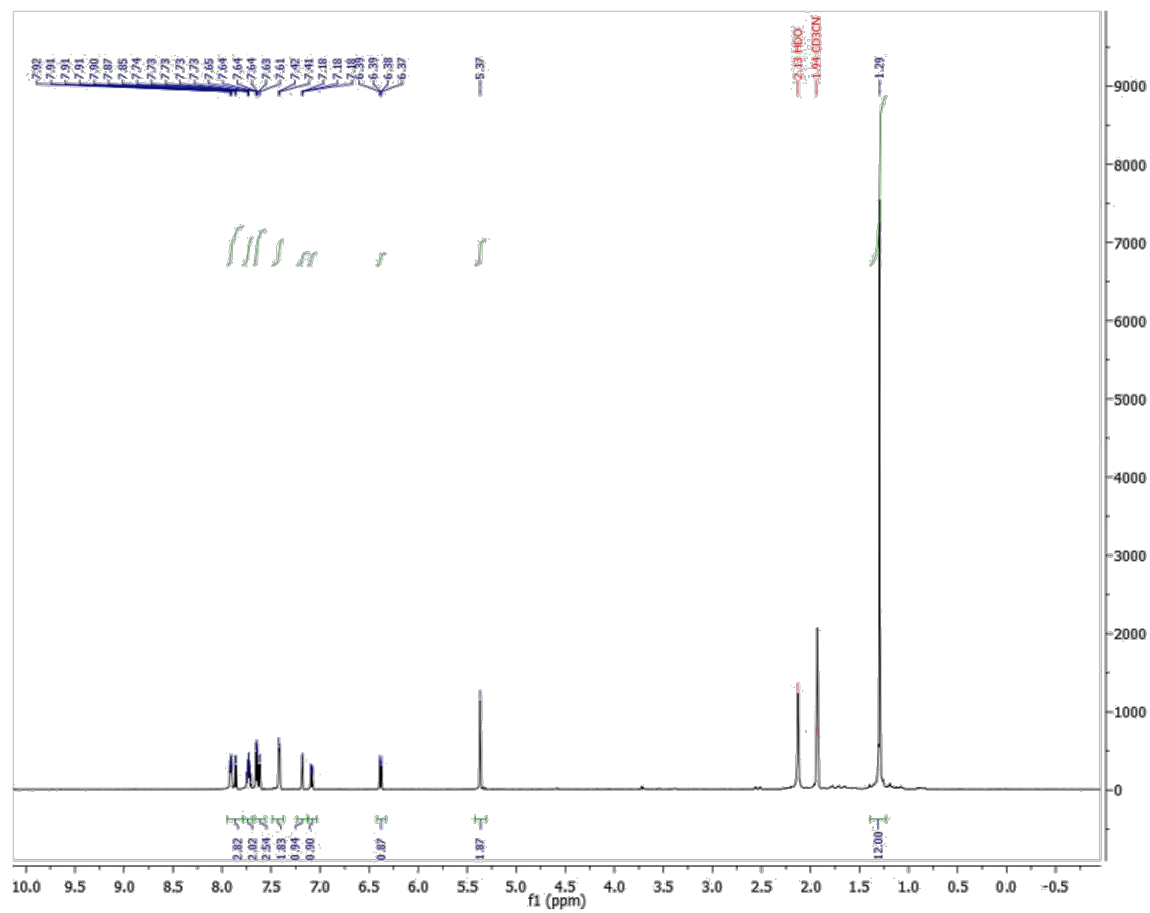
References:

- (1) Crofts, P. C.; Ghahhary, M.; Tajbakhsh-Jadidi, M. *OPPI Briefs* **1990**, *22*, 538.
- (2) Barrett, A.; Gross, T.; Hamprecht, D.; Ohkubo, M.; White, A.; Williams, D. *Synthesis*, 1998, 490.
- (3) Weiyang, L.; Long, L.; Tan, W. *Chem. Commun.*, 2010, **46**, 1503.

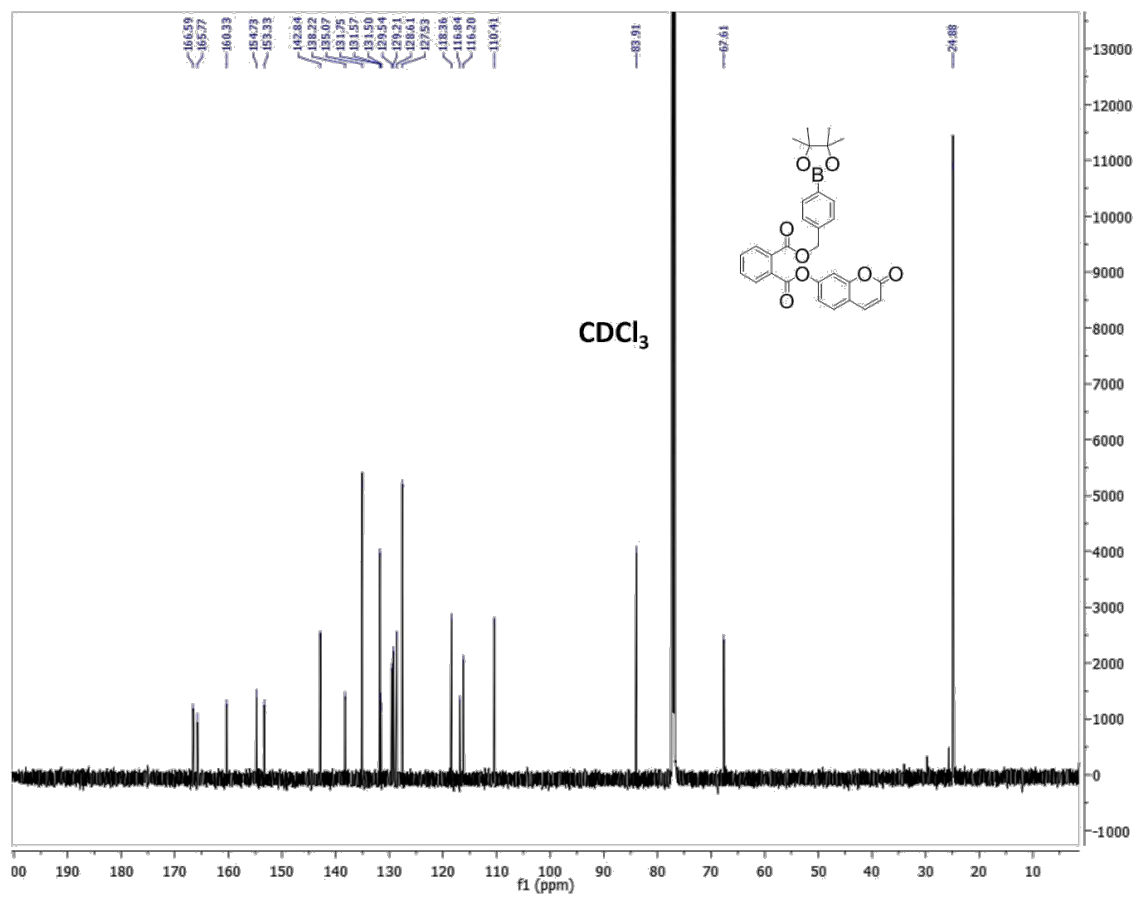
APPENDIX C: CHAPTER 6



Stability study of 7-hydroxycoumarinyl 2-(4-hydroxymethyl)benzeneboronic phthalate in water in the absence of hydrogen peroxide. The fluorescence intensity is so small that the water Raman band is seen at 397 nm. A small increase in fluorescence was seen in Compound 2 after a 16 hour period (red is initial scan and blue is after 16 hours), but insignificant compared to the increase in fluorescence intensity due to free dye.

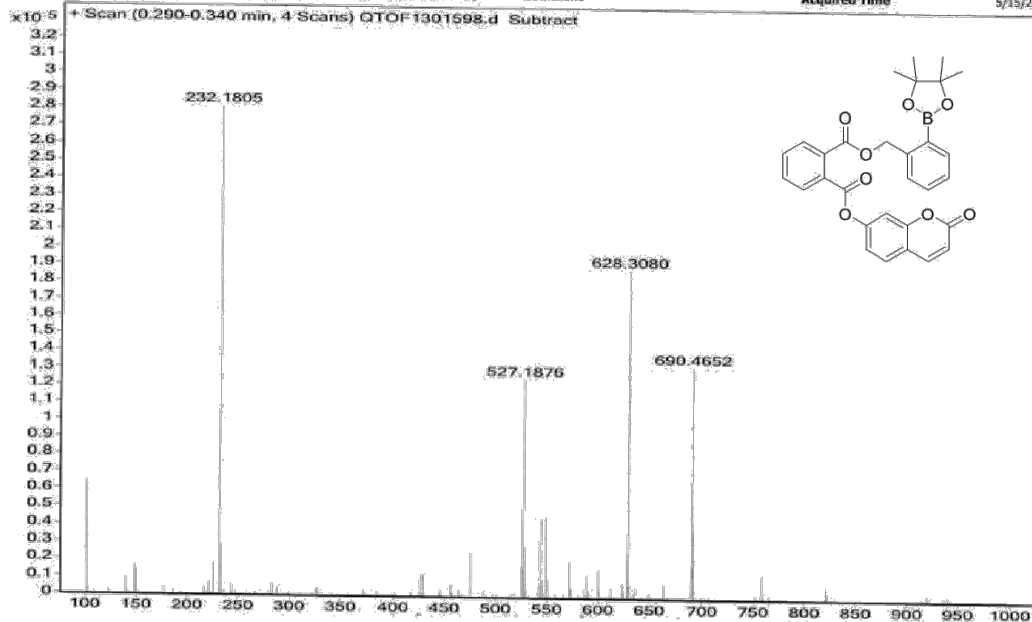


^1H NMR of Compound 2, 400 MHz.

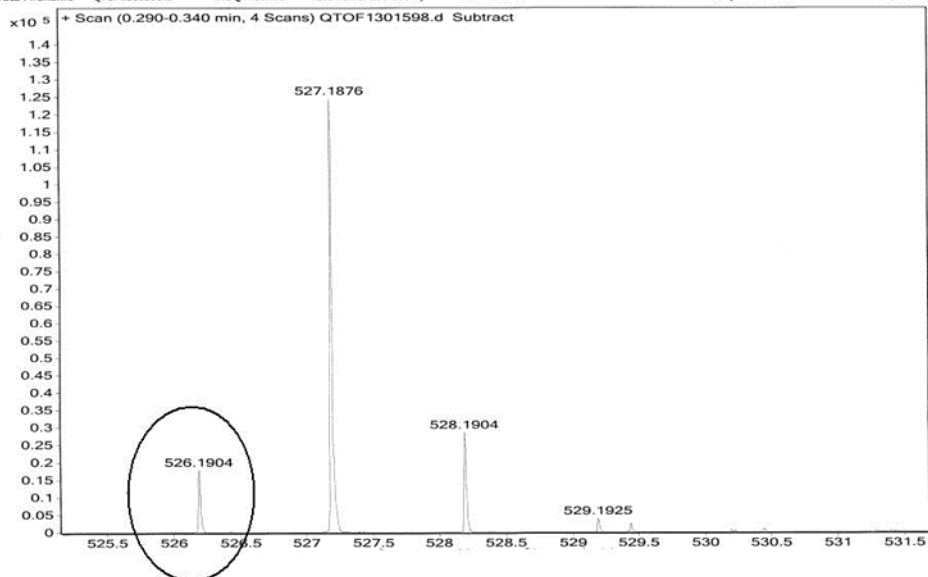


^{13}C of Compound 2, 150 MHz.

Sample Name	KM2060-2-2	Position	vial1	Instrument Name	QTOF	User Name	CIF-PC\admin
Inj Vol	1	InjPosition		SampleType	Sample	IRM Calibration Status	Success
Data Filename	QTOF1301598.d	ACQ Method	ESI-Kamel-100-1000-p	Comment		Acquired Time	5/15/2013 9:40:26 AM



Sample Name	KM2060-2-2	Position	vial1	Instrument Name	QTOF	User Name	CIF-PC\admin
Inj Vol	1	InjPosition		SampleType	Sample	IRM Calibration Status	Success
Data Filename	QTOF1301598.d	ACQ Method	ESI-Kamel-100-1000-p	Comment		Acquired Time	5/15/2013 9:40:26 AM



Mass Spec of Compound 2, (C₃₀H₂₇BO₈).